FLUORESCENCE IMAGING OF TUMOUR HYPOXIA IN XENOGRAFT TUMOUR MODELS

by

SOLMAZ SOBHANIFAR

BSc. (Biochemistry), The University of British Columbia, 2002

A THESIS SUBMITTED IN PARTIAL FULFILMENT OF
THE REQIREMENTS FOR THE DEGREE OF

MASTER OF SCIENCE

in

THE FACULTY OF GRADUATE STUDIES

(Department of Experimental Medicine)

THE UNIVERSITY OF BRITISH COLUMBIA

December 2004

ABSTRACT

Hypoxic cells in solid tumours are known to resist radiotherapy as well as forms of chemotherapy. Hypoxia is also believed to promote tumour aggressiveness and metastasis. It is therefore important to develop a practical method to identify hypoxic tumour cells in order to assess which patients could benefit from hypoxic cell-targeted therapies.

The goal of this study was to develop an immunohistochemical approach to the detection of hypoxia in xenograft models that may be applied to clinical samples. The hypotheses to be tested were that areas of chronic or transient hypoxia could be distinguished based on specific patterns of hypoxia markers, and that HIF-1α could be comparable as a hypoxia marker to pimonidazole. The objectives were: 1) to characterise the kinetics of development under anoxia and loss upon reoxygenation of the exogenous hypoxia marker pimonidazole and the endogenous hypoxia marker HIF-1α, 2) to use quantitative fluorescence image analysis to compare patterns of pimonidazole binding and HIF-1α expression in WiDr, SiHa and M006 human tumour xenografts, and to measure marker response under various oxygen- breathing conditions, and 3) to compare hypoxia marker patterns in xenograft tumours with patterns observed in cervical cancer biopsies.

HIF-1α and pimonidazole colocalised in regions distant from blood vessels; perinecrotic regions however showed pimonidazole binding but no HIF-1α expression. This lack was not a result of anoxia but likely a result of glucose and serum starvation. With time after pimonidazole administration, the extent of colocalisation with HIF-1α

was reduced from 60% at 90min to 7% at 48hr, consistent with the movement of pimonidazole-labelled cells into necrosis. Patterns of HIF-1α and pimonidazole binding in clinical samples confirmed the dissociation between the markers when pimonidazole was administered 24hr before tumour excision. Overall our xenograft results indicated HIF-1α to be a reliable indicator of tumour hypoxia; however, it over-estimated radiobiological hypoxia (<1% O_2) and was not expressed in the most hypoxic regions of tumours. The kinetics of marker development and loss, and occasional regions expressing one but not the other marker indicated that HIF-1α in combination with pimonidazole has the potential to measure the presence of transient hypoxia.

TABLE OF CONTENTS

LIST OF ABBREVIATONS

ARCON	Accelerated radiotherapy with carbogen and nicotinamide
ARNT	aryl hydrocarbon receptor nuclear translocator
bHLH/PAS	Basic-helix-loop-helix/Per-ARNT-Sim
BrdUrd	Bromodeoxyuridine
BOLD	Blood oxygen diffusion imaging
Carbogen	95% O_2 + 5% C O_2
CA	Carbonic anhydrase
CD31	Platelet endothelial cell adhesion molecule
CDK	Cyclin-dependent kinase
$CoCl_2$	Cobalt chloride
DAPI	6'-diamidino-2-phenylindol; nuclear stain
FBS	Fetal Bovine Serum
GLUT	Glucose transporter
HIF-1	hypoxia inducible factor 1
Hoechst 33342	2'-(4-ethoxyphenyl)-5-(4-methyl-1-piperazinyl)-2,5'-bi-1H-benaimidazole trihydrochloride
HRE	Hypoxia response element
i.p.	intraperitoneal
i.v.	intravenous
MAPK	Mitogen-activated protein kinase
MEM	Minimum essential medium
MVD	Microvessel density
NOD/SCID	Non-obese diabetic/severe-combined immunodeficient
OCT	Formulation of water-soluble glycols and resin
ODD	Oxygen-dependent degradation domain
PBS	Phosphate buffered saline
PET	Positron emission tomography
PI3K	Phosphatidylinositol 3 kinase
Pimonidazole	1-[(2-hydroxy-3piperidinyl)propyl]-2-nitroimidazole
PH	Prolylhydroxylase
pO_2	Oxygen partial pressure
PTN	PBS containing 1% BSA and 0.1% Tween 20
Rb	Retinoblastoma protein
SCID	severe combined immunodeficient
SPECT	Single photon emission computed tomography
TPZ	Tirapazamine
VEGF	Vascular endothelial growth factor
VHL	Von-Hippel-Lindau

LIST OF FIGURES

LIST OF TABLES

ACKNOWLEDGEMENTS

First and foremost I would like to thank my wonderful supervisor, Dr. Peggy L. Olive for allowing me the opportunity to work in her laboratory, and for imparting to me her keen interest and endless curiosity, for which I am ever grateful. Her great expertise in the field and generosity with her time was a great benefit, without which this project would not have been possible.

I am also very grateful to the members of my laboratory: Susan McPhail for seasoning me on the microscope, Laura Sinnott for her patience in teaching me how to handle and work with mice, Denise McDougle for her invaluable help with flow cytometric analyses, Eric Chu for his help with experiments when more than two hands were necessary, and Bojana Jankovic for helping me interpret my numbers.

I also wish to thank Dr. Christina Aquina-Parsons for providing me with clinical biopsies, the Durand, Minchinton, and Karsan laboratories for their valued assistance and for allowing me the use of their equipment, and Will Cottingham for her administrative support.

I furthermore thank the members of my supervisory committee, Dr. Ralph Durand, Dr. Vincent Duronio, and Dr. Paul Rennie for their guidance and direction.

Lastly, I would like to thank my family for enduring me, and of course for giving me much needed support, and friends for distracting me and thus keeping me functional.

1 INTRODUCTION

1A HYPOTHESIS AND OBJECTIVES

The overall goal of this study was to develop an immunohistochemical approach to the detection of chronic and transient forms of hypoxia in xenograft models that may be applied to clinical samples. The hypotheses to be tested were: 1) areas of chronic or transient hypoxia can be distinguished based on specific patterns of hypoxia marker binding and 2) HIF-1α would show sufficient agreement with pimonidazole as a hypoxic marker in xenograft tumours. The objectives of this thesis were:

1. To characterise the kinetics of development under anoxia and loss upon reoxygenation of the exogenous hypoxia marker pimonidazole and the endogenous marker HIF-1α.
2. To quantify patterns of expression or binding of pimonidazole and HIF-1α in WiDr, SiHa and M006 human tumour xenografts, and to measure marker response under various oxygen conditions. This included measurement of the degree of marker colocalisation, and the ability of markers to identify regions of transient as well as chronic hypoxia.
3. To compare hypoxia marker patterns in xenograft tumours with patterns observed in cervical cancer patients.

1B BACKGROUND

1B1 THE TUMOUR MICROENVIRONMENT

The tumour microenvironment is heterogeneous and often hostile, characterised by low glucose concentrations, high lactate concentrations, low extracellular pH, and low oxygen tensions (1). Focal necrosis and regions of hypoxia, as well as energy and nutrient deficiencies are therefore characteristic of most advanced solid tumours. These features often apply selective pressure for cell populations with survival and growth advantages under severe conditions, leading to tumour progression and metastasis.

1B1a Metabolism

The unfulfilled demand for oxygen in tumour cells is a natural consequence of the normal metabolic processes. Oxygen is necessary in two important steps of glucose metabolism: "the citric acid cycle" and "oxidative respiration". Not surprisingly, tumours often show a greater rate of metabolism than most normal tissue given that tumour cells undergo rapid growth, contain smaller, fewer, and often misshapen mitochondria, and have an almost five-fold increase in O_2 consumption (2). It is this high metabolic demand that throws the tumour into a state of hypoxia. In his influential studies, Warburg (3) noted that tumours underwent similar metabolic processes as normal tissue. However, he also showed that tumours are able to function both with insufficient glucose levels as well as a compromised vascular supply.

1B1b Vascular Architecture

Although the oxygen partial pressure (pO_2) in normal tissue, depending on tissue-type, ranges between 10-80mmHg, most tumours tend to have a median pO_2 of less than 10mmHg (4, 5). This difference is primarily the result of the abnormal vasculature that develops during tumour angiogenesis. Tumour blood vessels are shown to have very irregular vascular architecture whose features include blind ends, arterio-venous shunts, and high angle branching patterns. Furthermore, these vessels tend to be more "leaky" than those in normal tissue, given that they lack smooth muscle and enervation, and may contain an incomplete endothelial lining and basement membrane (6). A further cause of tumour hypoxia may be the phenomenon of "intravascular hypoxia", resulting from the relative lack of arteriolar input into tumours. In most normal tissue, the relative number of arteriolar vessels tends to be quite high. In fact there tends to be a redundancy in arteriolar supply, and the tissue volume supplied by a single arteriole is tightly regulated. However in tumours, the volume of tissue supplied by a single artery is often significantly greater, and the oxygen gradient across tumour cells extends >100-200μm away from a single capillary (7). The anatomical features of these relatively sparse arterioles result in a steep longitudinal gradient leading to vasculature and tissue hypoxia (8). Measuring the intravascular pO_2 in tumour vessels using microelectrodes, Dewhirst et al. (9) were able to demonstrate that the overall average pO_2 of tumour vessels was near 20mmHg, and that 25% of tumour blood vessels had pO_2 values of less than 1mmHg near the centre of the tumour mass, despite the fact that they contained flowing blood. They go further to show using window chamber tumours, that in Fischer-344 rats, the feeding oxygen concentration of arterioles averaged 32mmHg, whereas in arterioles of

healing tissue, this value was 50mmHg (10). Furthermore, it has been estimated that 8-9% of all tumour microvessels are plasma channels, which do not contain an appreciable red blood cell supply, possibly due to abnormal branching angles and altered rheology of red blood cells (11). Other groups have shown similar results in support of the existence of hypoxia in functional tumour vessels (12, 13).

1B2 TUMOUR HYPOXIA

Given the increased metabolic demand of tumour cells in light of an irregular and often inadequate vascular network, a heterogeneous microenvironment characterised by localised regions poor in oxygen and nutrients would seem the logical outcome. Cells have been defined as being modestly hypoxic (~2.5% 0_2), moderately hypoxic (~0.5% 0_2), and severely hypoxic (~0.1% 0_2) (14).

1B2a Chronic vs. Acute Hypoxia

Thomlinson and Gray (15) in 1955, were the first to report that some human tumours grew as nodules within stroma containing blood vessels, and that tumour cells at a distance exceeding 180μm from blood vessels became necrotic. Later another model for tumour hypoxia was described by Tannock et al. (16) that contained a central blood vessel, bordered by a cord of viable tumour cells ranging from 60-120μm, followed at larger distances by necrosis. Both such models provide for "chronic" or "diffusion limited" hypoxia, which occurs as a result of tumour cells having outpaced the growth of their blood supply. The diffusion distance of oxygen is influenced by several factors including the rate of blood flow, the presence of intravascular hypoxia, and the rate of

oxygen consumption. Surprisingly, hypoxia is also occasionally observed in close proximity to the blood vessels (17, 18). This presents the possibility of a second form of hypoxia termed "acute", "transient" or "perfusion limited" hypoxia, which likely arises from transient and localised changes in vascular perfusion. Chaplin et al. (19, 20) were the first to demonstrate that changes in blood flow and blood oxygen were sufficient to influence radiation response in tumours over 20min intervals. Furthermore, Hill et al. (21), using a multi-channel laser Doppler system that can detect micro-regional fluctuation in perfusion, have shown that transient micro-regional changes in erythrocyte flux are a common feature of both human and xenograft tumours. Previously it was assumed that the presence of transient hypoxia required total vascular stasis, and given that this event occurs less than 10% of the time (22, 23) as observed via micro-vessel flow in window chamber tumours, it was also believed that transient hypoxia was a rare event. Evidence suggests, however, that total vascular stasis is not a requirement for transient hypoxia, and that even a two-fold change in fluctuation of red blood-cell flux can reflect a change in vascular pO_2 and could substantially subject tumour regions to periods of transient hypoxia (24). This effect is even more pronounced in the case of poorly vascularised tumours. It does appear, therefore, that transient hypoxia is perhaps a more common phenomenon than previously assumed. Nevertheless, this categorisation of hypoxia still lends itself to the simplification of a very complex situation. Indeed, the abnormalities in tumour vasculature, as discussed above, lead to temporal shut-down of vessels, changes in oxygen and nutrient gradients in both transversal and longitudinal directions, as well as changes in the direction of blood flow (25). These changes can affect the status of both chronic and transient hypoxia, and can easily blur the boundary

between the two. Although most of the evidence for transient hypoxia thus far comes from murine models, there is growing evidence suggesting the existence of transient hypoxia in human tumours. These studies include the transient delivery of halogenated pyrimidines in human head and neck tumours (26) and implanted probes that directly measure changes in blood flow and oxygen (27).

1B2b Hypoxic Adaptation and Hypoxia Inducible Factor 1

Mammalian cells have developed adaptive systems that allow them to function under moderate and even severe hypoxia, which involve the expression of genes coding for proteins such as aldolase A and enolase α, lactate dehydrogenase, pyruvate kinase, and glucose transporter one (GLUT-1), all of which are responsible for the anaerobic production of ATP (28). Hypoxic cells also secrete the angiogenic vascular endothelial growth factor (VEGF), which promotes neovascularisation (29, 30). Several transcription factors have been found to respond to hypoxic stress, such as AP-1, NFκB, and Hypoxia-inducible factor-1 (HIF-1), among which HIF-1 appears to be unique with respect to its function as a global regulator of oxygen homeostasis (31).

The Structure of HIF-1

HIF-1 is a transcription factor for the activation of genes involved in erythropoiesis, angiogenesis, and cellular energy metabolism (32, 33). The protein is a heterodimer consisting of the HIF-1α subunit and a constitutively expressed HIF-1β subunit, known also as the aryl hydrocarbon receptor nuclear translocator (ARNT), both of which belong to a group of transcription factors termed basic-helix-loop-helix/Per-ARNT-Sim (bHLH/PAS) proteins (34). There exist at least two other members of the

HIF-α family, designated as HIF-2α (35) and HIF-3α (36). These HIFs show more cell type-specific expression patterns than HIF-1α, although the patterns do partially overlap. HIF-2α has biochemical properties similar to HIF-1α, including the ability to bind HIF-1β and to induce hypoxia-regulated gene expression. HIF-3α has several splice variants, one of which encodes an inhibitory PAS domain which is thought to negatively regulate hypoxia induced gene expression by competing with HIF-1α for HIF-1β binding (37).

The N-terminal domain of HIF-1α contains a basic helix-loop-helix domain and a PAS domain that are essential for dimerisation with HIF-1β, as well as for binding to hypoxia response element (HRE) DNA sequences (38). The C-terminal portion of HIF-1α contains several regulatory domains responsible for hypoxia-dependent gene expression, including the TAD-N and TAD-C terminal transactivation domains, which bind general transcriptional coactivators such as CBP/p300, SRC-1 and TIF-2 (39). Nuclear localisation signals are present at both the N and C terminals and translocate HIF-1α into the nucleus independent of dimerisation with HIF-1β (40). A critical component of the HIF-1α protein is its oxygen-dependent degradation domain (ODD) which is involved in protein stability and causes, under normoxic conditions, the rapid degradation of the HIF-1α protein through the ubiquitin-proteasomal pathway (41).

Oxygen-dependent Regulation of HIF-1 α

The oxygen dependency of HIF-1 is determined by the expression and activity of its HIF-1α subunit, whose levels increase in response to decreases in cellular oxygen concentrations (42). Under aerobic conditions, HIF-1α is bound to the Von-Hippel-Lindau (VHL) tumour suppressor, causing HIF-1α to be ubiquitinated and rapidly degraded (43, 44, 45, 46). However for this interaction to occur, HIF-1α must be

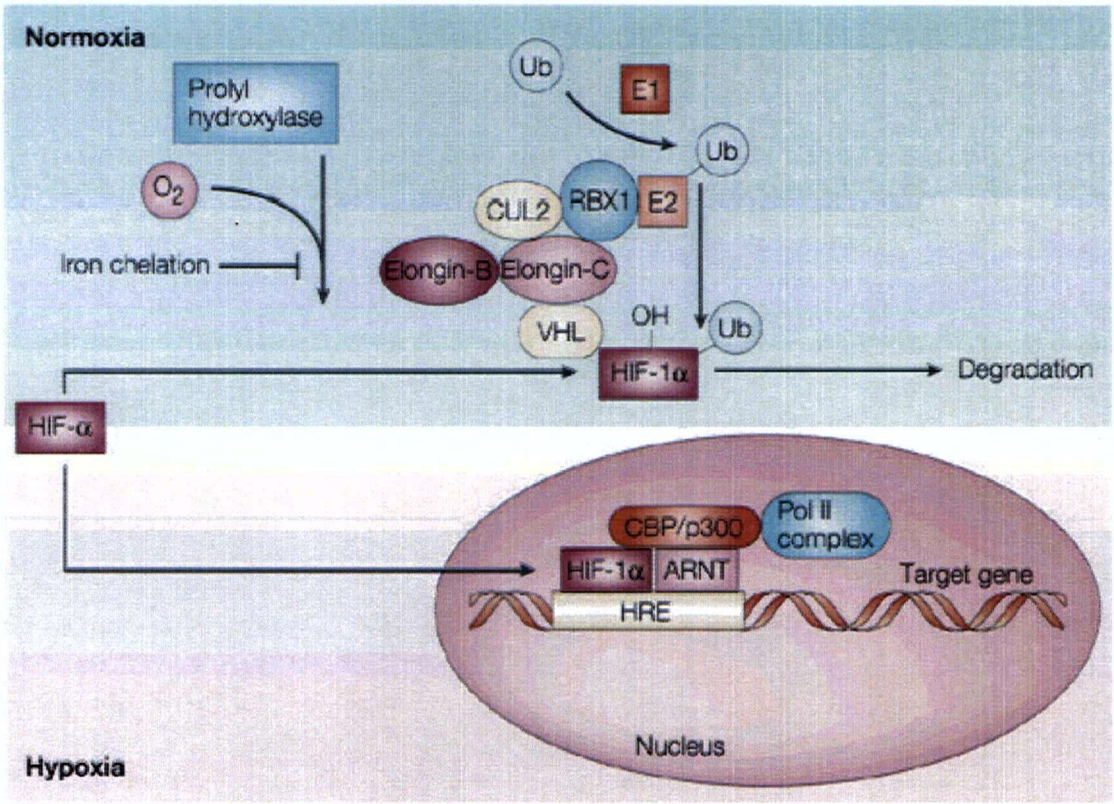

Figure 2. Oxygen-dependent HIF-1α regulation (47).

covalently modified to its hydroxylated form by an oxygen-requiring prolyl hydroxylase (PH) (48, 49, 50), and under hypoxic conditions, this modification no longer occurs. Furthermore, under hypoxia, HIF-1α dissociates from heat shock protein Hsp90 (51), a molecular chaperone, and is translocated to the nucleus (52). Nevertheless, to be fully active, it requires suitable redox conditions (53), as well as interaction with coactivators, namely CREB binding protein/p300 (CBP/p300), and steroid receptor coactivator-1 (SCR-1) (19). The subsequent increase in HIF-1α then allows the protein to bind HREs, which are sequences found in the promoter regions of genes involved in the increased delivery of oxygen or metabolic adaptation to oxygen deprivation (54).

1B3 TUMOUR PATHOPHYSIOLOGY

The progression of a malignant tumour is largely promoted by an increase in neoplastic cell load, microenvironment-induced phenotypic changes in neoplastic and stromal cells, as well as genotypic changes and clonal selection (55). Much evidence suggests that hypoxia, in addition to adapting cells to a hostile tumour microenvironment, also promotes genetic instability through point mutations, deletions, and gene amplification. These events may arise from errors in DNA repair and/or replication due to impairment of the activity of enzymes such as topoisomerases, helicases, and ligases (56, 57), as well as through reperfusion injury and oxidative damage to the DNA (58). The resulting genetic instability consequently may lead to an increase in the number of genomic variants selected to survive and proliferate under low oxygen conditions. This in turn may result in the clonal selection of p53-deficient tumour cells, due to the complex interaction of the p53 oncogene with HIF-1, whose relationship is discussed

below. To this effect, Kim et al. (59) have shown that in cervical cancer, hypoxia greatly accelerates the selection pressure for tumours with a compromised apoptotic potential. In addition, hypoxia can contribute to tumour progression by causing upregulation of VEGF, a most potent promoter of neoangiogenesis (60). Furthermore, hypoxia is involved in a number of other major tumourigenic pathways mainly through the actions of HIF-1, some of which are described below.

1B3a HIF-1α and Pathophysiology

Under physiological hypoxia, HIF-1α acts as a sensor and leads to the upregulation of hypoxia-inducible genes to adjust the cell to oxygen deprivation conditions and to attenuate the insult. Nevertheless in solid tumours, these benefits are largely lost, given that HIF-1 simply cannot respond to fully resolve hypoxic stress (61). Rapid tumour growth constantly produces new regions of hypoxia such that a uniform normoxic environment is never established. Indeed, as described above, such modifications often lead to increased pathogenesis. HIF-1 contributes to the pathogenic modulation of various processes leading to increased angiogenesis, local invasion, distant metastasis, and alteration of apoptotic programs.

Metabolism

HIF-1 has been shown to upregulate various genes involved in metabolic processes, inducing a shift from oxidative to anaerobic glycolytic pathways. This switch is crucial for cell survival, providing an alternative energy pathway during oxygen shortages. Expression studies performed in HIF-1α deficient embryonic stem cells have shown decreased expression of 13 different genes encoding both glucose transporters and

glycolytic enzymes, and HIF-1 has also been shown to upregulate fructose-2,6-bis-phosphate, a regulator of glycolytic flux (62). Anaerobic glycolytic end-products such as lactate and pyruvate have been shown to promote the stability of HIF-1α and HIF-1-dependent gene expression, possibly forming a feed-forward loop and propagating the effects of HIF-1α (63). Tumours are furthermore characterised by having an acidic extracellular microenvironment, much of this owing to the lactate produced during anaerobic glycolysis. Nevertheless, pH levels inside the cell are tightly regulated by transmembrane proteins such as carbonic anhydrases CA9 and CA12, which catalyse the reversible hydration of carbon dioxide to bicarbonate and protons (64). This process is thought to maintain intracellular homeostasis, while further aggravating extracellular acidosis as bicarbonate is exchanged for intracellular chloride. CA9 and CA12 have interestingly been identified as a new class of HIF-1 regulated proteins (65). In this way, HIF-1 appears not only to relieve hypoxic stress by allowing a switch to the anaerobic glycolytic pathway, but also to allow maintenance of the crucial physiological pH in cells, despite the acidity resulting from this switch.

Angiogenesis and Metastasis

Under normal physiological conditions, endothelial cells are tightly regulated as a result of the delicate balance between various pro- and anti-angiogenic factors. However, in solid tumours, metabolic stress, acidosis, mechanical strain, hypoglycemia, and hypoxia (the major physiological stimulus), disrupt this balance and turn on an "angiogenic switch", which leads to neoangiogenesis, allowing tumours to establish their own vascular networks (66). One of the key mediators of angiogenesis is VEGF, a protein responsible for the proliferation, survival, and migration of endothelial cells, and

an essential component for blood vessel formation (67). HIF-1 has been shown to be a key factor in the regulation of VEGF, its receptor, VEGFR, and many other angiogenic factors (68). Immunohistochemical analysis of human tumour biopsies has revealed the overexpression of HIF-1α in many common cancers and its association with tumour VEGF expression and vascularisation (69, 70). Furthermore, VEGF overexpression in several tumours has been correlated with high vascularity, lymph node metastasis, and liver metastasis (71, 72). The process of angiogenesis influences metastasis, and certain members of the VEGF family have been implicated in lymphangiogenesis (73, 74, 75). Lymphangiogenesis is the production of lymphatics, small thin channels similar to blood vessels which do not carry blood, but carry tissue fluid from the body to ultimately drain back into the blood-stream. Metastasis arises as a result of tumour cells gaining access to lymphatics, in theory by one of two ways: the first is that tumours metastasise solely by invasion of pre-existing tissue lymphatics at their margin, while the second theory proposes that metastasis can also occur via formation of new lymphatics within the body of the tumour itself (76). Nevertheless, VEGF plays a part not only in the formation of lymphatics, but also induces plasma protein leakage (77), stimulates basement-membrane degradation (78, 79), and induces endothelial cell migration and proliferation (80, 81).

Apoptosis

As stated previously, hypoxia has been shown to select for malignant cell clones having increased resistance to hypoxia-mediated apoptosis. The wild-type p53 is a multi-functional transcription factor that mediates responses to various cellular stresses, such as DNA damage and hypoxia, and is an integral component of the surveillance system that arrests cell cycle progression under unsuitable conditions (82). Somatic mutations in the

p53 tumour suppressor are the most common alterations in human tumours, occurring in approximately 50 percent of all cancers, and such defects are strongly associated with metastasis and tumour progression (83). There is increasing evidence that mutations in p53 play an important role in regulating both the survival and the angiogenic response of tumour cells to hypoxia. Various studies suggest that p53 negatively regulates VEGF induction (84, 85, 86). In agreement, it has been observed that when overexpressed, the wild-type p53 blocks transcription from numerous promoters lacking p53-binding sites, including those induced by HIF-1 (87). The body of evidence now available suggests a delicate balance in the interaction of HIF-1α and p53. p53 increases in response to hypoxia (88) and maintains a role as a tumour suppressor, where it is thought to either bind and lead to the proteosomal degradation of HIF-1α, independent of the VHL pathway (89, 90), or to out-compete HIF-1 for the p300 coactivator (91), thereby inhibiting the induction of genes required for angiogenesis. However, under prolonged and severe hypoxia, HIF-1α appears to bind and stabilise the p53 protein, facilitating apoptosis under unsuitable oxygen levels (92). A recent report by Kaluzova et al. (93) further suggests that hypoxia alone does not lead to significant overexpression of p53, but rather DNA damage in combination with hypoxia is necessary for p53 to lead to HIF-1α degradation. In light of these results, it would appear that p53 inactivation in cancers not only inhibits hypoxia-induced apoptosis, but also, through failure to inhibit HIF-1α, provides a potent stimulus for the activation of the angiogenic switch in tumours.

Proliferation

Cells under prolonged hypoxia are generally believed to be slow or non-proliferating, as revealed by studies in human tumour xenografts using pimonidazole

(marker of hypoxia), and BrdUrd (marker of proliferation) labelling, demonstrating that cells were very seldom marked by both (94). Furthermore, previous studies have indicated that HIF-1 activation prevents G1/S transition through at least two different mechanisms (95); HIF-1 may lead to the upregulation of cyclin-dependent kinase inhibitors (CKIs), $p21^{Cip1}$, and $p27^{Kip1}$, whose sustained expression suppresses cyclin/CDK2 activity, leading to the dephosphorylation of retinoblastoma protein (Rb), resulting in cell cycle arrest at the G1/S transition point. HIF-1 may also down-regulate cyclin E levels known to bind CDK2, again leading to arrest in G1/S. In fact, cyclin E/CDK2 kinase activity in HIF-1α-deficient cells was shown to be increased, resulting in only partial retardation, but still substantial cell growth under hypoxic conditions. Furthermore, hypoxic cells in vitro were shown capable of proliferation when the gene for HIF-1α was inactivated, again demonstrating its important role in this pathway (95). Nevertheless, experiments using exogenous markers of proliferation and hypoxia have shown the co-existence of a small but distinct number of proliferating cells in hypoxic tumour compartments (96, 97, 98). One also observes from in vitro studies that, when uncoupled from acidosis, hypoxia actually enhances tumour cell viability and clonogenicity (99). Moreover, an increased overlap between proliferative and hypoxic marker binding was observed after radiation in canine tumours, which is interesting in itself and of relevance to radiotherapy (100). It is possible that these groups of proliferating hypoxic cells may represent transient hypoxia, in that they are hypoxic enough for marker binding, but are able to proliferate in short windows of oxygenation, such as would be provided by reoxygenation after clearance of normoxic cells by

radiotherapy. Further investigation into this area would be valuable, in that it may provide information on methods to identify therapeutically relevant hypoxic cells.

1B4 HYPOXIA AND RESPONSE TO TREATMENT

1B4a Radioresistance

Hypoxic cells have long been notorious for their resistance to ionising radiation, and the survival of this fraction of cells is thought to lead to the reappearance of tumours after radiotherapy. Schwartz first observed the oxygen effect in 1912, and noted that the erythema reaction on the forearm was reduced when the radium applicator was pressed hard to the skin. In 1953, Gray et al. established the radioresistance of hypoxic tumour cells. It was later shown that these cells require three times the radiation dose of non-hypoxic cells to achieve the same biological effect (101); oxygen is highly electron affinic and is able to "fix" or make permanent radiation-induced radicals produced in DNA that might otherwise undergo charge recombination (102). Furthermore, hypoxia-induced radioresistance has been clearly shown in clinical studies on soft tissue sarcomas (103, 104), uterine cervical carcinomas (105, 106, 107), and head and neck carcinomas (108, 109, 110), where the presence of hypoxic regions in tumours has had adverse effects on locoregional control and/or disease-free survival after radiotherapy.

1B4b Chemo-resistance

It has been shown that hypoxia (and accompanying nutrient deprivation) reduces the proliferation rate or arrests progress through the cell-division cycle (111), and this occurs as a function of distance from the blood vessel (112). Given that most cancer drugs such as alkylating agents act by causing damage to DNA, thereby inducing

apoptosis during the synthesis phase of the cell cycle (113), such drugs lack efficacy on non-cycling hypoxic cells. Furthermore, drug delivery is also problematic since the drug is often metabolised by the intermediate layers of cells before reaching the hypoxic areas, causing a reduction in dose (114, 115). Drug uptake may also be a concern given that tumour cells are known to exhibit a lower extracellular pH than normal cells, but maintain a constant intracellular pH (116). This creates a pH gradient, leading to decreased uptake of weakly basic drugs such as vinblastine (117). Hypoxia in addition often leads to the production of stress proteins responsible for resistance to drugs such as doxorubicin (118), etoposide (119), and methotrexate (120).

1B4c Chronic vs. Transient Hypoxia

The effects of hypoxia on therapy described above are applicable primarily to chronic hypoxia, whereas the presence of transient hypoxia may yield still greater difficulties in obtaining an adequate treatment response. Firstly, the time course of transient hypoxia could have serious implications, such that if at the time of therapy, blood vessels are closed, cells may be protected from both radiation and chemotherapy-induced damage (121). Tumour cells, moreover, have been shown to undergo intermittent growth arrests (122) possibly due to transient changes in oxygen, which could render them still less susceptible to certain chemotherapeutic agents. It has also been reported that a great number of hypoxic cells in xenograft systems retain their viability and growth potential as a result of the intermittent availability of oxygen and nutrients (123, 124). It is thus very possible that following therapy, the surviving fraction

of these transiently hypoxic cells, upon reperfusion, may proliferate and result in tumour repopulation.

1B5 HYPOXIA-DIRECTED THERAPIES

1B5a Physiology-based Therapies

To date, breathing of hyperoxic gases has been the simplest method of decreasing diffusion-limited hypoxia. The breathing of carbogen gas, consisting of 95% O_2 and 5% CO_2, has been shown effective in raising the arterial partial pressure of oxygen (pO_2) in both tumour models and patient biopsies (125, 126, 127, 128, 129), although a few studies have found no significant effect or worsening of oxygenation status (130, 131). The rationale behind the small fraction of CO_2 is to induce an increase in respiratory drive, as well as improved blood perfusion, due to CO_2-induced vasodilation (132). However, when the tumour vasculature lacks responsive smooth muscle and is parallel to vasculature of the surrounding host tissue, carbogen can have a reverse effect; blood perfusion may be increased in the surrounding normal tissue but reduced in the tumour (the "steal phenomenon") (132). Furthermore, some patients lack tolerance for the 5% CO_2, due to feelings of dyspnoea. Thus, the CO_2 fraction in most patient studies has been reduced to a more tolerable 2% (133), which has been shown as effective as the 5% in increasing tumour oxygenation. A novel approach in radiotherapy is ARCON (accelerated radiotherapy with carbogen and nicotinamide). This approach combines accelerated fractionated radiotherapy to counteract cellular repopulation, carbogen to reduce diffusion-limited hypoxia, and nicotinamide, a vasoactive agent believed to reduce perfusion-limited hypoxia. Nicotinamide, the amide derivative of vitamin B_3, has been

studied extensively for its radiosensitising properties, and is likely to act by preventing intermittent vascular shut-down, as observed in a number of experimental and human tumours (134, 135). In clinical trials, the use of ARCON has been shown most effective for improved local control and survival for head and neck and bladder cancers (136, 137, 138), and phase 1 and 2 trials have shown the feasibility and tolerability of ARCON in various tumour types; the dose used, nevertheless, may be limited by the gastro-intestinal toxicity of nicotinamide. In addition, bioreductive drugs that require hypoxic conditions and the production of the appropriate set of reductase enzymes for activation have been used as hypoxia-selective cytotoxins (139). These drugs include indolequinones mitomycin C and E09, SR4233 (tirapazamine; TPZ), RSU1069, AQ4N, and CB1954, from which mitomycin C and TPZ, in combination with radiotherapy, have produced significant improvements in locoregional control and overall survival (140, 141).

1B5b Molecular-based Therapies

Given the wide array of oncogenes that are hypoxia-regulated, hypoxia-targeted molecular-based therapies have received much attention. The major role of HIF-1 in resistance to therapy and cancer progression has led to the development of various HIF-1-targeted therapies. One of these is the development of peptides that hinder interaction between HIF-1 and the co-activator p300/CREB, thereby disrupting the transcriptional activity of HIF-1 (142). Other techniques include the use of anti-sense technology, leading to the down regulation of HIF-1α via mRNA silencing (143), as well as high-throughput screening of small molecular inhibitors of the HIF-1 transcriptional pathway (144).

HRE-directed gene therapy involves the construction of therapeutic agents under control of hypoxia-inducible promoters (HREs), which restrict the therapeutic effect to hypoxic regions. An example is the enzyme cytosine deaminase, which although not toxic on its own, can convert the prodrug 5-fluorocytosine (5FC) into a cytotoxic agent, a process called gene-directed enzyme/prodrug therapy (GDEPT) (145, 146). This method could also be used to deliver pro-apoptotic, anti-proliferative, or anti-angiogenic genes to hypoxic tumour areas. Hypoxia-targeted gene delivery has been achieved using vehicles such as retro-and adenoviruses, liposomes, and naked DNA injections, along with novel vectors such as bacteria and macrophages known to accumulate in hypoxic regions (147).

1B6 MEASUREMENT OF HYPOXIA

Clinically relevant techniques used to assess the presence of hypoxia in individual human tumours can be classified as either direct or indirect, whereby direct techniques measure oxygen levels in tissue or blood, and indirect techniques provide a measure of the extent of "hypoxia" as opposed to measuring pO_2 levels. Each of these methods presents a set of advantages and disadvantages that are addressed below.

1B6a Direct measurement of Tumour Oxygenation

Direct assays for measuring tumour oxygen levels include those applied to circulating blood such as oxyhemoglobin saturation measurements (148) or blood oxygen diffusion imaging (BOLD) (149), or those applied to tissues using needle electrodes. This latter approach will be the focus of this discussion due to its widespread use. The first needle electrodes used widely in the clinic were small polarographic needle

electrodes developed by the Eppendorf Company (KIMOC 6650, Sigma-pO_2-Histograph, Eppendorf, Hamburg, Germany). This instrument functions by being mechanically and progressively moved through tissue in a ratcheting motion, while pO_2 measurements are collected via an electrolytic reaction that occurs at the cathode placed in the tip of the needle. Although this method has been widely and successfully used in many clinical studies, it does present significant limitations. These include the invasiveness of the technique, the difficulty in accessing the tumour, the failure to distinguish necrosis from hypoxia, the inability to provide information regarding hypoxic patterns or hypoxia at the single cell level, as well as the cost and dependence on a technically-skilled user (150, 151).

1B6b Indirect Measurement of Tumour Oxygenation

Indirect measurements of tumour oxygen levels involve the use of chemical or biological reporters, which provide a signal in the absence of oxygen. Non-invasive molecular imaging techniques include single photon emission computed tomography (SPECT) imaging and positron emission tomography (PET) imaging, which are based upon the emission and subsequent detection of photons emitted from the isotope decay of administered drugs. PET imaging is believed to be a more powerful technique than SPECT for several reasons, including ease of preparation of radiopharmaceuticals, higher resolution, and accuracy in quantitation of measurement; nevertheless, the advantage of PET comes at the cost of greater radioactivity (152). The resolution of PET imaging is inversely limited by the energy of the emitted positron, with the most widely studied imaging agent being ^{18}F-Miso, a relatively low energy positron emitter. Modern PET

instruments can provide high quality images with moderate spatial resolution and provide accurate quantitative results, although the ability to detect small percentages of hypoxic cells is questionable. Moreover, the cost and availability of such facilities currently limit their use.

Invasive molecular imaging techniques include reporters that can be categorised as exogenous or endogenous markers of tumour hypoxia. Exogenous markers are bioreductive drugs that were developed in the 1970s initially as hypoxic-cell sensitisers, and later proposed as chemicals that could be used to identify hypoxic cells. These agents form intracellular covalent bonds with thiol-containing molecules as a function of decreasing oxygen (153), and can then be detected using liquid scintillation methods (154), autoradiography (155), and more recently, specific antibody detection techniques (156). Although these markers can be used in the clinic and have the advantage of marking hypoxia with high resolution in the context of the tumour microenvironment, a disadvantage of using exogenous markers is that they must be administered before biopsy which may be costly and does not allow for the study of archival material.

A possible alternative that may overcome these problems is the use of endogenous markers such as hypoxia-regulated genes or gene products. As mentioned previously, these include HIF-1α and effectors such as GLUT-1, GLUT-3, and CA9. The advantage of these endogenous markers is their use in retrospective studies on archival material. Furthermore, CA9, GLUT-1, and GLUT-3 are non-diffusible and membranous (unlike targets such as VEGF), providing the added advantage that they need not be fixed for staining, and can be used for flow cytometry and sorting of viable cells. In this study,

the focus is placed on the exogenous marker pimonidazole and the endogenous marker HIF-1α.

Pimonidazole as a Hypoxia Marker

The use of pimonidazole as a hypoxia marker, developed by Dr. James A. Raleigh, has been validated in preclinical studies (157, 158) and is under current clinical investigation (159, 160, 161). Pimonidazole is a lipophilic 2-nitroimidazole compound that binds to thiol-containing hypoxic cells and forms adducts at oxygen partial pressures of less than 10mmHg (162, 163). This process requires the presence of one electron nitroreductases such as NADPH:cytochrome p450 reductase, xanthine oxidase, and aldehyde dehydrogenase, which reduce and activate the 2-nitroimidazoles in two separate one-electron reactions (figure 2). The first reaction is reversible in the presence of molecular oxygen, and the second can only take place in the presence of low oxygen concentrations (half-maximal inhibition at 4μM as measured by microelectrodes) (164). The first step in the reaction appears to be responsible for the hypoxic specificity in bioreductive activation and binding. The hydroxylamine that forms from the radical anion is the species believed to bind thiol-containing peptides to from stable adducts. However it must be considered that contrary to 1-electron reductases, 2-electron reductases such as DT diaphorase can bypass this first oxygen-dependent reductive step and cause reduction of pimonidazole irrespective of its oxygen status. To this effect, Janssen et al. (165) have demonstrated that pimonidazole staining of frozen sections under normoxia gave rise to some pimonidazole labelling, mainly in keratinising areas, suggesting that the concentration of non-specific oxygen-independent nitroreductases

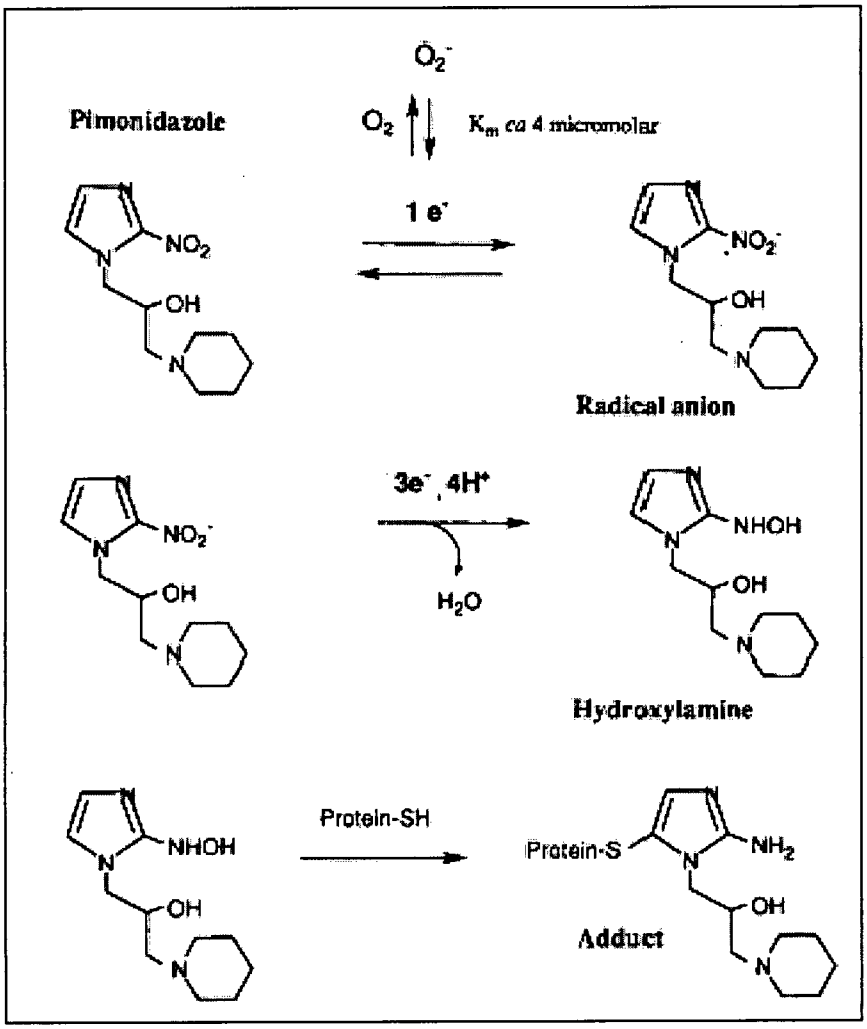

Figure 2. Oxygen-dependency of pimonidazole. Pimonidazole is reduced by nitroreductases in a two-step oxygen regulated process, and is activated for adduct formation (166).

may influence pimonidazole labelling, as detected in histological sections. Furthermore, it is important to be aware that the intracellular/extracellular concentration ratio and local concentration of pimonidazole adducts are pH-dependent, and enhanced at acidic pH (167). Despite these limitations, pimonidazole has proven to be an effective hypoxia marker both in animal and human studies, with no associated toxic effects (168, 169, 170).

Pimonidazole is administered to patients intravenously, is well distributed throughout the entire body, including the brain, and is excreted in part via the urinary tract with a plasma half-life of approximately 6 hours (171). A biopsy of the tissue is then taken typically 24 hours later, and pimonidazole adducts can be detected via immunohistochemistry, enzyme-linked immunosorbent assay, or flow cytometry.

HIF-1α as a Hypoxia Marker

Given the importance of HIF-1 in hypoxia and tumour progression, recent efforts have been made to use HIF-1α as a hypoxia marker that could be used in predicting response to therapy. Various studies, using archival formalin-fixed tumour biopsies, have correlated HIF-1α expression to outcome as well as parameters such as microvessel density (MVD) and Eppendorf electrode measurements. Table 1 shows that in 13 recent outcome studies performed on a range of tumour types, 8 correlated HIF-1α expression to poor survival, and/or local failure, 4 revealed no correlation, while 1 studies reported a positive correlation between overexpression and survival. Taken together, HIF-1α does appear to be useful as a prognostic marker. The correlation of HIF-1α expression with other measures of hypoxia, such as Eppendorf electrode measurements, pimonidazole

binding, and CA9 expression, has nevertheless yielded mixed results in patient studies. A source of these discrepancies may be sample handling. For example, a scattered rather than focal expression pattern may be due to the improper treatment of archival material; given the rapid stabilisation of HIF-1α under hypoxia, tumour biopsies or resections which become hypoxic upon removal must be prepared promptly to avoid high background levels of HIF-1α. Differences in kinetics between markers may also result in areas of mismatch due to transient changes in tumour oxygenation.

HIF-1 in addition plays an important role in tumourigenesis; the loss of HIF-1α in embryonic stem cells leads to dramatic retardation in the growth of solid tumours (172), and furthermore, HIF-1α is upregulated in the majority of human cancers (173). Given HIF-1α's important role in tumour progression, it is not surprising that its stabilisation promotes the survival of both hypoxic and *non-hypoxic* tumour cells under severe microenvironment conditions. Figure 3 illustrates some of the major tumourigenic pathways involved in HIF-1α expression, of which only some are hypoxia related.

1B7 SIGNALLING PATHWAYS THAT INFLUENCE HIF-1α EXPRESSION

1B7a The PI3K Pathway

The disregulation of signal transduction from tyrosine kinase and its effectors, which occurs via autocrine-stimulation or inactivation of the tumour suppressor PTEN, is a common phenomenon in many human cancers. Numerous studies have reported non-hypoxic stimuli such as growth factors including insulin (174), IGF (175), EGF (176), HGF/scatter factor (177), PDGF and TGFβ (178), as well as the inflammatory mediators NO and TNFβ (179) to induce HIF-1 activity through the PI3K/Akt pathway, and many

Table 1. HIF-1α Correlation. Overview of patient tumour studies on HIF-1α status and its prognostic value as well as its correlation to other parameters

Tumour site (patient cohort)	Tumour stage	Treatment modality	HIF-1α expression pattern	Analytic Parameters	Outcome and Correlations	Reference
Breast (n=206)	T1-2; N+	CT/HT/ Surg	Nuclear	Point system: scored # (+) cells and intensity	Independent prognostic factor	Schindl M et al. 2002 (180)
Cervix (n=91)	pT1-b	CT/RT/ Surg	Nuclear	Point system: scored # (+) cells and intensity	Strong independent prognostic factor	Birner et al 2000 (181)
Cervix (n=68)	FIGO I-IV	CT/RT/ Surg	Nuclear	Quantitative: positive nuclear fraction	No corr w/ survival; no corr w/ oxgen tesion and hypoxic fraction via eppendorf	Mayer et al. 2004 (182)
Cervix (n=42)	FIGO IB-III	RT	Nuclear	% (+) tumour area labelled	No corr w/ prognosis; corr w/ Eppendorf	Haugland et al. 2002 (183)
Endometrium (n=81)	FIGO I	Surg/RT	Nuclear/ scattered cytoplasmic	Semi-quant: absent/weak/strong staining	Corr w/ poor prognosis, MVD, VEGF	Sivridis et al. 2002 (184)
Esophagus (n=37)	Tis; T1	PDT/RT	Nuclear/ cytoplasmic	Qualitative: strong exp (+); weak/no exp (-)	Worse response to PDT; no response to salvage RT; no corr w/ survival.	Koukourakis et al. 2001 (185)
Gastrointestine (n=53)	Benign; borderline; malignant	Surg	Nuclear	distinct nuclear labelling: <10% (-); >10% (+)	Corr w/ poor prognosis, MVD, VEGF	Takahashi et al. 2003 (186)
H&N (n=75)	T3-4; N2b-3	CT/RT	6% nuclear; 36% cytoplasmic	% labelling above/below mean scored (-)/(+) respectively	Corr w/ local failure and poor overall survival	Koukourakis et al. 2002 (187)
NSCLC (n=108)	T1-2; NO-1	Surg	Nuclear/ cytoplasmic	Point system: scored # (+) cells and intensity.	Over-expression corr w/ increased survival	Giatromanolaki et al. 2001 (188)
Nasopharynx (n=90)	N1; N2-3; T1b	CT/RT	Nuclear	Semi-quant: scored based on staining pattern, not intensity	Trend for poor survival.; corr w/ CA9, VEGF	Hui et al. 2002 (189)
Oligodendroglioma (n=51)	Low grade	CT/RT/ Surg	Nuclear/ Cytoplasmic	Semi-quant: weak/strong staining	Corr w/ shorter overall survival, MVD	Birner et al 2001 (190)
Oropharynx (n=98)	T3-4; N1+	CT/RT	Nuclear: focal and scattered	Point system: scored # (+) cells and intensity	Corr w/ worse disease free and local failure survival	Aebersold et al. 2001 (191)
Ovary (n=102)	FIGO I-IV; LMP IA	Surg/CT	Nuclear	Point system: scored # (+) cells and intensity	No corr w/ survival unless combined w/ p53 expression data; corr w/ MVD	Birner et al. 2002 (192)

of these studies have identified mTOR/FRAP to work down-stream of Akt. Furthermore oncogenes such as V-SRC, H-RAS, erB2, and receptor tyrosine kinases, as well as loss of the PTEN tumour suppressor, have all led to the increase in activity of both the PI3K/Akt pathway and HIF-1. The mechanism by which PI3K induces HIF-1α, is independent of the VHL pathway that is functional under hypoxia (193), and appears to act by increasing the translation of HIF-1α mRNA (194, 195). Studies however have shown that the involvement of the PI3K/Akt pathway in the growth factor and oncogenic induction of HIF-1α is neither sufficient for the activation of HIF-1α nor essential for its induction under hypoxia, and is of a much lower magnitude than that caused by hypoxia (196). The involvement of a positive feedback loop has also been suggested, where VEGF has been shown to both activate and be activated by the PI3K/Akt pathway (197, 198). Therefore, the PI3K/Akt could possibly have an indirect role in the activation or maintenance of HIF-1α, which to varying degrees may be dependent on the initial activation of VEGF by a hypoxic stimulus.

1B7b The MAPK Pathway

Three well characterised MAPK signalling pathways in mammalian cells include the extracellular signal-related kinase (ERK) 1/2 (also known as p42/p44 MAPKs), the jun amino-terminal kinase (JNK/SAPK), and the p38 MAPK. The ERK-1/2 signalling pathway is activated primarily by mitogens, whereas the JNK/SAPK and the p38 MAPK pathways are regulated by pro-inflammatory cytokines, as well as a diverse array of cellular stresses, such as radiation, hydrogen peroxide, and heat and osmotic shock. Interestingly, the activation of all three pathways has been implicated in the regulation of

HIF-1α in response to various signals. It has been shown thus far that the hypoxic activation of the MAPKs is dependent on both cell type as well as the severity of the hypoxic stress (199). Although the ERK pathway is not primarily stress-responsive (200), it has been shown to be involved in the hypoxia-induced transactivation of HIF-1α (201, 202, 203, 204, 205), likely by indirect phosphorylation (206). Although MAPKs appear to play a role in the hypoxic activation of HIF-1α, there are still many HIF-1α inducing pathways that are hypoxia-independent. Hepatocyte growth factor (HGF), a cytokine that modulates mitogenesis (207), stimulation and promotion of matrix invasion (208), and angiogenesis (209) has been shown to enhance the DNA binding activity of HIF-1α via post-translational stabilisation through the stress kinase pathways, JNK/SAPK and p38 MAPK (210). Furthermore, it has been shown that transformation by viral oncogenes such as the G protein-coupled receptor (GPCR) from the Kaposi's sarcoma-associated herpes virus, can lead to the activation of HIF-1α as well as VEGF overexpression through the induction of both the p38 and ERK pathways (211). Oncogenic Ras mutations, which are very common in human cancers, can also lead to VEGF expression via either the PI3K pathway, as mentioned earlier, or the MAPK pathway, depending on cell type (212).

The regulation of HIF-1α appears to occur on multiple levels. It involves a number of mediators which in turn, may respond to various and at times, multiple physiological and pathological stimuli, often in a cell-type and context-specific manner. In light of these observations, HIF-1α may not be strictly predictive of the pattern of hypoxia in certain tumour types. Nevertheless, the majority of studies indicate that the upregulation of HIF-1α in response to such pathways is much less significant compared

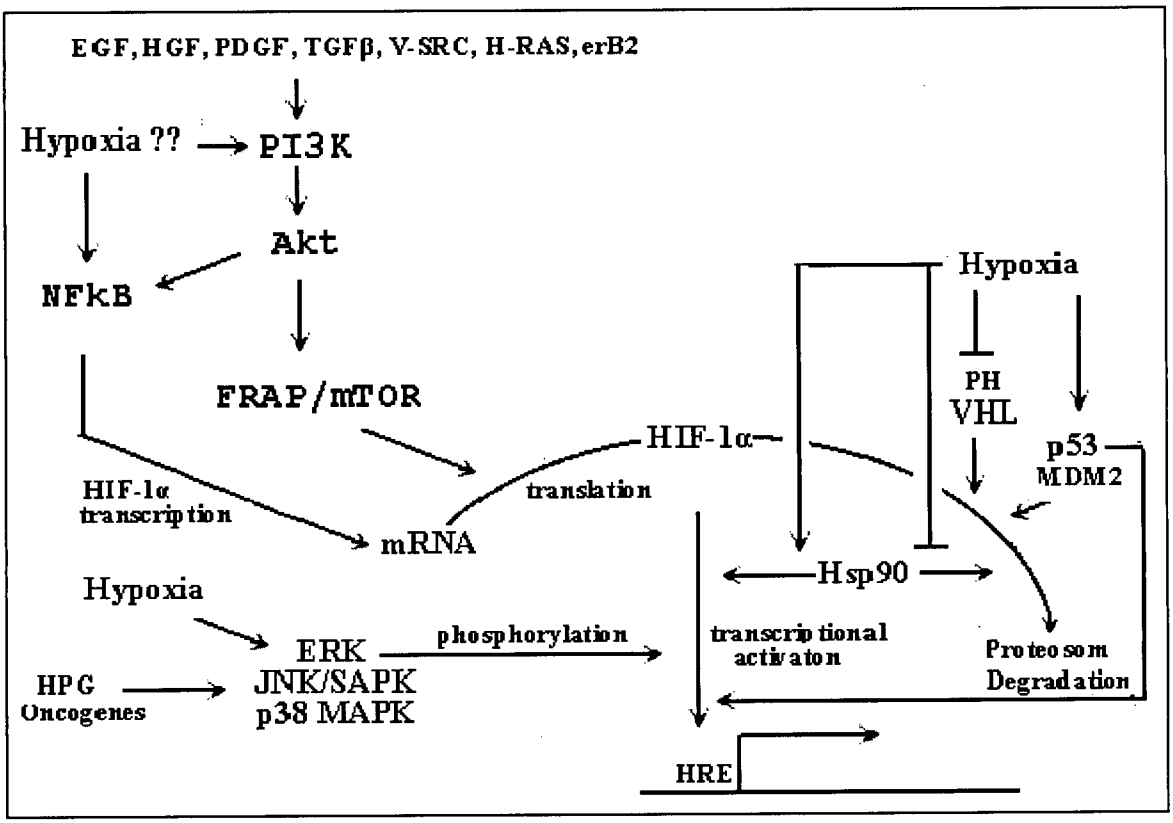

Figure 3. Signalling Pathways in HIF-1α regulation. The schematic illustrates the regulation of HIF-1α by both hypoxia and non-hypoxia-related stimuli, on levels of trascription and post-trascription.

to that of hypoxia, such that HIF-1α should in theory be applicable for the identification of regions of hypoxia in most tumour types. The involvement of such pathways, however, may lead to an increase in background levels of HIF-1α, in such a way thatproper thresholding must be carefully applied to minimise the measurement of hypoxia-independent HIF-1α expression.

1B8 USING HYPOXIA MARKERS IN COMBINATION

Given the prognostic value of HIF-1α, it is useful to investigate how well this marker relates to other hypoxia markers. By comparing pimonidazole binding and HIF-1α expression in tumours under various oxygen conditions, we hope to determine whether the use of HIF-1α presents an adequate measure of tumour hypoxia. The combination of hypoxia markers may also provide the opportunity to distinguish between chronic and transient forms of hypoxia based on differences in marker kinetics, and may allow one to follow the turnover of hypoxic cells in solid tumours. The current study aims to use the endogenous marker HIF-1α and the exogenous marker pimonidazole, believed to have different kinetics, for these purposes. Given that studies investigating the dynamics of the two markers in patient samples would be problematic due to both the lack of availability and heterogeneity of the material, studies are performed first using human tumour xenografts grown in immunodeficient mice. The rationale behind the use of this system follows the recognition that human cancers which are transplanted into mice very often retain many characteristics of the original tumour, including histology, chromosomal abnormalities, surface antigen expression, and vascular structure (113). Nevertheless, a limitation of this model remains that mice and humans have considerably

different physiology, and such differences must be taken into consideration both with rates of oxygen consumption and marker development.

Using a xenograft tumour model, an immunohistochemical method was developed to combine and to study HIF-1α and pimonidazole marker patterns in relation to each other. To do this, the development and loss kinetics of marker binding and expression were first determined, and the oxygen and nutrient dependency of the endogenous marker, HIF-1α were studied. These patterns were studied in a range of xenograft tumour types, and as a function of changing oxygen in SiHa xenografts via oxygen breathing experiments. The ability of the combination of the two markers to identify regions of transient hypoxia were examined, and the life-time of hypoxic cells was determined by measuring the progression of pimonidazole-labelled cells from areas of viability to those of necrosis as a function of time after chemical administration. The feasibility of this fluorescence immunohistochemical approach was then tested in cervical cancer biopsies, and the patterns obtained compared to those in the xenografts.

2. MATERIALS AND METHODS

2A CELL LINES AND CULTURE CONDITIONS

1) SiHa: human cervical squamous cell carcinoma cell-line; adherent; contains HPV-16 (1-2 copies per cell); pRb and p53 compromised; doubling time 20-22hr; obtained from the American Culture Collection (ATCC)
2) WiDr: human colon adenocarcinoma cell-line; adherent; expresses mutant p53 (273G-273A); expresses EGF; doubling time ~24hr; obtained from ATCC
3) MOO6 human astrocytoma cell-line; low mitotic index; prominent endothelial proliferation and extensive necrosis; doubling time ~24hr; obtained from Dr Alan Franko (214), Cross Cancer Institute, Edmonton AB

The above cell-lines were chosen for their ability to grow in monolayer culture and as xenografts in immunodeficient mice, and to represent a range of tumour types. These cell-lines were also chosen due to having been well-characterised in our laboratory. The SiHa cervical carcinoma cell-line in particular was chosen for comparison with patient cervical cancer biopsies. All three cell-lines were maintained in exponential monolayer growth in Eagle's minimum essential medium (MEM) (Sigma-Aldrich, Oakville, ON, Canada containing 10% (v/v) fetal bovine serum (FBS) (Gibco BRL, Grand Island, NY, USA). The cells were grown as monolayers in 100mm plastic tissue culture plates (Falcon 3003) at 37°C in a humidified atmosphere of 5% CO_2, 95% air. Cells were subcultivated twice weekly to maintain exponential growth, and were recovered from culture plates by removing the culture medium, rinsing the plates in 0.1% trypsin in citrate phosphate saline buffer (Gibco), leaving a thin layer of trypsin remaining after the

second rinse, and incubating cells for ~6min at 37°C. Cell counts were performed using a Coulter Counter cell analyser (Beckman/Coulter, Fullerton, CA).

2B XENOGRAFT TUMOUR MODELS

Xenograft tumours were grown from SiHa, WiDr, and MOO6 cell lines. Tumour cell suspensions (0.1ml at 10^6 cells/ml) were subcutaneously injected in the back of 7-8 week old NOD/SCID (non-obese diabetic/severe combined immunodeficient) mice. The tumour lines were maintained by serial implantation of the tumours in the flanks of NOD/SCID mice. NOD/SCID mice were kept in a pathogen-free unit in an air-conditioned facility, approved by the Canadian Council of Animal Care. Approval of the local animal care committee was obtained for all protocols.

To implant tumours, mice were shaved over the back. NOD/SCID mice were then anaesthetised with isoflurane, the areas swabbed with alcohol, and injected once subcutaneously with a minced tumour suspension or with single cell suspensions using a 20g needle. The area was swabbed again with alcohol and mice were allowed to recover in a warm environment before returning to the animal holding room. Tumours were used when they reached a size a 0.25 - 0.6g in approximately 3-4 weeks.

2C ADMINISTRATION OF CHEMICALS

Pimonidazole

Pimonidazole-hydrochloride (hypoxyprobe-1; Chemicon Int. Temecula, CA, USA), a bioreductive marker for hypoxia, was administered to mice intraperitoneally (i.p.) at 100mg/kg (215). Mice were sacrificed by cervical dislocation 90min to 48hr

following pimonidazole administration and the tumours excised. Pimonidazole was administered to patients intravenously (i.v.) at 500mg/m^2 and biopsies taken 24hr after administration. Informed consent was obtained from all patients and approval for the study was given by the British Columbia Cancer Agency and the University of British Columbia clinical investigations committee. The plasma half-life of pimonidazole is ~30min in mice (216), and ~6hr in humans (171).

Hoechst 33342

Hoechst 33342 (Sigma/Aldrich, St. Louis MO, USA), a fluorescent dye used as a marker for vascular perfusion, was administered to mice i.v. at a volume of 0.1ml and a concentration of 4mg/ml in PBS. Given its relatively short plasma half-life of 110s, Hoechst 33342 binds in the first few minutes after administration, and only produces extensive fluorescence in cells adjacent to perfused vasculature (217). Mice were sacrificed by cervical dislocation 10min following Hoechst 33342 administration. Given that a perfusion marker in humans has not yet been approved, the endothelial cell marker CD31 was used to identify vasculature in patient biopsies.

2D GAS-BREATHING PROCEDURES

Gas-breathing experiments were performed using a PROOX model 110 hypoxic chamber (BioSpherix, Redfield New York, USA), which equilibrates ambient air with nitrogen or oxygen gasses to create the desired gas concentration. Mice were placed in the chamber 5min prior to pimonidazole administration, and were returned to the chamber for 1.5-2hr at the desired oxygen concentration. Mice were then removed briefly, administered Hoechst 33342, and placed in the chamber for 10min, followed by

sacrifice. For carbogen (95% O_2, 5% CO_2), mice were placed inside a plexi-glass chamber and gassed with carbogen (PRAXAIR, ON, Canada).

2E PREPARATION OF FROZEN SECTIONS

Mice were sacrificed by cervical dislocation and the tumour excised within 30s. The tumour sample was embedded and frozen at -20°C in O.C.T.(Tissue-Tek). 10μm sections were obtained using a Cryostar HM560 (Microm International GmbH, Walldor, Germany). Frozen sections were melted for 30s on glass slides in preparation for immunohistochemistry and fluorescence microscopy.

2F IMMUNOHISTOCHEMISTRY

Sections were fixed in cold 2% paraformaldehyde (Sigma-Aldrich) in PBS for 15 minutes at 4°C. The sections were then rinsed sequentially in PBS, MeOH (-20°C), PBS, and immersed in PTN (PBS, 1% bovine serum albumin, 0.1% Tween) for 5min at room temperature. 30-40μl of antibody solution (table 2) were then applied to each slide and covered with $1cm^2$ paraffin strips (to prevent evaporation) for 30min in humidified containers at ambient temperature. The primary antibody was rinsed off in PBS and the slide immersed in PTN for 5min before addition of the fluorescent secondary antibody. In double-staining procedures, the slides were fixed in 2% paraformaldehyde before addition of the second primary antibody to prevent cross-reaction. Following all staining procedures, sections were rinsed for 5min in PBS, drained, covered with 10μl Fluorogard mounting medium (BioRAD, Mississauga, ON, Canada) and sealed with a cover-slip. Appropriate secondary antibody controls were performed for each experiment.

Table 2. List of antibodies. Primary (1°) and secondary (2°) antibodies are indicated. Typically, the HIF-1α primary antibody and Alexa 594 secondary antibody were administered before the anti-pimonidazole antibody and Alexa 488 secondary. Antibodies were diluted in PTN.

Antibody	**Origin**	**Source**	**Dilution**
HIF-1α (1°)	Mouse anti-human	BD Transduction Laboratories, Canada	1:100
Pimonidazole-HCl (1°)	Mouse anti-human	Natural Pharmaceuticals International Inc., NC	1:200
CD31 primary (1°)	Mouse anti-human	Dakocytomation, Mississauga, ON	1:50
Alexa 488 (2°)	Goat anti-mouse IgG F(ab')	Molecular Probes, USA	1:200
Alexa 594 (2°)	Goat anti-mouse IgG F(ab')	Molecular Probes, USA	1:200

2G IMAGE ACQUISITION AND ANALYSIS

Many studies use a semi-quantitative method of analysis in evaluating the presence and extent of maker binding, as displayed in table 1. However, much more information may be gained from a quantitative analysis, and the ease in evaluation due to image quality and definition in fluorescence imaging, as well as the possibility of a double staining protocol allowed us to evaluate marker patterns quantitatively. Slides were viewed with 488nm excitation (green light emission), 594nm excitation (red light emission), and UV excitation (blue light emission) using a 10x neofluor objective with a Zeiss Axioplan 2 epifluorescence microscope with an attached Retiga Exi mono cooled 12 bit CCD camera (Q Imaging, Canada). The images were digitised using Northern Eclipse 5.0 software (Empix, Toronto, ON, Canada). When possible, three sections were obtained from each tumour (proximal, mid, and distal), and five to ten 10x magnification images were obtained from each section.

10x magnification grayscale images (1360x1024 pixels, 1pixel/μ, 8bit) of sections showing HIF-1α, pimonidazole, and Hoechst 33342 were pseudocoloured, superimposed and analysed for degree of colocalisation or mismatch between the colours using software written for the Northern Eclipse 5.0 software by Hart Lambur. The mismatch software measured the number of pixels designated red (R; HIF-1α), green (G; pimonidazole), and yellow (RG; both), and the number of RG pixels were divided by the total number of R or G pixels to provide % colocalisation with respect to HIF-1α and pimonidazole respectively. To do this, each grayscale image was displayed individually and thresholded. This required manual application of thresholds to determine positive regions

of labelling. The thresholds chosen were typically 2x and 3x the level of background labelling for HIF-1α and pimonidazole respectively. A higher threshold was used for pimonidazole, which showed a lower level of background labelling. The number of pixels from each individual image was automatically counted and entered into a spreadsheet. The images were then superimposed, and matching pixels from both images were counted and entered into the spreadsheet, from which the % colocalisation was calculated, as described above.

Values for HIF-1α and pimonidazole development (start-point and end point with respect to distance from the blood vessel, as marked by Hoechst 33342) were obtained using ImageJ software (NIH Image: http://rsb.info.nih.gov/ij). Three to four regions from each image were selected by drawing a line from the centre of a blood vessel through a tumour cord. The regions were selected such that they encompassed one or a small group of blood vessels on one side, and were adjacent to a region of obvious necrosis on the other. Selection was necessary in order to model a simplified system, where the cord would start from an area of highest oxygen concentration (area stained with Hoechst 33342) and extend through to that of the lowest oxygen concentration (region of necrosis). The ImageJ RGB profiler function then produced a colour histogram of each selected region, from which the start and end points of HIF-1α and pimonidazole staining with respect to the blood vessel were obtained and calibrated in microns. Given the variation in the size of the tumour cords, the results were normalised. Values for the HIF-1α start points were first divided by the corresponding pimonidazole start points, and values for the HIF-1α end point were accordingly divided by the pimonidazole end points to obtain start and end point ratios. These ratios were then multiplied by the

average pimonidazole start and end points over all samples, to obtain relative HIF-1α start and end values, respectively.

2H WESTERN BLOT ANALYSIS

Approximately $6x10^6$ cells were lysed in RIPA lysis buffer (50mM Tris-HCL pH 7.4, 150mM NaCl, 1% NP-40, 0.5% sodium deoxycholate, 0.1% SDS, 1mM EDTA) to which 1mM PMSF, 1μg/ml aprotinin, 1μg/ml leupeptin, 1mM Na_3VO_4, and 1mM NaF were added before use (all reagents were obtained from Sigma Chemical Co., Oakville ON, Canada). Protein concentrations were standardised using the DC Protein Assay (BioRad). Proteins were separated on a 10% polyacrylamide precast gel system (BioRAD) and transferred to a nitrocellulose membrane (BioRAD). The membrane was immersed in 5% non-fat dry milk in TBS-T (25mM Tris-HCL, pH 7.04, NaCl, KCl, 0.05% Tween 20) for one hour at room temperature with shaking. Membranes were next incubated in anti-mouse monoclonal HIF-1α antibody (1:1000 dilution) overnight. After several washes in TBS-T, membranes were incubated in horseradish peroxidase anti-mouse antibody (1:5000 dilution; Sigma) for 1hr and developed using the ECL detection kit (Amersham, Oakville, ON, Canada). Membranes were exposed under a chemiluminescence imager (MultiImage Light Cabinet, Alpha Innotech Corp., CA) for 4-10min. Images were analysed for band density using FluorChem software (v.3.04A, Alpha Innotech). Relative band density was obtained by first adjusting (by division) to the band density of cells in air-equilibrated medium, and then to the highest band density obtained in each sample. Experiments were repeated twice.

2I FLOW CYTOMETRIC ANALYSIS

Approximately 10^5 to 10^6 cells were fixed in 70% EtOH in PBS. Cells were centrifuged, washed in PBS, and rehydrated in PST (PBS with 4% FBS and 0.1% triton X-100) for 15min. Cells were centrifuged and incubated in pimonidazole antibody (1:200) for 2hr on a shaker. Cells were then centrifuged, washed in PST, and incubated in Alexa 488 antibody (1:200) for 45min with shaking. Cells were again centrifuged, washed twice in PBS, and incubated in DAPI (1:50 dilution of 100ug/ml) for nuclear staining. Cells were then analysed using a dual laser Epics Elite-ESP flow cytometer (Coulter Corp., Hialeah, FL). Gates were set to discriminate against debris on the basis of cell size and time of flight. List mode files were collected and post processed

to determine parameters of interest using the WINLIST software package (Verity Software House Inc., Topsham, ME). Figure 4 depicts typical read-outs obtained from flow cytometric analyses. The means of the peak intensities, shown in Figures 4C and D were used as a measure of the amount of pimonidazole adducts. Experiments were repeated twice.

2J GRAPHICAL AND STATISTICAL ANALYSIS

For statistical analysis of data, the mean and SD values were determined. The one-way ANOVA followed by the Tukey-Kramer test was used to compare multiple means (JMP Start Statistics 2nd Ed., SAS Institute Inc.). p values of less than 0.05 were considered to represent significant changes. Graphical analysis of kinetics data was performed by fitting each curve to an appropriate exponential function using Gnu Plot software (Thomas Williams, Collin Kelly; 2004).

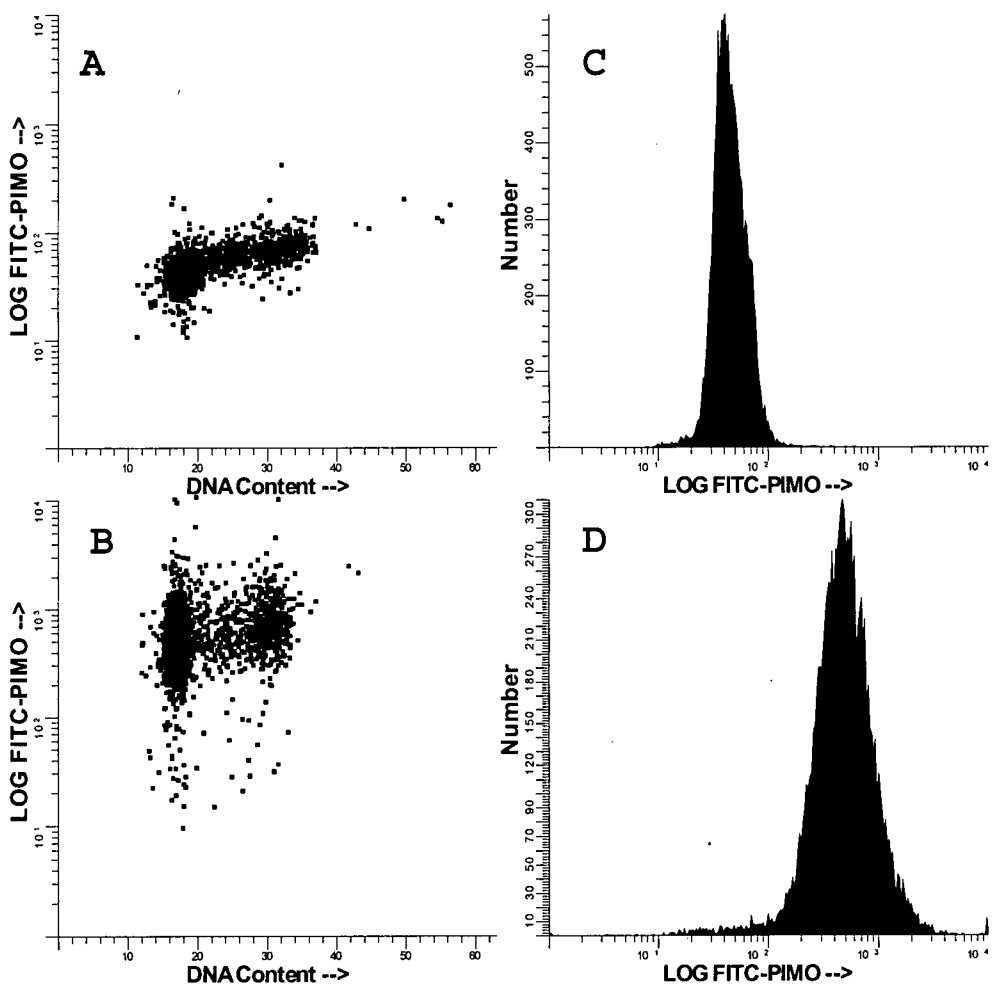

Figure 4. Flow cytometric analysis. SiHa cells were first gated on forward light scatter and time of flight to eliminate debris. Panels A and C are control cells, panels B and D are SiHa cells after 4hr incubation with pimonidazole under anoxic conditions.

3 RESULTS

Given the importance of tumour hypoxia in both tumour progression and response to therapy, hypoxia should be measured routinely in tumour biopsies. A method applicable to formalin-fixed paraffin-embedded sections could be easily incorporated into pretreatment analysis of patient biopsies. In this study 1) we examined the ability of an endogenous hypoxia marker, HIF-1α, to mark the same regions as an established chemical marker for hypoxia, pimonidazole. 2) The rate of development of the markers under hypoxic conditions and their rate of loss upon reoxygenation were examined, and 3) the role of oxygen and nutrients (glucose/serum) in marker binding were determined. 4) The localisation of the two markers within tumour cords and their response to oxygen modulation were also studied. 5) Lastly, two patient biopsies were examined to confirm the feasibility of using the staining protocol on human frozen-sections.

3A MARKER KINETICS

All marker kinetics experiments were performed using cultured SiHa cells. Cells were removed from culture plates using trypsin and transferred as cell suspensions to medium-containing (MEM/10%FBS unless otherwise specified) pre-gassed glass spinner culture flasks (150 rpm) equilibrated with 0% O_2 in nitrogen and with 5% carbon dioxide to maintain the pH of the bicarbonate buffer. Cells were maintained with continuous gassing at 0% O_2 as required at 37°C. High cell density ($2x10^5$ cells/ml) compensated for any small oxygen leakage into the flasks to maintain oxygen concentrations as close as possible to 0%.

3A1 HIF-1α BUILD-UP UNDER ANOXIA

Cell suspensions were incubated under anoxia as described above for up to 16hr, after which the cells were rapidly removed into ice-cold medium containing cobalt chloride ($CoCl_2$; final concentration of 100μM) to inhibit HIF-1α degradation. $CoCl_2$ binds the oxygen-dependent degradation (ODD) domain of HIF-1α and inhibits VHL binding, thereby inhibiting degradation (218). As shown using western analysis, HIF-1α was stabilised quickly under anoxia, and by 2hr, the half-maximal signal was reached (figure 5). This is consistent with the presence of a steady state level of HIF-1α that is ready to be stabilised upon exposure to hypoxic stress.

3A2 HIF-1α HALF-LIFE UPON REOXYGENATION

Cell suspensions were incubated under anoxic conditions as described for 4hr. Subsequently, cells were removed and reoxygenated by immersion in air-equilibrated medium. Further degradation of HIF-1α was inhibited by adding $CoCl_2$. Cells were lysed and analysed by western blot analysis (figure 6). The half-life of HIF-1α upon reoxygenation was found to be < 1min.

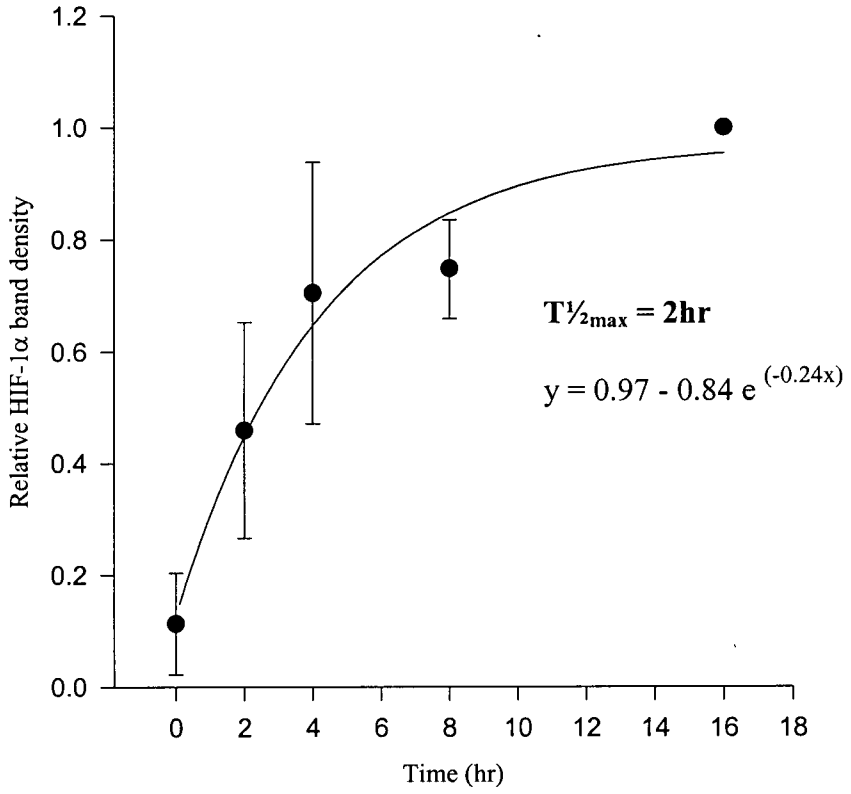

Figure 5. Stabilisation of HIF-1α under anoxia. SiHa cells were incubated under anoxia, and cell lysates were subjected to western blot analysis. Relative band densities were obtained as described (refer to 2H), and an exponential function was fitted to data points.

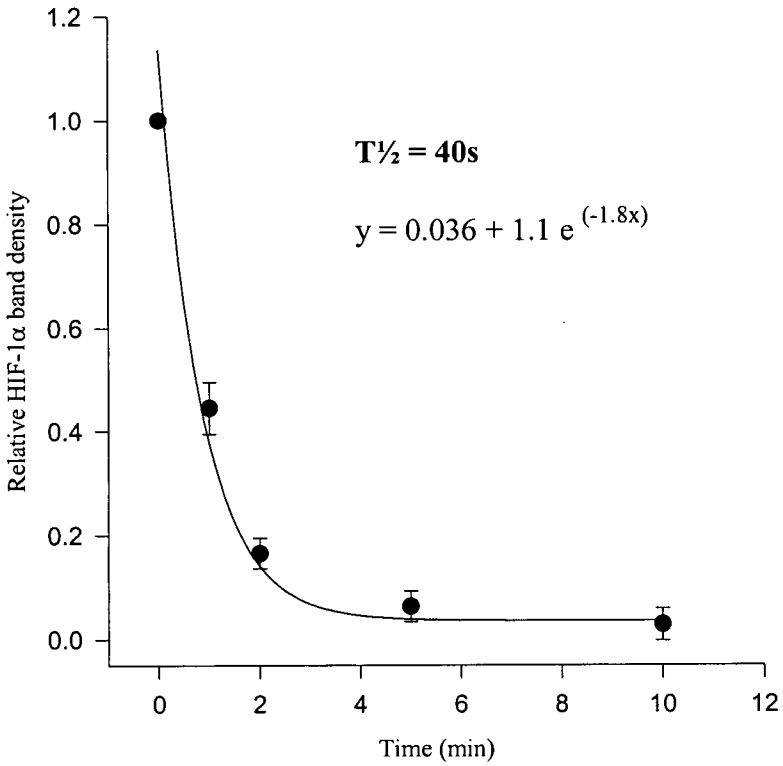

Figure 6. Loss of HIF-1α after reoxygenation. SiHa cells were incubated for 4hr under anoxia and were reoxygenated. Cell lysates were subjected to western blot analysis. Relative band densities were obtained as described (refer to 2H), and an exponential function was fitted to data points.

3A3 PIMONIDAZOLE BINDING UNDER ANOXIA

Cell suspensions were equilibrated under anoxia as described, and incubated with 2, 10, and 50μg/ml pimonidazole hydrochloride. Cells were then sampled from each flask at various times, fixed in 70% ethanol, immunostained with anti-pimonidazole antibodies, and analysed for fluorescence by flow cytometry (figure 7). At high concentrations of pimonidazole, the initial rate of pimonidazole adduct formation was greater than at the lower concentrations, possibly related to the Km of the system. At 10 and 50μg/ml of pimonidazole, the curves start to level at ~2hr, likely due to saturation, although cell toxicity effects cannot be excluded. The half-maximum signal was obtained at 20min and 40min for 50μg/ml and 10μg/ml, respectively. As mice were administered 100mg/kg pimonidazole, the higher doses are probably more typical of the *in vivo* exposure.

3A4 PIMONIDAZOLE HALF-LIFE UPON REOXYGENATION

Cells were incubated under anoxia as described in 50μg/ml of pimonidazole for 4 hours, after which they were removed, placed in culture dishes and allowed to recover under ambient oxygen. Cells were trypsinised and removed from the plates at the indicated times, fixed in ethanol, and analysed by flow cytometry. The doubling time of the same cell population was also assessed by counting the cells after typsinisation. The half-life of the pimonidazole adducts was 45hr (figure 8A) and the doubling time of the cell line was 21hr (figure 8B). Although one would expect adduct half-life to be equal or less than cell doubling time, the observed effect may be due to anti-body binding affinity. Therefore, these results still suggest that loss of pimonidazole adducts may largely be a

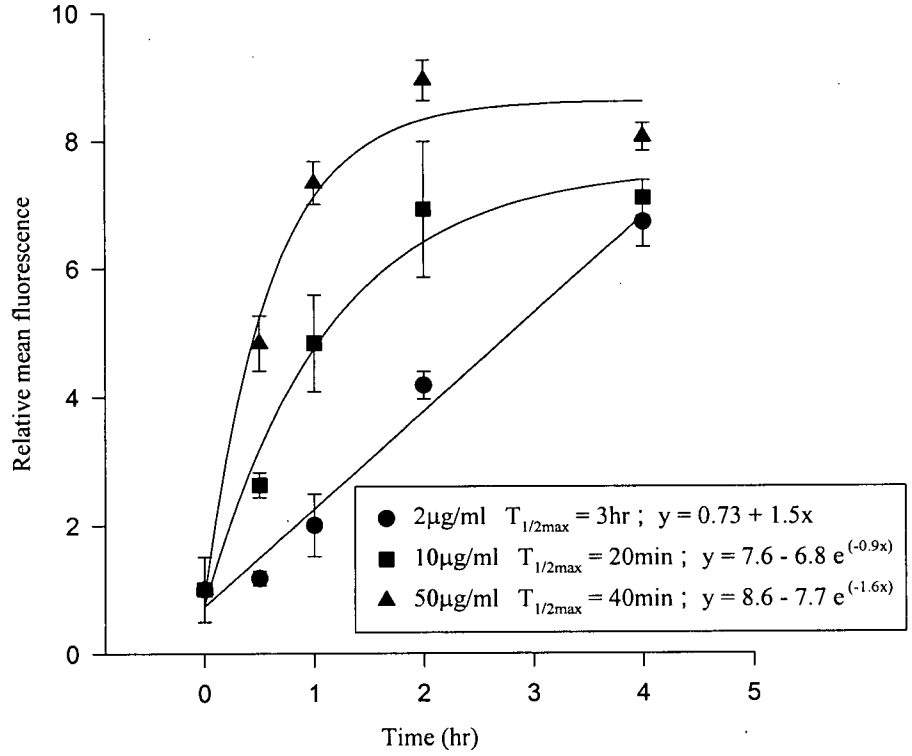

Figure 7. Formation of pimonidazole adducts under hypoxia. Different concentrations of pimonidazole were added to SiHa cells that were incubated in spinner flasks under anoxia for various times. Mean fluorescence was detected using flow cytometry. Relative values were obtained by dividing by the mean fluorescence of cells incubated in air-equilibrated medium for each time point. Appropriate functions were fitted to data points.

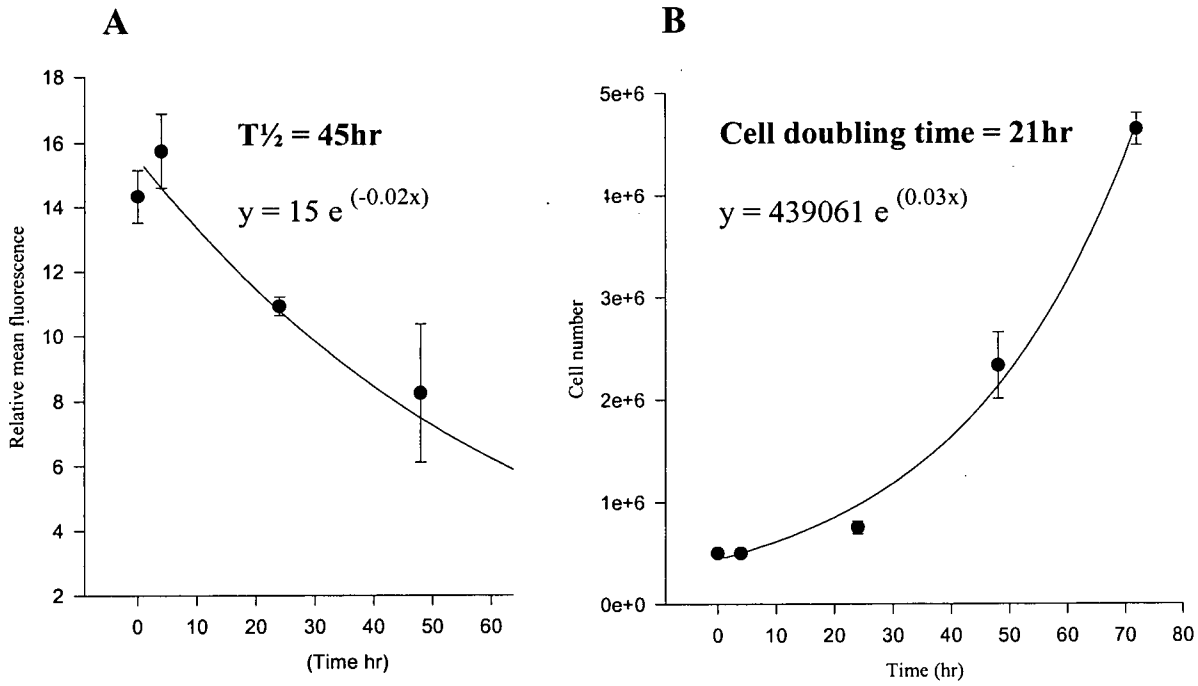

Figure 8A. Loss of pimonidazole adducts after reoxygenation. SiHa cells were incubated in spinner flasks under 50 μg/ml pimonidazole and anoxia for 4hr, and then cultured under ambient oxygen. Mean fluorescence was detected by flow cytometry. Relative values were obtained by division by the mean fluorescence of cells incubated in air-equilibrated medium for each time point. **Figure 8B.** Cell doubling after reoxygenation. Cells from the same experiment were allowed to recover in ambient oxygen *in vitro* to examine the relation between loss of pimonidazole adducts and cell division. Exponential functions were fitted to data points.

result of cell division. Furthermore, the doubling time of 21hr, which is the same for cells under normal conditions, suggests that pimonidazole at 50μl/ml is likely not very toxic.

3B MARKER COLOCALISATION STUDIES

Three different human tumour cell lines, WiDr colon carcinoma cells, SiHa cervical carcinoma cells, and MOO6 glioma cells, were grown as xenografts for use in the following experiments.

3B1 MARKER COLOCALISATION IN XENOGRAFT TUMOURS

Frozen sections from xenograft tumours were incubated with antibodies to HIF-1α and pimonidazole as described, with Hoechst 33342 used as a marker of perfusion. HIF-1α showed a nuclear labelling pattern as expected, and pimonidazole showed a cytoplasmic labelling pattern, confirming no cross-reaction between the two monoclonal antibodies (figure 9). Regarding the pattern of labelling, in all three xenograft types, HIF-1α appeared closer to the Hoechst 33342-labelled perivascular regions than pimonidazole. Unexpectedly, the region binding pimonidazole antibody extended beyond that labelled for HIF-1α. Occasionally hypoxic regions of the tumour showed very low levels of, or lacked altogether only one of the two markers. The colocalisation between HIF-1α and pimonidazole was determined for each xenograft type. The mean colocalised fraction with respect to HIF-1α in SiHa, WiDr, and MOO6 xenografts was 60 ± 11%, 59 ± 17%, and 50 ± 14%, respectively, and the mean colocalised fraction with respect to pimonidazole was 45 ± 13%, 23 ± 9%, and 27 ± 12%, respectively (figure 10).

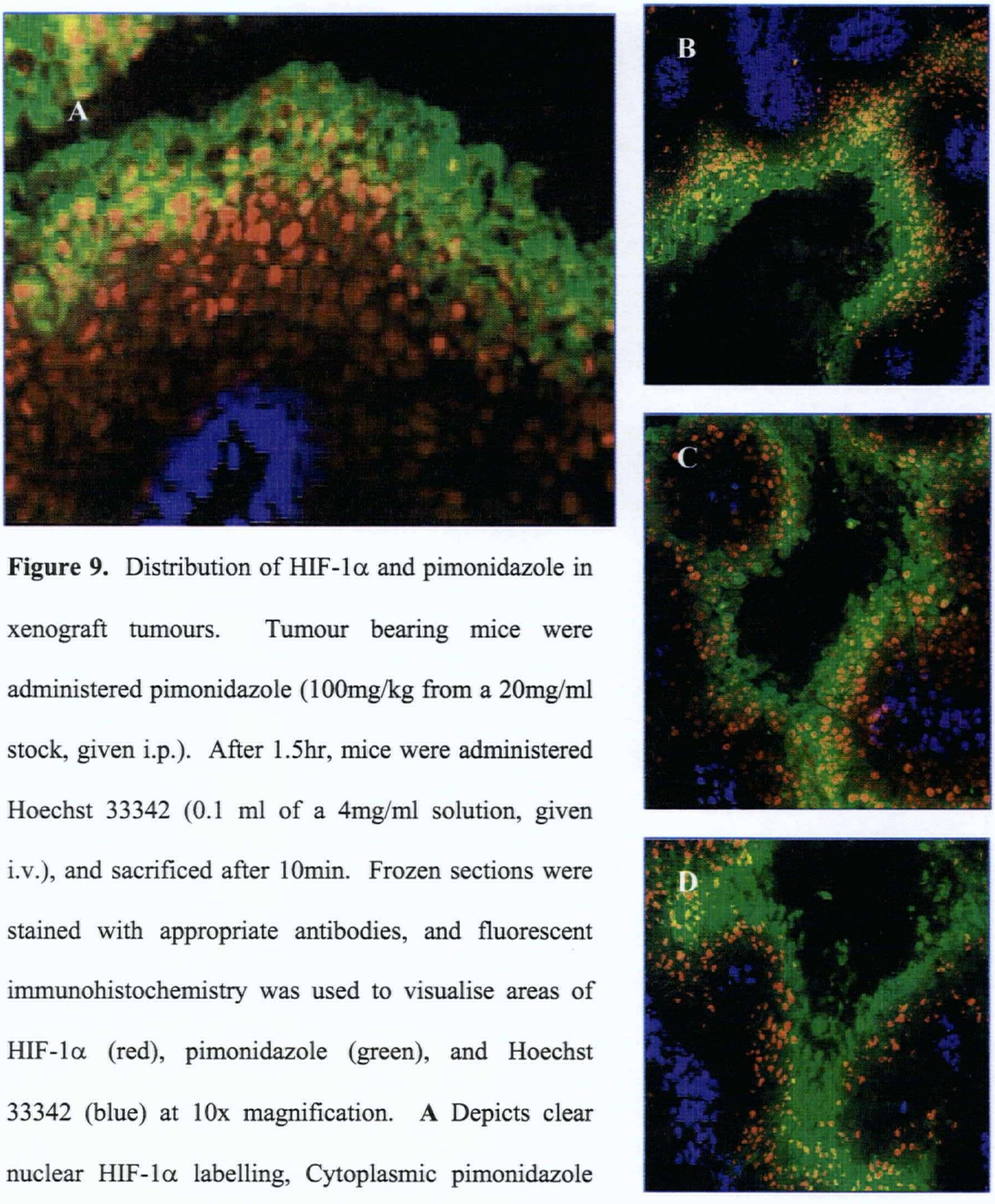

Figure 9. Distribution of HIF-1α and pimonidazole in xenograft tumours. Tumour bearing mice were administered pimonidazole (100mg/kg from a 20mg/ml stock, given i.p.). After 1.5hr, mice were administered Hoechst 33342 (0.1 ml of a 4mg/ml solution, given i.v.), and sacrificed after 10min. Frozen sections were stained with appropriate antibodies, and fluorescent immunohistochemistry was used to visualise areas of HIF-1α (red), pimonidazole (green), and Hoechst 33342 (blue) at 10x magnification. **A** Depicts clear nuclear HIF-1α labelling, Cytoplasmic pimonidazole labelling, and nuclear Hoechst 33342 labelling in a SiHa xenograft tumour. **B**, **C** and **D** represent SiHa, WiDr, and MOO6 xenografts respectively.

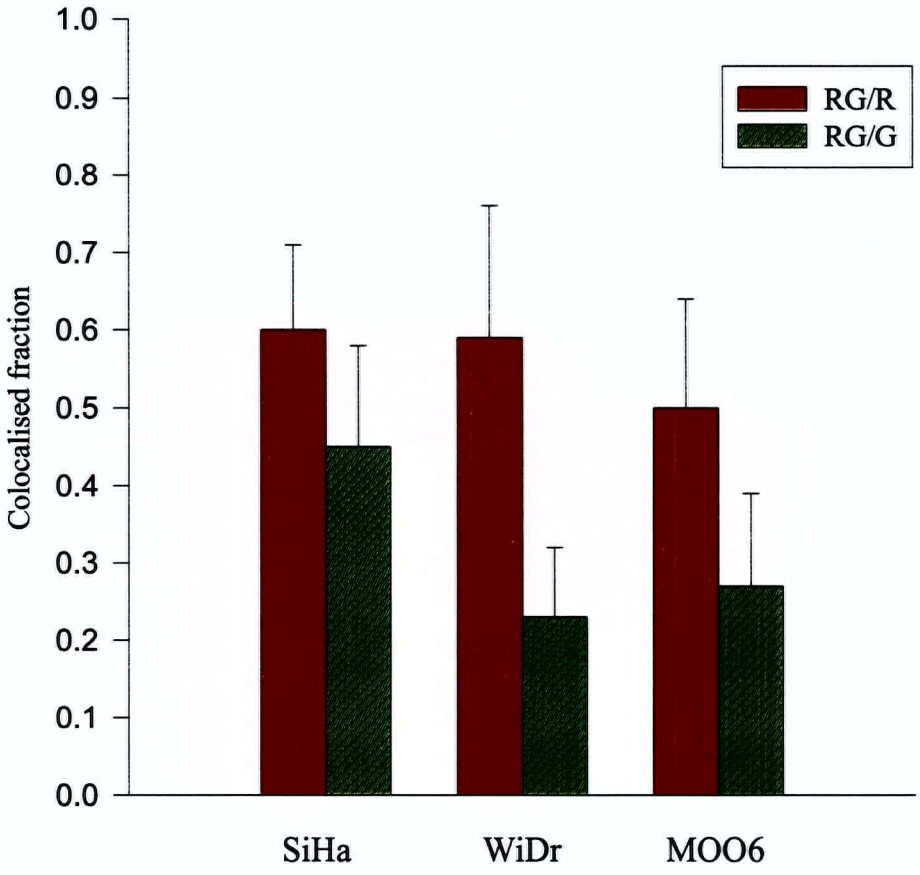

Figure 10. Colocalisation of HIF-1α and pimonidazole in xenografts. Data were obtained by studying antibody staining patterns in SiHa (n=5), WiDr (n=5) and MOO6 (n=5) xenografts using 10x magnification fluorescent images. The fraction colocalised was determined by dividing the number of colocalised pixels of red and green (HIF-1α and pimonidazole respectively: RG) by the total number of red (R) or green (G) pixels (refer to 2G). RG/R represents fraction of total HIF-1α colocalised with pimonidazole, and RG/R represents the fraction of total pimonidazole colocalised with HIF-1α.

No significant difference was observed in the mean colocalised fraction with respect to HIF-1α in the tumour types, but the mean colocalised fraction with respect to pimonidazole in SiHa xenografts was significantly higher than both WiDr and MOO6 xenografts ($p = 0.05$; Tukey-Kramer). It should be noted that given the different localisation of the two markers (nuclear vs. cytoplasmic), the colocalised fraction may have been underestimated. The thickness of the frozen sections (10μ) however, may have compensated for this difference; most cells were imaged in three dimensions, so that the cytoplasmic staining anterior and posterior to that of the nucleus would provide sufficient staining signal to coincide with the latter.

Atypical Marker Patterns

Marker colocalisation studies above revealed occasional hypoxic regions in all three xenograft types where labelling of only one of the two markers was very low or altogether missing. Figure 11A shows an area where HIF-1α labelling occurs in the absence of pimonidazole labelling. The reverse was also observed, where pimonidazole labelling occurred in the absence of HIF-1α labelling (figure 11B). Both of these patterns could be indicative of transient changes in perfusion (transient hypoxia), whereas areas labelled with both markers, as are more commonly observed, would represent primarily chronic hypoxia. Often, HIF-1α and pimonidazole labelling occurred inside areas labelled with Hoechst 33342, possibly indicating a very low oxygen gradient despite plasma flow through the vessel (figure 11C). These patterns however were relatively rare (<5% blood vessels), as observed by others (219), so that they did not greatly contribute to decreases in marker colocalisation.

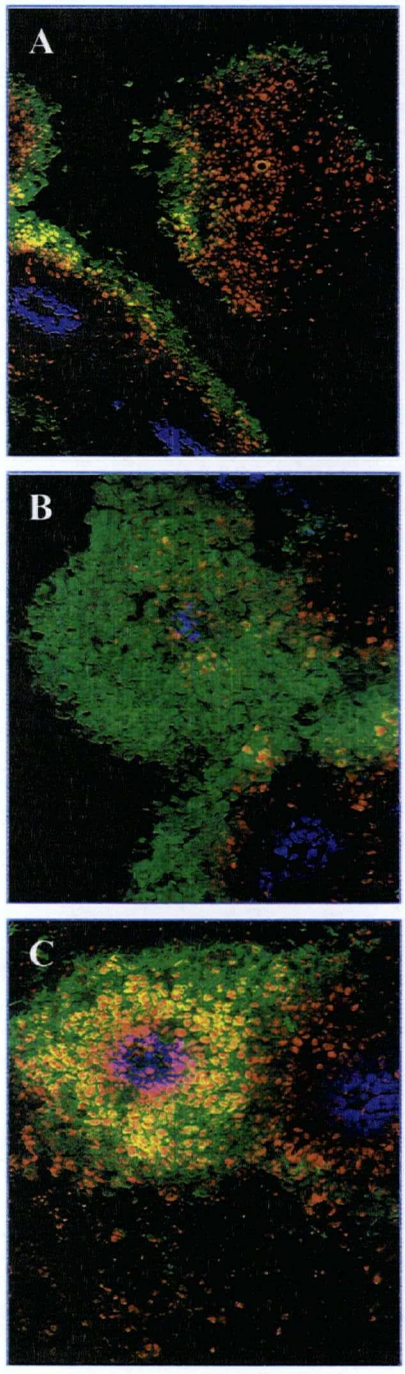

Figure 11. Atypical marker patterns in xenograft tumours. Fluorescent immunohistochemistry was used to visualise areas of HIF-1α (red), pimonidazole (green), and Hoechst 33342 (blue). **A** HIF-1α staining with little pimonidazole labelling and lack of Hoechst 33342 staining (SiHa). **B** Pimonidazole and Hoechst 33342 labelling with little HIF-1α labelling (MOO6). **C** Pimonidazole and HIF-1α labelling very close to the Hoechst 33342 labelled area (SiHa).

3C HIF-1α: OXYGEN-DEPENDENCY AND NUTRIENT REQUIREMENTS

3C1 IN VITRO OXYGEN AND NUTRIENT DEPENDENCE

The lack of HIF-1α labelling in perinecrotic tumour regions was investigated by studying the oxygen and nutrient-dependency of HIF-1α expression. SiHa cultured cells were incubated in spinner flasks for 4hr at various oxygen concentrations. The cells were then removed and HIF-1α degradation was inhibited by adding $CoCl_2$ and placing cells on ice. Figure 12 shows that as oxygen concentration was decreased, the relative amount of HIF-1α increased accordingly, and that the highest level of HIF-1α was seen under anoxic conditions. Cells from the same population were incubated for 4hr at 0% O_2 in serum and glucose-free medium, glucose-free medium with 10% serum, 1% serum-containing medium, and 10% serum containing medium (figure 13). HIF-1α was not observed under the first two conditions, but increased as the percent serum was increased.

3C2 REOXYGENATION OF PERINECROTIC CELLS IN XENOGRAFTS

To test whether the lack of HIF-1α in regions distal to the blood vessels was due to in vivo changes in oxygen, tumour oxygen levels were modified by increased oxygen-breathing; this would increase oxygen diffusion distances and oxygen levels in perinecrotic areas, possibly allowing stabilisation of HIF-1α in these regions. Mice with SiHa xenografts were administered pimonidazole and after 2hr (by which time the pimonidazole should be metabolised and largely eliminated from the blood) were given 60% O_2 to breathe for another 2hr (experimental group), or were left in air for a further 2hr (control group). Mice were then administered Hoechst 33342. The tumours

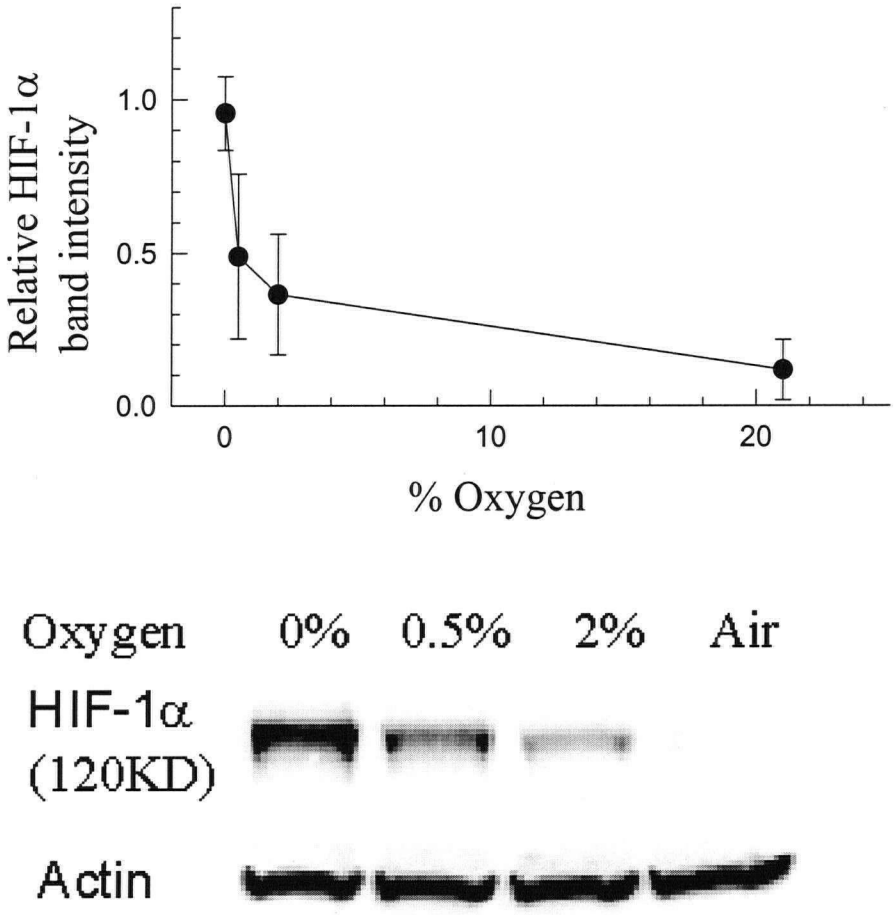

Figure 12. Effect of oxygen on HIF-1α protein level. SiHa cells were incubate in spinner flasks under various oxygen concentrations for 4hr, and the cell lysates subjected to western blot analysis. Band densities were adjusted as described (refer to 2H).

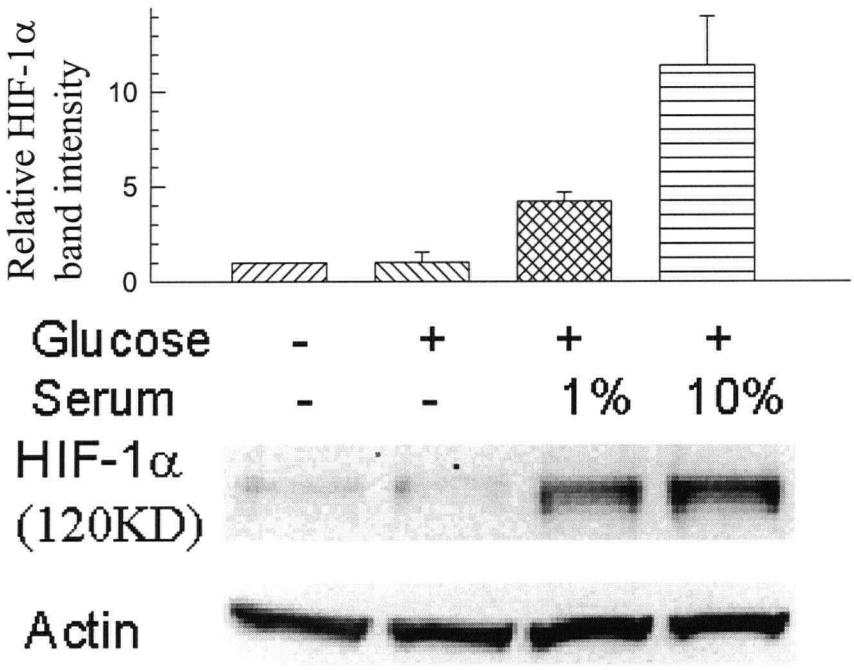

Figure 13. Effect of glucose and serum on HIF-1α protein level. SiHa cells were incubated in spinner flasks at % O_2 for 4hr in glucose-free MEM, or in MEM containing 0%, 1% or 10% FBS. Cell lysates were subjected to western blot analysis and band densities were adjusted as described (refer to 2H).

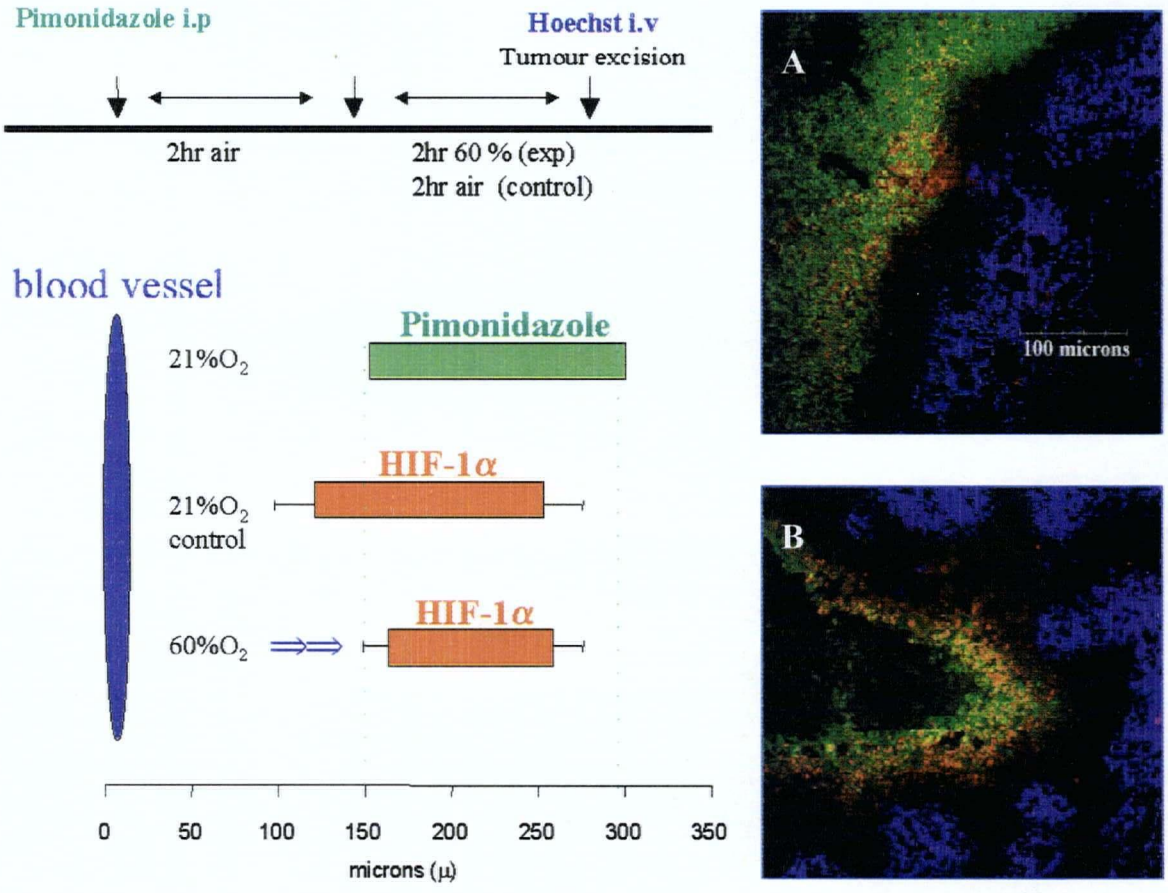

Figure 14. Reoxygenation of distal cells in SiHa xenograft tumours. Tumour bearing mice were administered pimonidazole (100mg/kg at 20mg/ml i.p.). After 2hr, mice were given 60% oxygen (**B**; n=4) or air (**A**: control; n=3) to breathe, administered Hoechst 33342 (4mg/ml 100μl i.v.), and sacrificed after 10min. Fluorescent immunohistochemistry was used to visualise areas of HIF-1α (red) and pimonidazole (green). 10x magnification images were analysed by measuring start and end points of marker-labelled regions with respect to the blood vessel, using histograms of the marker profiles (refer to 2G).

were excised and frozen sections were stained for pimonidazole, HIF-1α, and Hoechst 33342. The average distance from the blood vessels to the cord edge (~300μ) is larger than those normally encountered in most solid tumours (~100-200μ). These large distances are a result of cord selection. Larger cords rather than small ones were selected for the reason that when mice were give 60% oxygen to breath, oxygen diffusion in smaller cords resulted in perinecrotic oxygen concentrations which were likely too high for HIF-1α stabilisation, as indicated by the overall absence of HIF-1α in the entire tumour cord, including regions that had previously bound pimonidazole. Since these perinecrotic regions were of interest in this study, larger cords were necessary so that the level of oxygen in these regions would increase, but would still be low enough to allow HIF-1α stabilisation. In the 60% oxygen-breathing mice, the area stained for HIF-1α was reduced past the region that stained for pimonidazole under ambient air breathing conditions, but still did not extend into the perinecrotic regions (figure 14). This result indicates that increasing oxygen level alone is not sufficient for the stabilisation of HIF-1α in perinecrotic xenograft regions.

3D OXYGEN MODULATION OF XENOGRAFTS VIA GAS-BREATHING

Mice carrying SiHa xenografts were administered pimonidazole and exposed to either air (21% O_2), 10% O_2, or carbogen (95% O_2, 5% CO_2) for 1.5hr. They were then administered Hoechst 33342 and sacrificed after 10min. The tumour was excised and frozen sections were stained for pimonidazole, HIF-1α, and Hoechst 33342 (figure 15). To quantify markers with respect to oxygen changes, 60% O_2 instead of carbogen was used, given that 95% O_2 decreased staining to such an extent that accurate quantification

became problematic. Images were manually thresholded and analysed for the fraction of marker mismatch as already described. The percent area labelled by HIF-1α showed a significant decrease ($p = 0.05$; Tukey-Kramer) with increase in oxygen. The percent area labelled by pimonidazole however showed a significant decrease ($p = 0.05$; Tukey Kramer) from air-breathing to 60% O_2-breathing mice, but shows no significant difference from air breathing to 10% O_2-breathing mice (figure 16). Changing oxygen-breathing conditions also affected colocalisation ratios (figure 17). The colocalised fraction with respect to HIF-1α significantly differed ($p = 0.05$; Tukey Kramer) between the air breathing and the 10 and 60% O_2-breathing conditions and the colocalised fraction with respect to pimonidazole differed significantly ($p = 0.05$; Tukey-Kramer) between the 10% O_2-breathing and the air and 60% O_2-breathing conditions. Lack of a consistent pattern in these changes suggests these differences to possibly be the result of inconsistent increase in the percent pimonidazole staining upon decrease in oxygen level.

3E HYPOXIC CELL HALF-LIFE IN XENOGRAFT TUMOURS

Mice with SiHa xenografts were administered pimonidazole and at times up to 48hr later, were administered Hoechst 33342 10min before sacrifice. Frozen sections were stained with antibodies against HIF-1α and pimonidazole and analysed for colocalised fraction. Fluorescent images showed that over time, mismatch between the two markers increased and pimonidazole-labelled cells appeared to move further into necrotic regions (figure 18). Furthermore, with time after pimonidazole administration, there was an increase in areas lacking one marker all together (figures 19A, B and C).

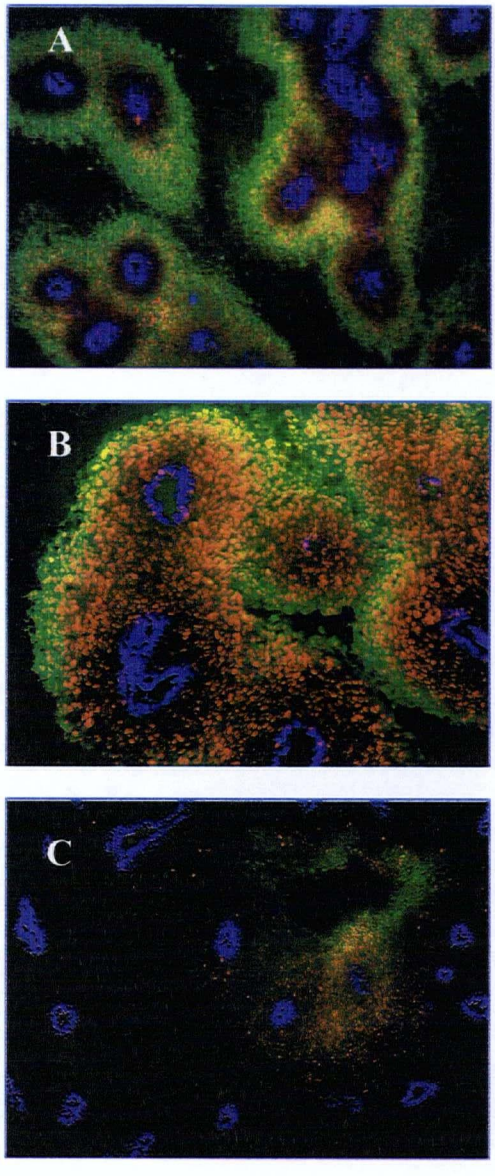

Figure 15. Oxygen modulation of SiHa xenograft tumours. Tumour bearing mice were administered pimonidazole (100mg/kg at 20mg/ml i.p.) and were given **A**: air (21% O_2,) **B**: 10% O_2 , or **C**: carbogen (95% O_2, 5% CO_2,) to breathe. After 1.5hr, mice were administered Hoechst 33342 (4mg/ml 100µl i.v.), and sacrificed after 10min. Fluorescent immunohistochemistry was used to visualise areas of HIF-1α (red), pimonidazole (green), and Hoechst 33342 (blue).

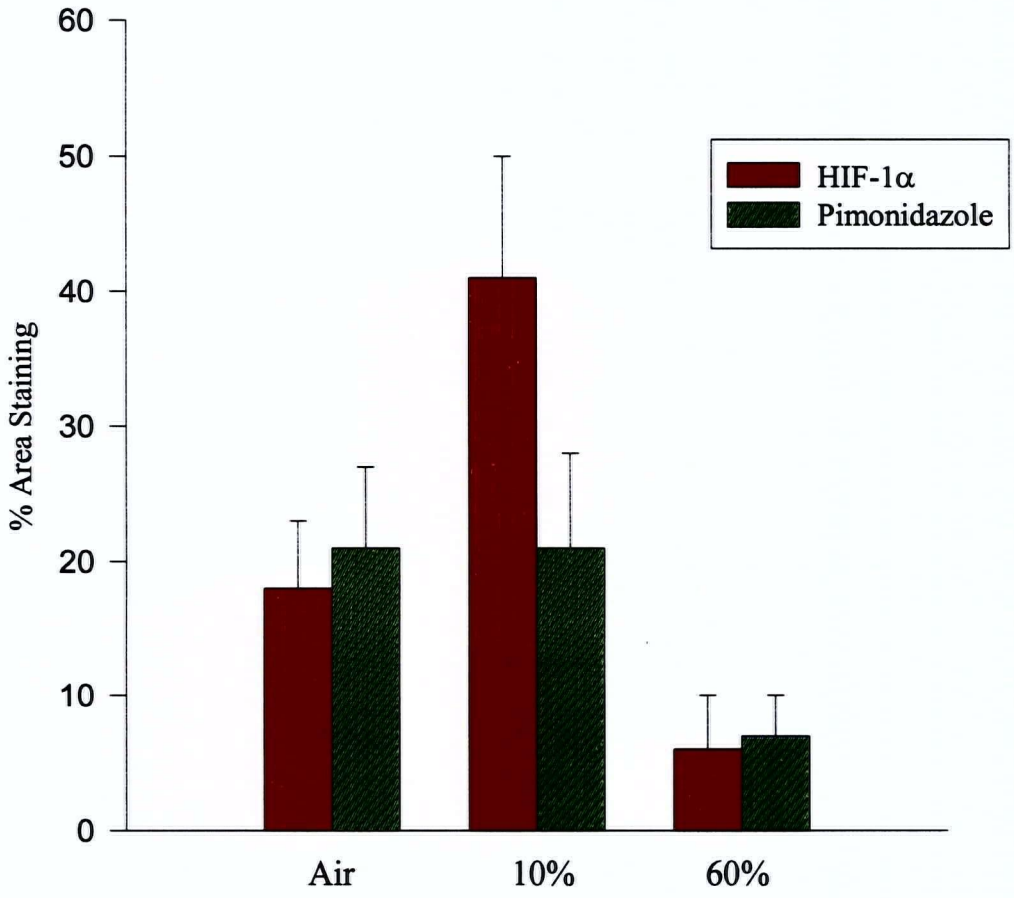

Figure 16. Effect of oxygen modulation on percent area staining in xenografts. Tumour bearing mice were exposed to 10% O_2 (n=3), air (21% O_2; n= 5) and 60% O_2 (n=3) for 1.5hr. 10x magnification fluorescent images were analysed to obtain the number of red pixels (HIF-1α) and green pixels (pimonidazole) over the total number of pixels to obtain % area staining.

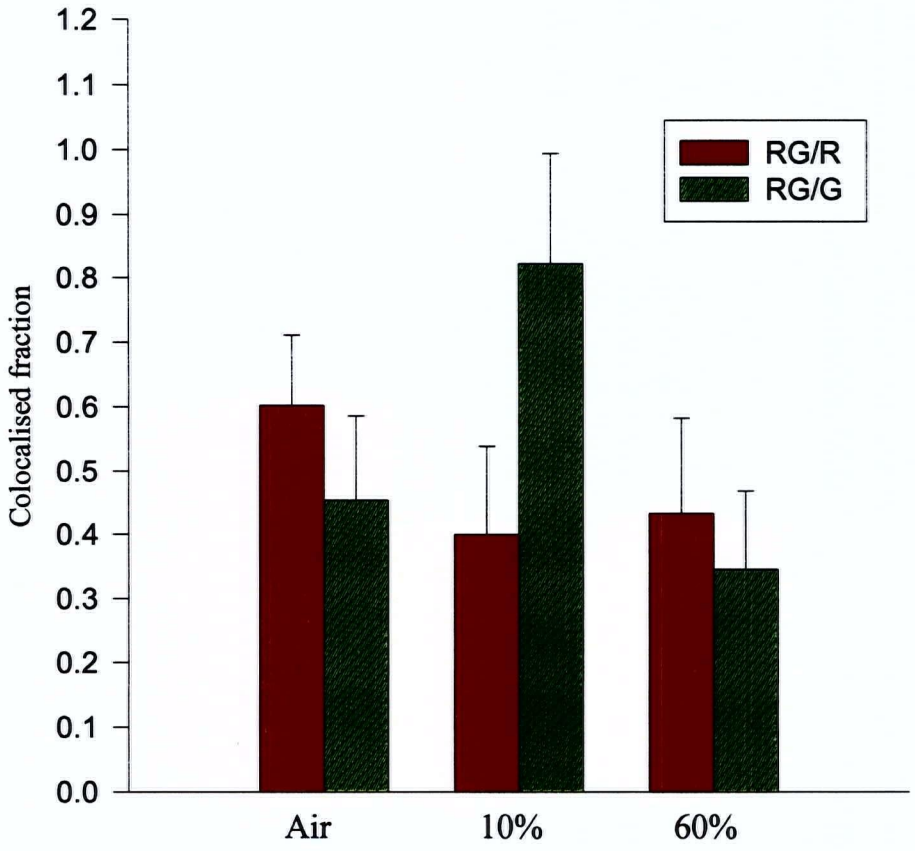

Figure 17. Effect of oxygen modulation on marker colocalisation in xenografts. Tumour bearing mice were exposed to 10% O_2 (n=3), air (21% O_2; n= 5) and 60% O_2 (n=3) for 1.5hr. Data were obtained by studying mismatch patterns using 10x magnification fluorescent images. The fraction colocalised was determined by dividing the number of colocalised pixels of red and green (HIF-1α and pimonidazole respectively: RG) by the total number of red (R) or green (G) pixels (refer to 2G). RG/R represents the fraction of HIF-1α colocalised with pimonidazole, and RG/R represents the fraction of pimonidazole colocalised with HIF-1α.

Figure 19D shows an area where pimonidazole appears to have accumulated in perinecrotic areas, and 19E a region where very little pimonidazole is observed, very likely due to loss of necrotic tissue upon slide processing. Necrotic cells were distinguished from viable cells based on morphology. In viable hypoxic regions, pimonidazole shows cytoplasmic and nuclear staining and appears to cover nearly the whole cell (figure 19A). In necrotic areas however, pimonidazole shows a "honey-comb" morphology, where the nucleus appears unlabelled and the staining looks moe membranous (figures 19B, C, and D). The rate at which pimonidazole stained cells moved into regions of necrosis was taken as a measure of hypoxic cell life-time, given that cells capable of metabolising pimonidazole must have been viable at the time of pimonidazole administration. Hypoxic cell half-life was obtained by measuring changes in the fraction of HIF-1α colocalised with pimonidazole, to measure the rate at which pimonidazole moved away from the HIF-1α labelled region (considered viable) to regions of necrosis. HIF-1α levels remained constant throughout the images at the various times, and did not contribute to changes in co localised fraction. Images were manually thresholded and analysed for the fraction of marker mismatch as already described (2G). The hypoxic half-life was found to be 16hr (figure 20).

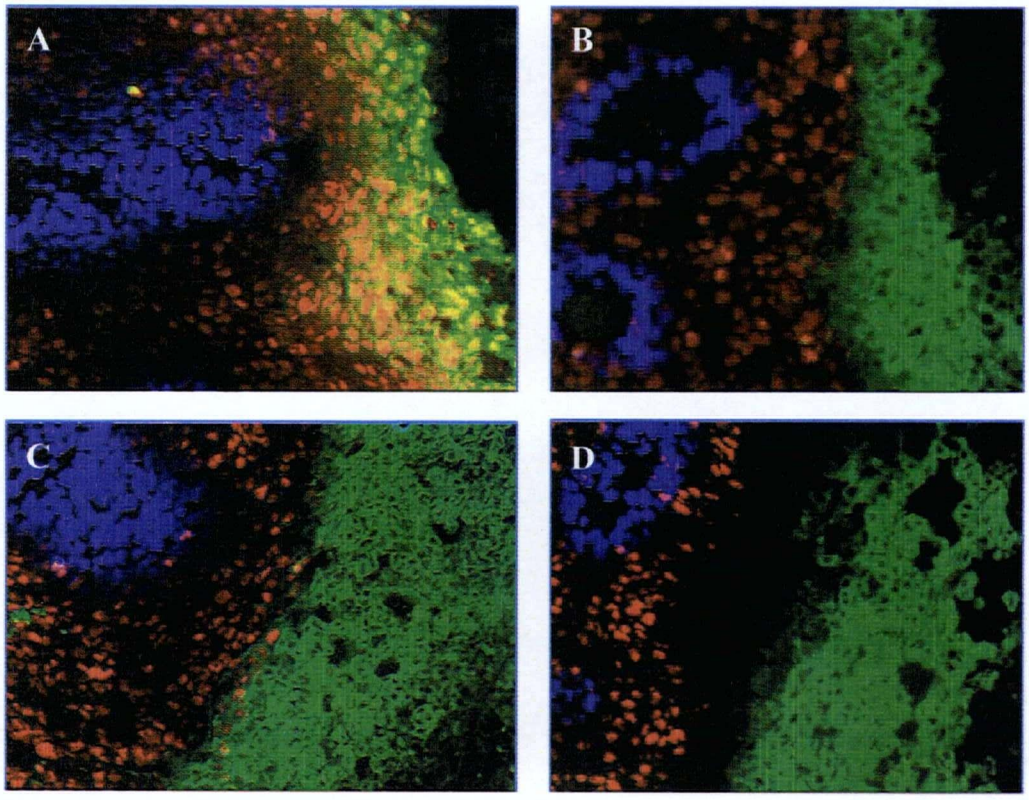

Figure 18. Changes in colocalisation with time after pimonidazole administration. Tumour bearing mice were administered pimonidazole 1.5hr (**A**), 12hr (**B**), 24hr (**C**), and 48hr (**D**) before biopsy, and the mismatch between pimonidazole and HIF-1α was studied as a function of time.

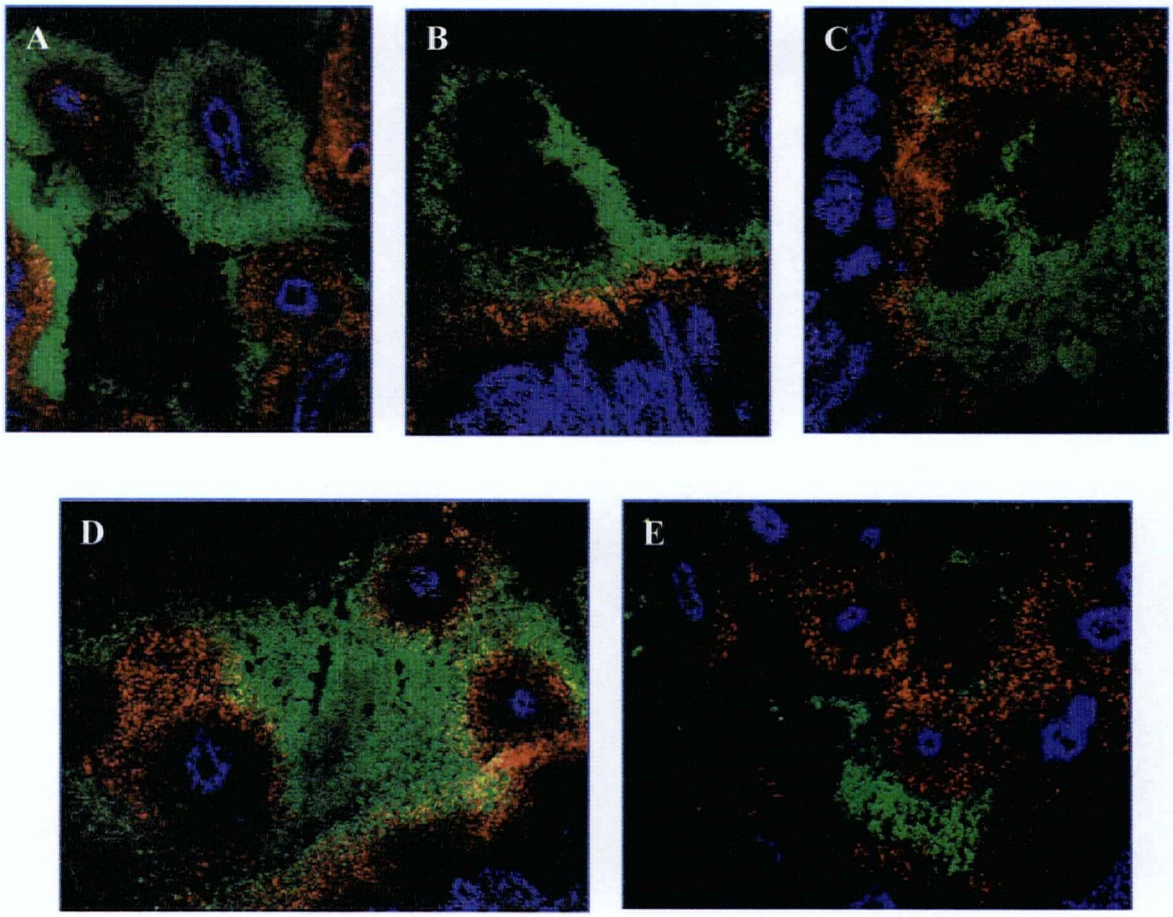

Figure 19. Atypical marker patterns with time after pimonidazole administration. Fluorescent immunohistochemistry was used to visualise areas of HIF (red), pimonidazole (green), and Hoechst 33342 (blue). **A, B,** and **C** reveal very typically observed areas of mismatch in xenografts excised 12, 24, and 48hr after pimonidazole administration, respectively. **D** and **E** show the accumulation of pimonidazole-labelled cells in obvious necrotic areas, and the loss of pimonidazole labelling due to slide processing respectively, in xenografts excised 24hr after pimonidazole administration.

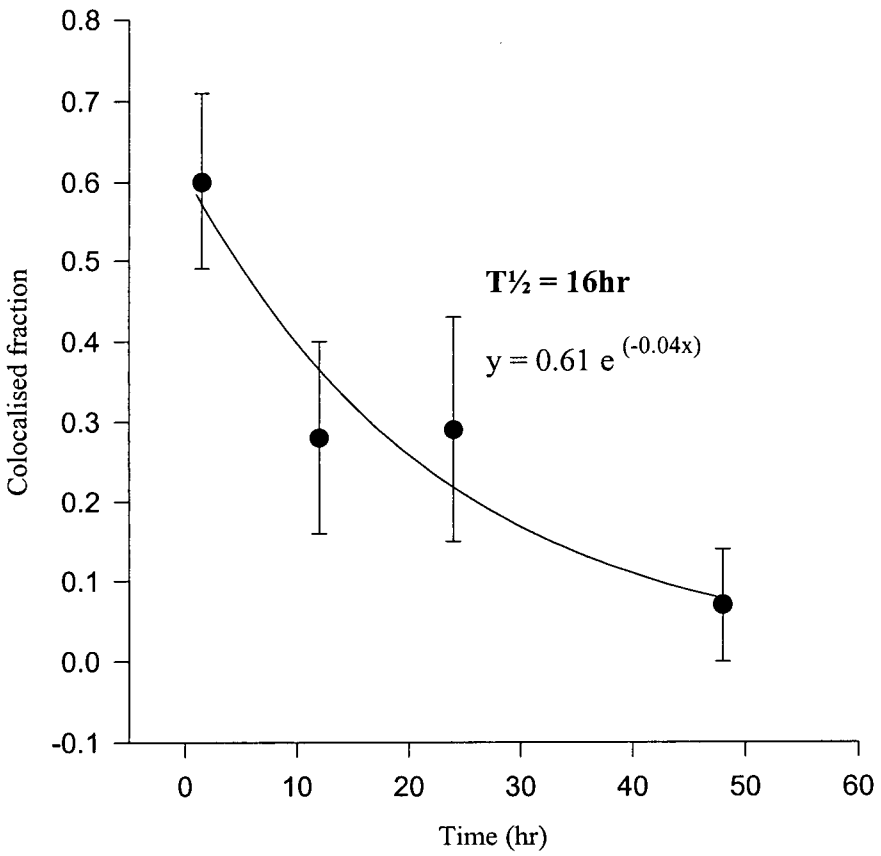

Figure 20. Hypoxic cell half-life in xenograft tumours. Tumour bearing mice were administered pimonidazole at 1.5hr and tumours were excised up to 48hr later. The colocalised fraction with respect to HIF-1α was determined as described (2G). Each point shows the mean and standard deviation for up to 8 sections per tumour for 3-5 tumours. An exponential function was fitted to data points.

3F COMPARISON OF PATIENT BIOPSIES AND XENOGRAFT MODELS

Having established the staining protocols and kinetics for the human tumour xenografts, a feasibility study was performed using frozen sections obtained from biopsy samples of patients with cancer of the cervix being treated at the B.C. Cancer Agency. Patients were part of a study headed by Dr. Christina Aquino-Parsons to examine expression of pimonidazole and correlation of this marker with outcome. Patients were administered pimonidazole 24hr before biopsy, and the biopsy was placed in ice-cold buffer, returned to the Research Centre on ice and immediately frozen. Two consecutive sections were stained for HIF-1α and pimonidazole, and for pimonidazole and CD31 respectively. Images from the two sections were superimposed using the pimonidazole staining pattern, and a triple stained image was then constructed. Figure 21 shows that the patient biopsy displayed similar patterns of HIF-1α and pimonidazole staining as the xenograft tumours. The amount of mismatch between the two markers, however, appears greater than that seen for the cervical xenografts, possibly due to the 24hr separation between pimonidazole administration and biopsy.

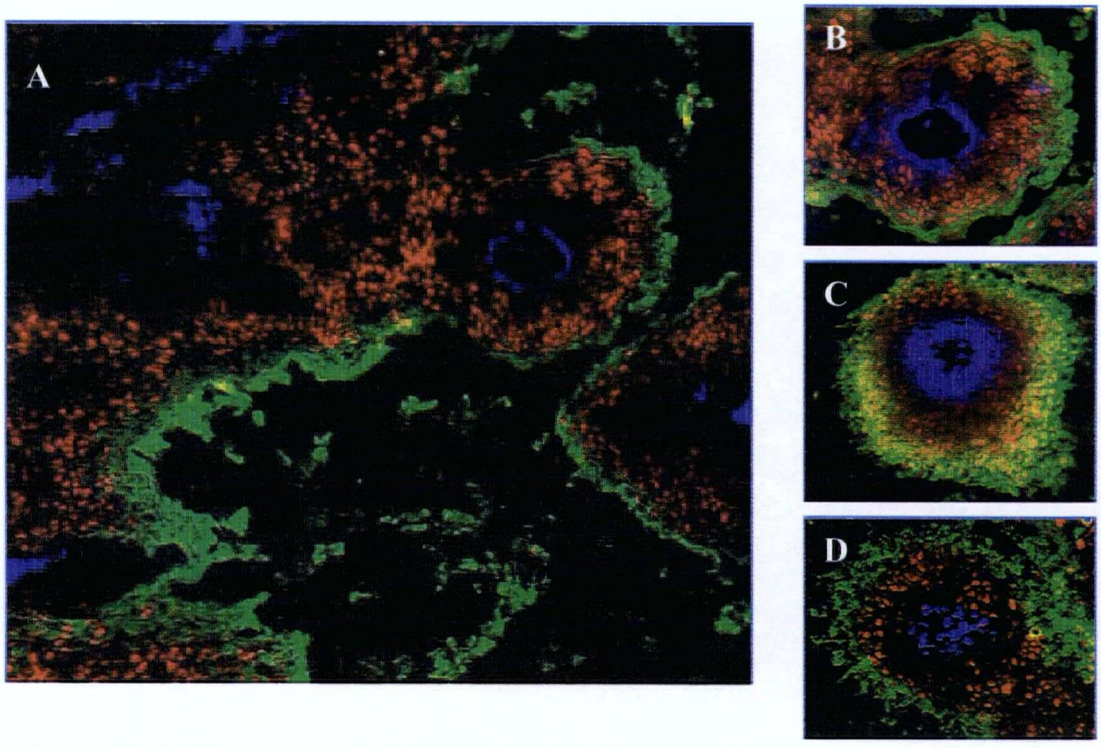

Figure 21. The distribution of HIF-1α and pimonidazole in cervical tumour biopsies. **A.** Patients were administered pimonidazole (500mg/m^2 i.v.) 24hrs before biopsy. Fluorescent immunohistochemistry was used to visualise areas of HIF-1α (red) and pimonidazole (green), and the vascular marker CD31 (blue). **B** is an image of a cervical tumour biopsy cord, and **C** and **D** are SiHa cords from xenografts excised 1.5hr and 24hr after pimonidazole administration, respectively.

4. DISCUSSION

4A MARKER KINETICS

The nature of hypoxia, whether chronic or transient, poses different challenges in both tumour progression as well as in therapy, and may require different strategies for treatment. Therefore markers with kinetics that, when applied together, allow one to identify these two forms of hypoxia, would be advantageous. Kinetics studies of HIF-1α in SiHa cells revealed that the protein is quickly stabilised (half-max ~2hr) and rapidly degraded (t½ <1min). In accordance, other studies reveal HIF-1α half-life to be on the order of minutes (220, 221), whereas there appear to be differences in kinetics of development. Similar to the results from this study, Vordermark et al, using U87 MG human glioblastomas observed HIF-1α levels to peak at 6hr and to maintain these levels up to 18hr (222), and in Fadu and HT1080 cells, to increase sharply at 1hr and continue to increase up to 24hr (223). In contrast, Jewell et al. (221), studying HeLaS3, cells observed a half-maximum level of HIF-1α as early as 13.3min and a maximal level at 1hr. A possible explanation for these variations may be cell-type differences (224), or differences in assay technique; HIF-1α is a very labile molecule, such that small differences in protocol can affect its stability. As observed from SiHa cells, the quick response to changes in oxygen make this marker an ideal candidate for the study of transient changes in perfusion. Although pimonidazole adducts form very quickly in the absence of oxygen (half-max = 20-40min), they are lost very slowly (t½ ~2dy). Therefore once pimonidazole adducts are formed, they will not respond to subsequent changes in oxygen. These characteristics allow pimonidazole to be predictive of hypoxic past, and when combined with the HIF-1α, to allow the determination of areas where

only one of the markers maybe mainly present (transient hypoxia), and regions where both markers are present (mostly chronic hypoxia).

4B MARKER COLOCALISATION

Fluorescent imaging revealed HIF-1α labelling to be strictly nuclear and focal, and pimonidazole labelling to be focal and cytoplasmic. Furthermore, mismatch was found to occur close to the blood vessel, where HIF-1α was stabilised in the absence of pimonidazole binding. The principle explanation for this is that pimonidazole requires lower oxygen levels (~1%) for binding than does HIF-1α (~2%), and an additional possibility may be that HIF-1α expression is higher in more metabolically active cells, located closer to the blood vessels. Mismatch was also observed at the perinecrotic edge, where pimonidazole adducts were found in the absence of HIF-1α. Possible explanations for this observation are discussed in section 4D. Areas showing atypical marker patterns, defined as those deviating from the normal pattern as shown in figure 9, were a further source of mismatch. In all three xenograft types, there were occasional cords where labelling of one or the other marker was low or absent, suggesting that transient changes in perfusion may have occurred in the short time frame of about 1-2hr. However, tumour cords are three dimensional, and so the contribution of out-of-plane blood vessels cannot be excluded. The two most common patterns of this type seen were: a) HIF-1α labelling in the presence of little or no pimonidazole and an absence of Hoechst 33342, and b) pimonidazole labelling close to the centre of the tumour cord in the presence of Hoechst 33342 but little or no HIF-1α labelling. The first pattern may be suggestive of a tumour cord having been well perfused at the time of pimonidazole administration and

later becoming much less perfused, possibly due to vessel closure. This would allow HIF-1α to become stabilised very near the centre of the cord in the absence of both pimonidazole and Hoechst 33342. The latter pattern may be indicative of the recent reopening of the blood vessel, where the tumour cord may have been sufficiently hypoxic at time of pimonidazole administration, but may have become reperfused sometime before Hoechst 33342 administration. This would result in most of the HIF-1α being degraded, whereas pimonidazole, which does not respond to subsequent oxygen changes, would remain stable. The most commonly observed atypical pattern in the xenografts occurred where both HIF-1α and pimonidazole maintained their normal pattern relative to each other, but labelled very near, and in the case of HIF-1α, within a brightly-labelled Hoechst 33342 area. This is suggestive of the existence of hypoxia in functional blood vessels, possibly due to a steep longitudinal oxygen gradient inside the vessel, or the presence of plasma channels, having a low supply of red blood cells.

Despite these occasional patterns, studies revealed that the two markers generally showed a reasonable degree of colocalisation, as observed in three different xenograft types. This result agrees with the findings of Vukovic et al. (225) who showed that overlap between HIF-1α and EF5, another exogenous hypoxic marker, was statistically significant in SiHa xenografts, although associations in the present study were stronger. Vordermark et al. (222), however, found low colocalisation between HIF-1α and pimonidazole in U87 MG glioblastoma xenografts using a double staining protocol for flow cytometry. Discrepancies may result from differences in methods used (flow cytometry vs. fluorescence imaging), as well as thresholding techniques, which are to some extent subjective.

The use of endogenous markers such as HIF-1α would allow the study of archival material and would be more convenient and less expensive, given no administration of costly drug would be necessary. It would, therefore, be useful to assess the hypoxic marker pattern in the xenograft model in relation to the pattern seen in the patient biopsies, as will be discussed in section 4E.

4C RESPONSE TO OXYGEN MODULATION

To see how our xenograft model system responded to changes in oxygen, mice bearing xenograft tumours were subjected to carbogen, ambient oxygen, and 10% O_2-breathing. The response of the system was very significant in the carbogen -breathing mice to the extent that the range of labelling of both markers decreased dramatically and in many regions, disappeared completely. For this reason, 60% O_2 rather than carbogen was used in order to allow quantification of marker labelling, given that the latter images contained so little of the markers that analysis of representative sections became problematic. In the 60% O_2-breathing mice, the system showed a significant response, and the labelling of both markers decreased approximately to the same extent (figure 16). In the 10% O_2-breathing mice, however, the range of labelling of HIF-1α significantly increased, while that of pimonidazole remained largely unchanged. Similar observations were made by Vordermark et al. (222) who showed in flow cytometry studies performed on U87 glioblastoma xenografts that the percentage of pimonidazole-positive cells did not increase following 10% oxygen-breathing, despite the increase in the percentage of HIF-1α positive cells. Olive et al. (226) showed in SCC7 xenograft tumours using a flow cytometric assay, that ~15% of cells were labelled under air-breathing, ~35% labelled

under 10% O_2-breathing, and ~90% in clamped tumours. The flow cytometry data suggests 10% O_2-breathing to have a much lesser effect on hypoxic fraction than clamping. Interestingly, Raleigh et al. (227), using fluorescence imaging in C3H mammary xenograft tumours, showed that clamping greatly increased the extent of pimonidazole staining from ~10% in air-breathing to ~40%, but that immunostaining did not completely cover perivascular regions. This again suggests, in light of the flow cytometry data, that since clamping only produced 40% immunostaining, decreasing oxygen breathing from 21% (air) to 10% would not have had a drastic effect in the percentage of pimonidazole labelling (on a tumour that is already quite hypoxic) using a fluorescence imaging method. One possible explanation for these results may be that reducing oxygen-breathing by half produces a greater population of intermediately hypoxic than highly hypoxic cells; given that vascular oxygen levels in tumours average from 2-3%, a drop from 20% to 10% in oxygen breathing may easily push vascular oxygen levels below 2%, allowing HIF-1α to be stabilised, but may not be as effective in dropping oxygen levels below 1% in order to allow pimonidazole adduct formation. Another explanation may involve the concentration of pimonidazole administered to mice. Durand et al. (215) observed that the percentage of pimonidazole-positive tumour cells increased as a function of dose in the range of 0-200mg/kg. In the current study and that of Vordermark et al., pimonidazole was given i.p. at 100mg/kg, and in the study by Raleigh et al., the dose was administered i.v. at 60mg/kg. The possibility thus may exist that the doses used in these studies may have been insufficient to label the increased number of hypoxic cells. Mismatch studies revealed that the amount of overlap between the markers was not maintained among the different oxygen-breathing conditions,

although there were greater similarities observed between the air-breathing and 60% O_2-breathing mice. This likely reflects differences in the oxygen thresholds of the markers, and further suggests that the relationship between change in the number of intermediately and highly hypoxic cells as a function of oxygen-breathing levels may not be spatially and/or numerically proportional.

4D HIF-1α: OXYGEN AND NUTRIENT EFFECTS

The observation that pimonidazole adducts form in perinecrotic areas in the absence of HIF-1α led us to question whether certain conditions in these regions are suitable for HIF-1α stabilisation. Jiang et al. (228) have previously suggested that the stabilisation of HIF-1α peaks at 0.5% O_2 and diminishes under anoxic conditions. It was therefore necessary to investigate whether anoxia in perinecrotic regions may be the reason for the absence of HIF-1α. However, both our *in vitro* and *in vivo* studies suggest that this is unlikely, since HIF-1α showed greatest stabilisation at 0% O_2, and when the oxygenation of perinecrotic regions of xenograft tumours was increased by having mice breath 60% O_2, HIF-1α still failed to appear in these regions. The lack of agreement in the *in vitro* results may be due to differences in experimental design. Whereas the experiments in this study were performed in spinner culture flasks, Jiang et al. used vessels wherein cells, immersed in a thin film of medium, were equilibrated with gasses. It is possible that these cells may have exhausted their nutrient supplies given the 4hr incubation time and the small amount of medium available to them, so that not only hypoxia, but also lack of nutrients may have contributed to the observations. We next investigated nutrient requirements for HIF-1α stabilisation. *In vitro* experiments under

anoxia revealed that the decrease in stabilisation may be due to lack of serum factors and glucose in these regions. With respect to serum levels, this observation appears reasonable given that certain growth factors are responsible for the transcriptional and translational induction of the steady state level of HIF-1α via the PI3K and MAPK pathways respectively. Furthermore, although glucose deprivation alone did not seem to affect HIF-1α stabilisation, its combination with serum factors may be important in HIF-1α induction; glucose levels in anoxic regions would be most critical, given that the lack of oxygen forces cells to rely on anaerobic glycolysis alone, which is a much less efficient method of ATP production than oxidative reduction. Therefore, in the absence of both serum and glucose, the production of HIF-1α may be very costly and the upregulation of other genes by HIF-1 may not be possible with limited cellular resources. Pimonidazole, nevertheless, which is easily metabolised by cells with little cost in energy, led to adduct formation in nutrient-deprived perinecrotic cells, although there is evidence that cells incubated under very low glucose levels (0.015mM) bind 2.5 times less misonidazole, a chemically related drug (229). This raises the question of whether hypoxic perinecrotic cells marked by pimonidazole are of radio-biological significance; given that HIF-1α is a major survival protein under hypoxia and is believed to be a prognostic marker for survival, cells that have ceased to produce HIF-1α may be very sick and of little threat to repopulation following therapy. It is possible, however, that upon clearance of normoxic cells, these perinecrotic cells, upon reperfusion, may recover sufficiently to once more produce HIF-1α. There are difficulties in investigating this theory *in vivo*. Flow cytometric analysis of disaggregated SiHa xenografts, where pimonidazole-labelled cells were sorted based on intensity of Hoechst 3334 staining,

revealed that cells with the lowest Hoechst 3334 staining (i.e., pimonidazole-labelled cells furthest from the blood vessel) were able to divide and form colonies when plated (230). This cell population, however, may not represent the perinecrotic pimonidazole labelled cells in the xenograft, since these could have been lost upon enzyme digestion. Perhaps one approach is to use a double staining protocol where cells stained for pimonidazole and not HIF-1α are sorted, but the problem arises that upon homogenisation of the xenograft, the resultant reoxygenation would lead to HIF-1α degradation, and even minimal loss in the presence of $CoCl_2$ may make the data difficult to interpret. Thus whether this population of cells is relevant to therapy remains unknown and will impact on the interpretation of hypoxia marker binding in clinical samples.

4E HYPOXIC CELL HALF-LIFE AND RELATION WITH PATIENT BIOPSIES

To see how well the xenograft model system represented patient biopsies, cervical tumour biopsies from two patients were stained for HIF-1α, pimonidazole, and CD31. The pattern seen in the patient biopsies was very similar to that observed in the xenografts, where HIF-1α and pimonidazole showed focal nucleic and cytoplasmic labelling respectively, both occurring at a distance from blood vessels. Although the spatial patterns of HIF-1α and pimonidazole were maintained with respect to the blood vessels, there was little overlap between the two markers; HIF-1α was expressed closer to the blood vessels as expected, but pimonidazole appeared to be present further out along the edges of the tumour cord. One possibility for this lack of overlap could be the 24hr time-period between administration of pimonidazole and biopsy; dividing tumour

cells from the centre of the cord may have pushed the once viable pimonidazole-labelled cells further into regions of perinecrosis and necrosis. To investigate this, mice with SiHa xenografts were administered pimonidazole 1.5, 12, 24, and 48hrs prior to tumour excision. Images from these xenografts revealed that longer intervals between pimonidazole administration and tumour excision caused a decrease in the degree of overlap between the two markers, and that pimonidazole-labelled cells appeared to be progressively driven into necrotic areas. Accumulated changes in perfusion resulted in even greater mismatch between the two markers. It was also observed that on some slides, necrotic areas were lost during the staining process, consequently resulting in the loss of a considerable percentage of pimonidazole-labelled cells. Indeed the colocalised fraction with respect to HIF-1α decreased from ~60% at 1.5hr to ~30% at 24hr, and ~7% at 48hr. One concern in these studies was that the plasma half-life in humans is considerably longer than that in mice (6hr vs. 30min) so that pimonidazole is available and metabolised over a longer period of time. Nevertheless a large degree of mismatch was observed even at the 12hr time point, so that the longer plasma half-life of pimonidazole does not compensate for the long wait period between pimonidazole administration and biopsy. Furthermore, colocalisation between the 12hr and 24hr time points was very similar, which may owe to the fact that mice at the 12hr time point were administered pimonidazole overnight, and murine rates of metabolism and blood flow increase nocturnally (231, 232). Overall, the hypoxic half-life in SiHa xenografts was measured to be ~16hr. This result agrees with those of Durand et al. who, using flow cytometric measurement of pimonidazole labelling in SiHa xenografts, found a tumour cell half-life of ~4dy (233), and an average hypoxic cell half-life of ~17hr (unpublished

data). Ljungkvist et al., using a fluorescent imaging techniques with two different chemical hypoxic markers, found hypoxic turnover rates to vary between tumour types, and to be related to both the organisation of hypoxic cells as well as their potential doubling times (in press).

In an experiment conducted on patients with squamous cell carcinoma of the head and neck, Janssen et al. (234) found no significant colocalisation between HIF-1α and pimonidazole. In their study, nuclear HIF-1α staining was observed in 0-18% of the tumour tissue, and colocalisation with respect to HIF-1α varied from 0.02-25%. Furthermore, from the 6 evaluable tumours, HIF-1α labelling was greatest distal from the blood vessel in only 1. Nevertheless, Aebersold et al. (191) in a study of 98 patients with squamous cell cancer of the oropharynx found focal expression of HIF-1α distal from the blood vessel in 65% of the biopsies, where as diffuse staining independent of vessel proximity was observed in 35%. Other studies have also found increased focal expression of HIF-1α distal from the blood vessels (235, 236). The very low fraction of biopsies having focal staining in Janssen's study therefore may be the result of a small sample size. The diffuse HIF-1α staining observed in both studies may be due to improper handling of biopsies, since the material becomes hypoxic upon removal, and HIF-1α stabilises within minutes of hypoxic exposure. A further reason may be the genetic heterogeneity of the biopsies, where in some tumours, pathogenic pathways involved in HIF-1α regulation may be active. The low colocalisation of HIF-1α and pimonidazole in the above study may also be due to the patients having been administered pimonidazole the day before biopsy, which may, as observed in the current study, result in even less overlap between the two markers.

Evidence from xenograft studies, as well as results obtained from a small number of cervical cancer biopsies in our study suggest that HIF-1α may be a good endogenous marker for the detection and quantification of hypoxia in cervical tumours, provided care is taken to promptly fix or freeze tumours after biopsy. Results also indicate that waiting too long after administration of pimonidazole to take a biopsy may provide an inadequate representation of the hypoxia in the tumour, and may lead to underestimation if pimonidazole-labelled necrotic areas are lost during slide processing. The recommendation is therefore made that if possible, biopsies be taken no more than 12hr following pimonidazole administration. This is the time course typically used by the Nordsmark et al. (237), so it will be of interest to compare our results in an ongoing pimonidazole study with theirs. A larger study examining the relationship of HIF-1α and pimonidazole in cervical cancer tumours would be furthermore necessary to properly assess the suitability of the use of HIF-1α as a hypoxia marker in these patients.

CONCLUSIONS

Given the importance of hypoxia in tumour progression and the obstacles it poses to therapy, effective methods to measure hypoxia in order to identify patients who would benefit most from hypoxia-directed therapies should be established. The present study supports the use of HIF-1α as reliable endogenous hypoxic marker in cervical tumours. Xenograft models reveal substantial overlap in antibody staining of HIF-1α and pimonidazole, and also suggest that HIF-1α may be a more immediate representation of the hypoxia within a tumour due to its rapid stabilisation under anoxia and rapid loss upon reoxygenation. In considering whether HIF-1α and pimonidazole label the same cells within a tumour, it is apparent from these results that mismatch between these markers is related not only to differences in oxygen dependency of binding/expression, notably in perivascular regions, but also to differences in nutrient requirements for binding/expression, notably in perinecrotic regions. A further consideration is that mismatch can occur if there is a long delay between pimonidazole administration and biopsy. Regions labelled with pimonidazole can progress quite quickly into areas of necrosis. The type of hypoxia within a tumour is also of great importance since transient and chronic hypoxia may present different challenges upon the effectiveness of tumour therapy, as well as choosing an appropriate hypoxia-directed therapy. The use of both markers together with a perfusion marker suggested the presence of regions of transient hypoxia, a method that once validated can possibly be applied to patient biopsies, given that an appropriate time course for marker stabilisation or binding is permitted.

BIBLIOGRAPHY

1. Vaupel P. Tumour microenvironmental physiology and its implications for radiation oncology. Semin Radiat Oncol 2004;14:198-206.

2. Hoberman HD. Is there a role for mitochondrial genes in carcinogenesis? Cancer Res 1975;35:3332-3335.

3. Warburg O. The metabolism of tumours. London, Costable & Co. 1930.

4. Hockel M, Schlenger K, Arad D, Miltze M, Shaffer U, Vaupel P. Association between tumour hypoxia and malignant progression advanced cancer of the uterine cervix. Cancer Res 1996;56:4509-4515.

5. Brizel DM, Sibley GS, Prosnitz LR, Scher RL, Dewhirst MW. Tumour hypoxia adversely affects the prognosis of carcinoma of the head and neck. Int J Radiat Oncol Biol Phys 1997;38:285-289.

6. Dewhirst MW. Concepts of oxygen transport at the microcirculatory level. Semin Radiat Oncol 1998;8:143-150.

7. Dunn, JF, Swartz HM. Blood oxygenation. Heterogeneity of hypoxic tissues monitored using BOLD MR imaging. Adv Exp Med Biol 1997;428:645-650.

8. Dewhirst MW Ong ET, Braun RD, Smith R, Klitzman B, Evans SM, Wilson D. Quantification of longitudinal tissue pO_2 in window chamber tumours: impact on tumour hypoxia. Br J Cancer 1999;79:1717-1722.

9. Dewhirst MW, Ong ET, Klitzman B, Secomb TW, Vinuya RZ, Dodge R, Brizel D, Gross JF. Perivascular oxygen tension in a transplantable mammary tumour growing in a dorsal flap window chamber. Radiat Res 1992;130:171-182.

10. Dewhirst MW Ong ET, Rosner GL, Rehmus SW, Shan S, Braun RD, Brizel DM, Secomb TW. Arteriolar oxygenation in tumour and subcutaneous arterioles: Effects of inspired air oxygen content. Br J Cancer 1996;74(suppl):S241-S246.

11. Dewhirst MW, Kimura H, Rehmus SW, Braun RD, pepahadjopoulos D, Hong K, Secomb TW. Microvascular studies on the origins of perfusion-limited hypoxia. Br J Cancer 1996;74:S247-S251.

12. Helmlinger G, Yuan F, Dellian M, Jain RK. Interstitial pH and pO_2 gradients in solid tumours in vivo: high-resolution measurements reveal a lack of correlation. Nature Med 1997;3:177-182

13. Fenton BM, Boyce DJ. Micro-regional mapping of HbO_2 saturation and blood flow following nicotinamide administration. Int J Radiat Oncol Biol Phys 1994;29:459-462.

14. Evans SM, Koch CJ. Prognostic significance of tumour oxygenation in humans. Cancer Lett 2003;195:1-16.

15. Thomlinson R, Gray L. The histological structure of some human lung cancers and the possible implications for radiotherapy. Br J Cancer 1955;9:539-549.

16. Tannock IF. The relation between cell proliferation and the vascular system in a transplanted mouse mammary tumour. Br J Cancer 1968;22:258-273.

17. Brown JM, Giaccia AJ. The unique physiology of solid tumours: opportunities (and problems) for cancer therapy. Cancer Res 1998;58:1408-1416.

18. Vukovic V, Nicklee T, Hedley DW. Multiparameter fluorescence mapping of nonprotein sulfhydryl status in relation to blood vessels and hypoxia in cervical carcinoma xenografts. Int J Radiat Oncol Biol Phys 2002;52:837-43.

19. Chaplin DJ, Olive PL, Durand RE. Intermittent blood flow in a murine tumour: Radiobiological effects. Cancer Res 1987;47:597-601.

20. Chaplin DJ, Trotter MJ, Durand RE, Olive PL, Minchinton AL. Evidence for intermittent radiobioligical hypoxia in experimental tumour systems. Biomed Biochim Acta 1989;48:S255-S259.

21. Hill SA, Pigott KH, Saunder MI, Powell ME, Arnold S, Obeid A, Ward G, Leahy M, Hoskin PJ, Chaplin DJ. Microregional blood flow in murine and human tumours assessed using laser Doppler microprobes. Br J Cancer 1996;74:S260-S263.

22. Eddy HA, Casarett GW. Development of the vascular system in the hamster malignant neurilenoma. Microvasc Res 1973;6:63-82.

23. Yamaura H, Matsuzawa T. Tumour regrowth after irradiation. An experimental approach. Int J Radiat Biol 1979;35:201-219.

24. Kimura H, Braun RD, Ong ET, Hsu R, Secomb TW, Papahadjopoulos D, Hong K, Dewhirst MW. Fluctuations in red cell flux in tumour microvessels can lead to transient hypoxia and reoxygenation in tumour parenchyma. Cancer Res 1996;56:5522-5528.

25. Walenta S, Snyder S, Haroon ZA, Braun RD, Amin K, Brizel D, Mueller-Klieser W, Chance B, Dewhirst MW. Tissue gradients of energy metabolites mirror oxygen tension gradients in rat mammary carcinoma model. Int J Radiat Onc Biol Phys 2001;51:840-848.

26. Kotelnikov VM, Coon JS IV, Haleem A, Taylor S IV, Hutchinson J, Panja W, Caldarelli DD, Griem K, Preisler HD. In vivo labelling with halogenated pyrimidines of

squamous cell carcinomas and adjacent non-involved mucosa of head and neck region. Cell Prolif 1995;28:497-509.

27. Pigott KH, Hill SA, Chaplin DJ, Saunders MI. Microregional fluctuations in perfusion within human tumours detected using laser Doppler flowmetery. Radiother Oncol 1996;40:45-50.

28. Semenza GL, Jiang BH, Leung SW, Passantino R, Concordet JP, Maire P, Giallongo A. Hypoxia response element in the aldolase A, enolase α, and lactate dehydrogenase A promoters contain essential binding sites for hypoxia-inducible factor 1. J Biol Chem 1996;271:32529-32537.

29. Ryan HE, Lo J, Johnson RS. HIF-1α is required for solid tumour formation and embryonic vascularisation. EMBO J 1998;17:3005-3015.

30. Levy AP, Levy NS, Wegner S, Goldberg MA. Transcriptional regulation of the rat vascular endothelial growth factor gene by hypoxia. J Biol Chem 1995;270:13333-13340.

31. Faller DV. Endothelial cell responses to hypoxic stress. Clin Exp Pharmacol Physiol 1999;26:74-84.

32. Wang GL, Semenza GL. Purification and characterisation of hypoxia-inducible factor 1. J Biol Chem 1995;270:1230-1237.

33. Wegner RH. Mammalian oxygen sensing, signalling and gene regulation. J Exp Biol 2000;203:1253-1263.

34. Wang GL, Jiang JH, Rue EA, Semenza GL. Hypoxia-inducible factor 1 is a basic-helix-loop-helix-PAS heterodimer regulated by cellular O_2 tension. Proc Natl Acad Sci USA 1995;92:5510-5514.

35. Ema M, Taya S, Yokotani N, Sogawa K, Matsuda Y, Fujii-Kuriyama Y. A novel bHLH-PAS factor with close sequence similarity to hypoxia-inducible factor 1 alpha regulates the VEGF expression and is potentially involved in lung and vascular development. Proc Natl Acad Sci USA 1997;94:4273-4278.

36. Gu YZ, Moran SM, Hogenesch JB, Wartman L, Bradfield CA. Molecular characterisation and chromosomal localisation of a third alpha-class hypoxia inducible factor subunit, HIF3alpha. Gene Expr 1998;7:205-213.

37. Maynard MA, Qi H, Chung J, Lee EH, Kondo Y, Hara S, Conaway RC, Conaway JW, Ohh M. Multiple splice variants of the human HIF-3 alpha locus are targets of the von Hippel-Lindau E3 ubiquitin ligase complex. J Biol Chem 2003;278:11032-11040.

38. Wang GL, Jiang BH, Rue EA, Semenza GL. Hypoxia-inducible factor 1 is a basic-helix-loop-helix-PAS heterodimer regulated by cellular O_2 tension. Proc Natl Acad Sci USA 1995;92:5510-5514.

39. Arany Z, Huang LE, Eckner R, Bhattacharya S, Jiang C, Goldberg MA, Bunn HF, Livingston DM. An essential role for p300/CBP in the cellular response to hypoxia. Proc Natl Acad Sci USA 1996;93:12969-12973.

40. Kallio PJ, Okamoto K, O'Brien S, Carrero P, Makino Y, Tanaka H, Poellinger L. Signal transduction in hypoxic cells: inducible nuclear translocation and recruitment of the CBP/p300 co-activator by the hypoxia-inducible factor-1 alpha. EMBO J 1998;17:6573-6586.

41. Ivan M, Kondo K, Yang H, Kim W, Valiando H, Ohh M, Salic A, Asara JM, Lane WS, Kaelin WG. HIF alpha targeted for VHL-mediated destruction by proline hydroxylation: implications for O_2 sensing. Science 2001;292:464-468.

42. Jiang BH. Mammalian oxygen sensing, signalling and gene regulation. J Exp Biol 2000;203:1253-1263.

43. Huang LE, Gu J, Schau M, Bunn HF. Regulation of hypoxia-inducible factor 1 alpha is mediated by an O_2 –dependant degradation domain via the ubiquitin-proteasome pathway. Proc Natl Acad Sci USA 1998;95:7987-7992.

44. Kallio PJ, Wilson WJ, O'Brien S, Makino Y, Poellinger L. Regulation of the hypoxia-inducible transcription factor 1 alpha by the ubiquitin-proteosome pathway. J Biol Chem 1999;274:6519-6525.

45. Cockman ME, Masson N, Mole DR, Jaakkola P, Chang GW, Clifford SC, Mahler ER, Pugh CW, Ratcliffe PJ, Maxwell PH. Hypoxia inducible factor-1alpha binding and ubiquitylation by the von Hippel-Lindau tumour suppressor protein. J Biol Chem 2000;275:25733-25741.

46. Ohh M, Park CW, Ivan M, Hoffman MA, Kim TY, Huang LE, Pavletich N, Chau V, Kaelin WG. Ubiquitination of hypoxia-inducible factor requires direct binding to the β-domain of the von Hippel-Lindau protein. Nature Cell Biol 2000;2:423-427.

47. Harris AL. Hypoxia-a key regulatory pathway in tumour growth. Nat Rev Cancer 2002;2: 38-47

48. Jaakkola, P, Mole DR, Tian YM, Wilson MI, Gielbert J, Gaskell SJ, Kriegsheim AV, Hebestreit HF, Mukherji M, Schofield CJ, Maxwell PH, Pugh CW, Ratcliffe PJ. Targeting of HIF-1α to the von Hippel-Lindau ubiquitylation complex by O_2 -regulated factors for oxygen-dependant proteolysis. Nature 2001;292:468-472.

49. Ivan M, Kondo K, Yang H, Kim W, Valiando H, Ohh M, Salic A, Asara JM, Lane WS, Kaelin WG. HIF-1α targeted for VHL-mediated destruction by proline hydroxylation: implications for O_2-sensing. Science 2001;292:464-468

50. Masson N, William C, Maxwell PH, Pugh CW, Ratcliffe PJ. Independent function of two destruction domains in hypoxia-inducible factor- α chains activated by prolyl hydroxylase. EMBO J. 2001;20:5197-5206.

51. Lando D, Pongratz I, Poellinger L, Whitelaw ML. A redox mechanism controls differential DNA binding activities of hypoxia-inducible factor (HIF)1alpha and the HIF-like factor. J Biol Chem 2000;4618-4627.

52. Minet E, Mottet D, Michel G, Roland I, Raes M, Remacle J, Michiels C. Hypoxia-induced activation of HIF-1: role of HIF-1alpha-Hsp90 interaction. FEBS Lett 1999;251-256.

53. Kallio, Okamoto K, O'Brien S, Carrero P, Makino Y, Tanaka H, Poellinger L al. Signal transduction in hypoxic cells: inducible nuclear translocation and recruitment of the CBP/p300 coativator by the hypoxia-incuible factor-1alpha by the ubiquitin-proteasome pahtway. J Biol Chem 1999;460:251-256.

54. Semenza GL, Jiang BH, Leung SW, Passantino R, Concordet JP, Maire P, Giallongo A. Hypoxia response elements in the aldolase A, enolase α, and lactate dehydrogenase A gene promoters contain essential binding sites for hypoxia-inducible factor 1. J Biol Chem 1996;271:32529-32537.

55. Cheng KC, Loeb LA. Genomic instability and tumour progression: mechanistic considerations. Adv Cancer Res 1993;86:361-367.

56. Reynolds TY, Rockwell S, Glazer PM. Genetic instability induced by the tumour microenvironment. Cancer Res 1996;56:5754-5757.

57. Russo CA, Weber TK, Volpe CM, Stoler DL, Petrelli NJ, Rodriguez-Bigas M, Burhans WC, Anderson GR. An anoxia inducible endonuclease and enhanced DNA breakage as contributors to genomic instability in cancer. Cancer Res 1995;55:1122-1128.

58. Janssen YM, Van Houten B, Borm PJ, Mossman BT. Cell and tissue responses to oxidative damage. Lab Invest 69:261-274.

59. Kim CY, Tsai MH, Osmanian C, Graeber TG, Lee JE, Giffard RG, DiPaolo JA, Peehl DM, Giaccia AJ. Selection of human cervical epithelial cells that possess reduced apoptotic potential to low oxygen conditions. Cancer Res 1997;57:4200-4204.

60. Ferrara N. Role of vascular endothelial growth factor in regulation of physiological angiogenesis. Am J Cell Physiol 2001;280:C1358-1366.

61. Dvorak HF. Tumours: wounds that do not heal. Similarities between tumour stroma generation and wound healing. N Engl J Med 1986;315:1650-1659.

62. Iyer NV, Kotch LE, Agani F, Leung SW, Laughner E, Wener RH, Gassmann M, Gearhar JD, Lawler AM, Yu AY, Semenza GL. Cellular and developmental control of O_2 homeostasis by hypoxia-inducible factor 1 alpha. Genes Dev 1998;12:149-162.

63. Lu H, Forbes RA, Verma A. Hypoxia-inducible factor 11 activation by aerobic glycolysis implicates the Warburg effect in carcinogenesis. J Biol Chem 2002;277:23111-23115.

64. Yamagata M, Hasuda K, Stamato T, Tannock IF. The contribution of lactic acid to acidificationof tumours: studies of variant cells lacking lactate dehydrogenase. Br J Cancer 1998;77:1726-1731.

65. Wykoff CC, Beasley NJ, Watson PH, Turner KJ, Pastorek J, Sibtain A, Wilson GD, Turley H, Talks KL, Maxwell PH, PughCW, Ratcliffe PH, Harris AL. Hypoxia-inducible expression of tumour-associated carbonic anhydrases. Cancer Res 2000;60:7075-7083.

66. Moeler BJ, Cao Y, Vujaskovic Z, Li CY, Haroon ZA, Dewhirst MW. The relationship between hypoxia and angiogenesis. Semin Radiat Oncol 2004;14:215-221.

67. Ferrara N. VEGF and the quest for tumour angiogenesis factors. Nat Rev Cancer 2002;2:795-803.

68. Shi YH, Fang WG. Hypoxia-inducible factor-1 in tumour angiogenesis. World J Gastroenterol 2004;10:1082-1087.

69. Bos R, Zhong H, Hanrahan CF, Mommers EC, Semenza GL, Pinedo HM, Abeloff MD, Simons JW, van Diest PJ, van der Wall E. Levels of hypoxia-inducible factor-1 alpha during breast carcinogenesis. J Natl Cancer Inst 2001;93:309-314.

70. Giatromanolaki A, Koukourakis MI, Sivridis E, Turley H, Talks K, Pezzella F, Gatter KC, Herris AL. Relation of hypoxia inducible factor 1 alpha and 2 alpha in operable non-small cell lung cancer to angiogenic/molecular profile of tumours and survival. B J Cancer 2001;85:881-890.

71. Toi M, Hoshina S, Takayangi T, Tominaga T. Association of vascular endothelial growth-factor expression with tumour angiogenesis and with early relapse in primary breast-cancer. Jpn Cancer Res 1994;85:1045-1049.

72. Maeda K, Chung YS, Ogawa Y, Takatsuka S, Kang SM, Ogawa M, Sawada T, Sowa M. Prognostic value of vascular endothelial growth factor expression in gastric carcinoma. Cancer 1996;77:585-863.

73. Enholm B, Karpanen T, Jeltsch M, Kubo H, Stenback F, Prevo R, Jackson DG, Yla Hertualla S, Alitalo K. Adenoviral expression of vascular endothelial growth factor C induces lymphangiogenesis in the skin. Circ Res 2001;88:623-629.

74. Jeltsch M, Kaipainen A, Joukov V, Meng X, Lakso M, Rauvala H, Swartz M, Fukumura D, Jain RK, Alitalo K. Hyperplasia of lymphatic vessels in VEGF-C transgenic Mice. Science 1997;276:1423-1425.

75. Veikkola T, Jussila L, Makinen T, Karpanen T, Jeltsch M, Petrova TV, Kubo H, Thurston G, McDonald DM, Achen MG, Stacker SA, Alitalo K. Signalling via vascular endothelial growth factor receptor 3 is sufficient for lymphangiogenesis in transgenic mice. EMBO J 2001;20:1223-1231.

76. Pepper MS. Lymphangiogenesis and tumour metastasis. Myth or reality? Clin Canc Res 2001;7:462-468.

77. Dvorak HF. Tumours: wounds that do not heal. Similarity between tumour stroma generation and wound healing. N Eng J Med 1986;315:1650-1658.

78. Unemori EN, Ferrara N, Bauer EA, Amento EP. Vascular endothelial growth factor induces interstitial collagenase expression in human endothelial cells. J Cell Phys 1992;153:557-562.

79. Mandriota SJ, Seghezzi G, Vassalli JD, Ferrera N, Wasi S, Mazzieri R, Mignatti P, Pepper MS. Vascular endothelial growth factor increases urokinase receptor expression in vascular endothelial cells. J Biol Chem 1995;270:9707-9716.

80. Plouet J, Schilling J, Gospodarowitcz D. Isolation and characterisation of a newly identified endothelial cell mitogen produced by AtT-20 cells. EMBO J 1989;8:3801-3806.

81. Ferrara N. Vascular endothelial growth factor. Eur J Cancer 1996;32A:2413-2422.

82. Giaccia, AJ, Kastan MB. The complexity of p53 modulation: Emerging patterns from divergent signals. Genes Dev 1998;12:2973-2983.

83. Levine, A.J. p53, the cellular gatekeeper for growth and division. Cell 1997;88: 323–331.

84. Mukhopadhyay DL, Tsiokas L, Sukhatme VP. Wild-type p53 and v-src exert opposing influences on human vascular endothelial growth factor gene expression. Cancer Res 1995;55:6161-6165.

85. Bouvet M, Ellis LM, Nishizaki M, Fujiwara T, Liu W, Bucana CD, Fang B, Lee JJ, Roth JA. Adenovirus-mediated wild-type p53 gene transfer down-regulates vascular

endothelial growth factor expression and inhibits angiogenesis in human colon cancer. Cancer Res 1998;58:2288-2292.

86. Fontanini G, Boldrini L, Vignati S, Chine S, Basolo F, Silvestri V, Lucchi M, Mussi A, Angeletti CA, Bevilacqua G. Bcl2 and p53 regulate vascular endothelial growth factor (VEGF)-mediated angiogenesis in non-small cell lung carcinoma. Eur J Cancer 1998;34:718-723.

87. Blagosklonny MV, An WG, Romanova LY, Trepel J, Fojo T, Neckers L. p53 inhibits hypoxia inducible factor-stimulated transcription. J Biol Chem 1988;273:11995-11998.

88. Graeber TG, Peterson JF, Tsai M, Monika K, Fornace AJ Jr, Giaccia AJ. Hypoxia induces accumulation of p53 protein, but activation of a G1-phase checkpoint by low-oxygen conditions is independent of p53 status. Mol Cell Biol 1994;14:6264-6277.

89. Hansson LO, Friedler A, Freund S, Rudiger S, Fersht AR. Two sequence motifs from HIF-1α bind to the DNA-binding site of p53. PNAS 2002;99:10305-10309.

90. Ravi R, Mookerjee B, Bhujwalla ZM, Sutter CH, Artemov D, Zeng Q, Dillehay LE, Madan A, Semenza GL, Bedi A. Regulation of tumour angiogenesis by p53-induced degradation of hypoxia-inducible factor 1alpha. Genes Dev 2000;14:34-44.

91. Kern SE, Pietenpol JA, Thiagalingam S, Seymour A, Kinzler KW, Vogelstein B. Oncogenic forms of p53 inhibit p53 regulated gene expression. Science 1992;256:827-830.

92. Suzuki H, Tomida A, Tsuruo T. Dephosphorylated hypoxia-inducible factor 1alpha as a mediator of p53-dependent apoptosis during hypoxia. Oncogene 2001;20:5779-5788.

93. Kaluzova M, Kaluz S, Lerman MI, Eric, Standbridge EJ. DNA damage is a prerequisite for p53-mediated proteasomal degradation of HIF-1α in hypoxic cells and downregulation of the hypoxia marker carbonic anhydrase IX. Mol Cell Biol 2004;24:5757-5766.

94. Durand RE, Raleigh JA. Identification of nonproliferating but viable hypoxic cells in vivo. Cancer Res 1998;58:3547-3550.

95. Goda N, Ryan HE, Khadivi B, McNulty W, Rickert RC, Johnson RS. Hypoxia-inducible factor 1 alpha is essential for cell cycle arrest during hypoxia. Mol Cell Biol 2003;23:359-369.

96. Bussink J, Kaanders JH, Van der Kogel AJ. Vascular architecture and microenvironmental parameters in human squamous cell carcinoma xenografts: effects of carbogen and nicotinamide. Radiother Oncol 1999;50:173-184.

97. Kennedy AS, Raleigh JA, Perez GM, Calkins DP, Thrall DE, Novotny DB, Varia MA. Proliferation and hypoxia in human squamous cell carcinoma of the cervix: first report of combined immunohistochemical assays. Int J Radiat Oncol Biol Phys 1997;37:897-905.

98. Webster L, Hodgkiss RJ, Wilson GD. Simultaneous triple staining for hypoxia, proliferation, and DNA content in murine tumours. Cytometry 1995;21:344-351.

99. Schmaltz C, Hardenbergh PH, Wells A, Fisher DE. Regulation of proliferation-survival decision during tumour cell hypoxia. Mol Cell Biol 1998;18:2845-2854.

100. Zeman EM, Calkins DP, Cline JM, Thrall DE, Raleigh JA. The relationship between proliferative and oxygenation status in spontaneous canine tumours. Int J Radiat Oncol Biol Phys 1993;27:891-898.

101. Chapman JD, Dugle DL, Reuvers AP, Meeker BE, Borsa J. Letter: Studies on the radiosensitising effect of oxygen in Chinese hamster cells. Int J Radiat Biol Relat Stud Phys Chem Med 1974;26(4):383-9

102. Hall EJ. Radiobiology for the radiologist. Philadelphia Lippincott Williams and Wilkins 2000, p588.

103. Brizel DM, Scully SP, Harrelson JM, Layfield LJ, Bean JM, Pronitz LR, Dewhirst MW. Tumour oxygenation predicts for the likelihood of distant metastases in human soft tissue sarcoma. Cancer Res 1996;56:941-943.

104. Nordsmark M, Alsner J, Keller J, Nielsen OS, Jensen OM, Horsman MR, Overgaard J. Hypoxia in human soft tissue sarcomas: Adverse impact on survival and no association with p53 mutation. Br J Cancer 2001;84:1070-1075.

105. Fyles AW, Milosovic M, Wong R, Pintilie M, Kavanagh MC, Levin W, Manchul LA, Keane TJ, Hill RP. Oxygenation predicts radiation response and survival in patients with cervix cancer. Radiother Oncol 1988;48:149-156.

106. Knocke TH, Wietmann HD, Feldmann HJ, Seltzer E, Potter R. Intratumoral pO_2-measurements as predictive assays in the treatment of carcinonoma of the uterine cervix. Radiother Oncol 1999;53:99-104.:711-715.

107. Hockel M, Schlenger K, Aral B, Milze M, Schaffer U, Vaupel P. Association between tumor hypoxia and malignant progression in advanced cancer of the uterine cervix. Cancer Res 1996;56:4509-4515.

108. Nordsmark M, Overgaard J. Pre-treatment oxygenation predicts radiation response in advanced squamous cell carcinoma of the head and neck. Radiother Oncol 2000;57:39-43.

109. Brizel DM, Sibley GS, Prosnitz LR, Scher RL, Dewhirst MW. Tumour hypoxia adversely affects the prognosis of carcinoma of the head and neck. Int J Radiat Oncol Biol Phys 1997;38:285-289.

110. Brizel DM, Dodge RK, Clough RW, Dewhirst MW. Oxygenation of head and neck cancer: Changes during radiotherapy and impact on treatment outcome. Radiother Oncol 1999;53:113-117.

111. Durand RE, Raleigh JA. Identification of non-proliferating but viable hypoxic tumour cells in vivo. Cancer Res 1998;58:3574-3550.

112. Minchinton AI, Durand RE, Chaplin DJ. Intermittent blood flow in the KHT sarcoma-flow cytometry studies using Hoechst 33342. Br J Cancer 1990;62:195-200.

113. Rang HP, Dall MM, Ritter JM. In: Pharmacology. 4th and. Churchill Livingstone: Edinburgh, 1999;670-677.

114. Tannock I. Response of aerobic and hypoxic cells in a solid tumour to adriamycin and cyclophosphamide and interaction of the drugs with radiation. Cancer Res 1982;42:4921-4926.

115. Durand RE. Distribution and activity of antineoplastic drugs in a tumour model. J. Natl Cancer Inst 1989;81:146-152.

116. Griffiths JR. Are cancer cells acidic? Br J Cancer 1991;64:425-427.

117. Chaplin DJ, Olive PL, Durand RE. Intermittent blood flow in a murine tumour: Radiobiological effects. Cancer Res 1987;16:1131-1135.

118. Shen J, Hughes C, Chao C, Cai J, Bartels C, Gessner T, Subjeck J. Coinduction of glucose-regulated proteins and doxorubicin resistance in Chinese hamster cells. Proc Natl Acad Sci USA 1987;84:3278-3282.

119. Hughes CS, Shen JW, Subjeck JR. Resistance to etoposide induced by three glucose-regulated stresses in Chinese hamster ovary cells. Cancer Res 1989;49:4452-4454.

120. Sanna K, Rofstad EK. Hypoxia-induced resistance to doxorubicin and methotrexate in human melanoma cell lines in vitro. Int J Cancer 1994;58:258-262.

121. Olive PL, Durand RE. Misonidazole binding in SCCVII tumours in relation to the tumour blood supply. Int J Radiat Oncol Biol Phys 1989;16:775-761.

122. Durand RE, Aquino-Parsons C. Clinical relevance of intermittent tumour blood flow. Acta Oncologica 2001;40:929-936.

123. Durand RE. Intermittent blood flow in solid tumours—an under appreciated source of drug resistance. Cancer Metast Rev

124. Durand RE, Sham E. The lifetime of hypoxic human tumour cells. Int J Radiat Oncol Bio Phys

125. Siemann DW, Hill RP, Bush RS. The importance of pre-irradiation breathing of O_2 and carbogen ($5\%O_2$: 95% O_2) on the in vivo radiation response of a murine sarcoma. Int J Radiat Oncol Biol Phys 1977;22:903-911.

126. Thews O, Kelleher DK, Vaupel P. et al. Dynamics of tumour oxygenation and red blood cell flux in response to inpiratory hyperoxia combined with different levels of inspiratory hypercapnia. Radiother Oncol 2002;62:77-85.

127. Ljungkvist AS, Bussink J, Rijken PF, Raleigh JA, Denekamp J, Van Der Kogel AJ. Changes in tumour hypoxia measured with a double hypoxic marker technique. Int Radiat Oncol Biol Phys 2000;48:1529-1538.

128. Bussink J, Kaanders JH, Strik AM, Vand Der Kogel AJ. Effects of nicotinamide and carbogen on oxygenation in human tumour xenografts measured with luminescence-based fibre optic probes. Radiother Oncol 2000;57:21-30.

129. Hill SA, Collingridge DR, Vojnovic B, Chaplin DJ. Tumour radiosensitisation by high-oxygen-content gases: influence of the carbon dioxide content of the inspired gas on pO_2 , microcirculatory function and radiosensitivity. Int Radiat Oncol Biol Phys 1988;40:943-951.

130. Brizel DM, Lin S, Johnson JL, Brooks J, Dewhirst MW, Piantadosi CA. The mechanisms by which hyperbaric oxygen and carbogen improve tumour oxygenation. Br J Cancer 1995;72:1120-1124.

131. Robinson SP, Rodrigues LM, Ojugo AS, McSheehy PM, Howe FA, Grifith JR. The response to carbogen breathing in experimental tumour models monitored by gradient-recalled echo magnetic resonance imaging. Br J Cancer 1997;75:1000-06.

132. Kaanders JH, Bussink J, Van Der Kogel AJ. ARCON: a novel biology-based approach in radiotherapy. Lancet Oncol 2002;3:728-737.

133. Powell MEB, Collingridge DR, Saunders MI. Improvements in human tumour oxygenation with carbogen of varying carbon dioxide concentrations. Radiother Oncol 1999;50:167-171.

134. Horsman MR, Chaplin DJ, Brown JM. Tumour radiosensitisation by nicotinamide: a result of improved perfusion and oxygenation. Radiat Res 1989;118:139-150.

135. Chaplin DJ, Horsman MR, Trotter MJ. Effect of nicotinamide on the microregional heterogeneity of oxygen delivery within a murine tumour. J Natl Cancer Inst 1990;82:672-676.

136. Kaanders JH, Pop LA, Marres HA, Liefers J, Van Den Hoogen FJ, Van Daal WA, Van Der Kogel AJ. Accelerated radiotherapy with carbogen and nicotinamide (ARCON) for laryngeal cancer. Radiaother Oncol 1998;45:115-122.

137. Kaanders JH, Pop LA, Marres HA, Bruaset I, Van Den Hoogen FJ, Merkx MA, Van Der Kogel AJ. ARCON: experience in 215 patients with advanced head-and-neck cancer. Int J Radiat Oncol Biol Phys 2002;52:769-778.

138. Hoskin PJ, Saunder MI, Dische S. Hypoxic radiosensitizers in radical radiotherapy for patients with bladder carcinoma: hyperbaric oxygen, misonidazole, and accelerated radiotherapy, carbogen, and nicotinamide. Cancer 1999;86:1322-1328.

139. Greco O, Marples B, Joiner MC, Scott SD. How to overcome (and exploit) tumour hypoxia for targeted gene therapy. J Cell Physiol 2003;197:312-325.

140. Haffty BG, Son YH, Papac R, Sasaki CT, Weissberg JB, Fischer D, Rockwell S, Sartorelli AC, Fischer JJ. Chemotherapy as an adjunct to radiation in the treatment of squamous cell carcinoma of the head and neck: Results of the Yale randomised trials. J Clin Oncol 1997;15:268-276.

141. Rischin D, Peters L, Hicks R, Hughes P, Fisher R, Hart R, Sexton M, D'Costa I, Von Roemeling R. Phase I trial of concurrent tirapazamine, cisplatin and radiotherapy in patients with advanced head and neck cancer. J Clin Oncol 2001;19:535-542.

142. Kung AL, Wang S, Klco JM, Kaelin WG, Livingston DM. Suppression of tumour growth through disruption of hypoxia-inducible transcription. Nat Med 2000;6:1335-1340.

143. Sun X, Kanwar JR, Leung E, Lehnert K, Wang D, Krissansen GW. Gene transfer of antisense hypoxia-inducible factor-1α enhances the therapeutic efficacy of cancer immunotherapy. Gene Ther 2001;8:638-645.

144. Rapisarda A, Uranchimeg B, Scudiero DA, Selby M, Sausville EA, Shoemaker RH, Mellilo G. Identification of small molecule inhibitors of hypoxia-inducible factor-1 transcriptional activation pathway. Cancer Res 2002;62:4316-4324.

145. Dachs Gu, Patterson AV, Firth JD, Ratcliffe PJ, Townsend KM, Stratford IJ, Harris AL. Targeting gene expression to hypoxic tumour cells. Nat Med 1997;3:515-520.

146. Greco O, Dachs GU. Gene directed enzyme/prodrug therapy of cancer: Historical appraisal and future prospectives. J Cell Physiol 187;22-36.

147. Greco O, Scott SD, Marples B, Dachs GU. Cancer gene therapy; Delivery, delivery, delivery. Front Biosci 2002;7:d1516-d1524.

148. Fenton BM, Paoni SF, Lee J, Kock CJ, Lord EM. Quantification of tumour vasculature and hypoxia by immunohistochemical staining and HbO_2 saturation measurements. Br J Cancer 1999;79:464-471.

149. Taylor NJ, Baddeley H, Goodchild KA, Powel ME, Thoumine M, Culver LA, Stirling JJ, Saunders MI, Hoskin PJ, Phillips H, Padhani AR, Griffiths JR. BOLD MRI human tumour oxygenation during carbogen breathing. J Magnet Reson Imaging 2001;14:156-163.

150. Jenkins WT, Evans SM, Kock CJ. Hypoxia and necrosis in rat 9L glioma and Morris 7777 hepatoma tumours: comparative measurements using EF5 binding and Eppendorf needle electrode. Int J Radiat Oncol Biol Phys 2000;46:1005-1017.

151. Nozue M, Lee I, Yuan F, Teicher BA, Brizel DM, Dewhirst MW, Milross CG, Milas L, Song CW, Thomas CD, Guichard M, Evans SM, Koch CJ, Lord EM, Jain RK, Suit HD. Interlaboratory variation in oxygen tension measurement by Eppendorf histograph and comparison with hypoxic marker. J Surg Oncol 1997;66:30-38.

152. Alavi A, Kung JW, Zhuang H. Implications of PET based molecular imaging on the current and future practice of medicine. Sem Nucl Med 2004;34:56-69.

153. Raleigh JA, Koch CJ. Importance of thiols in the reductive binding of 2-nitromidazoles to macromolecules. Biochem Pharmacol 1990;40:2547-2464.

154. Garrecht BM, Chapman JD. The labelling of EMT-6 tumours in balb/c mice with ^{14}C-misonidazole. Br J Radiol 1983;56:745-753.

155. Franko AJ, Chapman JD. Binding of ^{14}C-misonidazole to hypoxic cells in V79 spheroids. Br J Cancer 1982;45:694-699.

156. Woods ML, Koch CJ, Lord EM. Detection of individual hypoxic cells in multicellular spheroids by flow cytometry sing the 2-nitromidazole. EF5 and monoclonal antibodies. Int J Radiat Oncol Biol Phys 1996;34:93-101.

157. Arteel GE, Thurman RG, Yates JM, Raleigh JA. Evidence that hypoxia markers detect oxygen gradients in liver: pimonidazole and retrograde perfusion of rat liver. Br J Cancer 1995;72:889-895.

158. Raleigh JA et al. Comparisons among pimonidazole binding, oxygen electrode measurements, and radiation response in C3Hmouse tumours. Radiat Res 1999'151:580-589.

159. Kaanders JH, Wijfells KI, Marres HA, Ljungkvist AS, Pop LA, Van Der Hoogan FJ, De Wilde PC, Bussink J, Raleigh JA, Van Der Kogel AJ. Pimonidazole binding and tumour vascularity predict for treatment outcome in head and neck cancer. Cancer Res 2002;62:7066-1074.

160. Kennedy AS, Raleigh JA, Perez GM, Calkins DP, Thrall DE, Novotny DB, Varia MA. Proliferation and hypoxia in human squamous cell carcinoma of the cervix: first report of combined immunohistochemical assay. Int J Radiat Oncol Biol Phys 1997;37:897-905.

161. Raleigh JA, Calkins-Adams DP, Rinker LH, Ballenger CA, Weissler MC, Fowler WC Jr, Novotny DB, Varia MA. Hypoxia and vascular endothelial growth factor expression in human squamous cell carcinomas using pimonidazole as a hypoxia marker. Cancer Res 1998;58:3765-3768.

162. Chapman AD, Franko AJ, and Sharplin J. A marker for hypoxic cells in tumours with potential clinical applicability. Br J Cancer 1981;43:546-550.

163. Gross MW, Darbach U, Groebe K, Franko AJ, and Mueller-Dlieser W. Calibration of misonidazole labelling by simultaneous measurement of oxygen tension and labelling density in multicellular spheroids. Int J Radiat Oncol Biol Phys 1995;61:567-573.

164. Mueller-Klieser W, Schlenger KH, Walenta S, Gross M, Karbach U, Hoeckel M, Vaupel P. Pathophysiological approaches to identifying tumour hypoxia in patients. Radiother Oncol 1991;20:21-28.

165. Janssen HL, Hoebers FJ, Sprong D, Goethals L, Williams KJ, Stratford IJ, Haustermans KM, Balm AJ, Begg AC. Differentiation-associated staining with anti-pimonidazole antibodies in head and neck tumours. Radiother Oncol 2004;70:91-97.

166. Azuma C, RaleighJA. Longevity of pimonidazole adducts in spontaneous canine tumours as an estimate of hypoxic cell life-time. Radiat Res 1997;148:35-42.

167. Dennis MF, Stratford MR, Wardman P, Watts ME. Cellular uptake of misonidazole and analogues with acidic or basic functions. Int J Radiat Biol Relat. Stud. Phys., Chem. Med. 1985, 629-643.

168. Arteel GE, Thurman RG, Yates JM, Raleigh JA. Evidence that hypoxia markers detect oxygen gradients in liver: Pimonidazole and retrograde perfusion of rat liver. Br J Cancer 1995;72:895,1995.

169. Azuma C, RaleighJA, Thrall DE. Lifetime of hypoxic cells in spontaneous canine tumours. Radiat Res 1996;148:35-42.

170. Kennedy AS, Raleigh JA, Perez GM, Calkins DP, Thrall DE, Novotny DB, Varia MA. Proliferation and hypoxia in human squamous cell carcinoma of the cervix: First

report of combined immunohistochemical assays. Int J Radiat Oncol Biol Phys 1997;37:897-905.

171. Saunders MI, Anderson JP, Benett MH, Dische S, Minchinton A, Stratford MR, and Tothill M. The clinical testing of Ro 03-8799—pharmakinetics, toxicology, tissue and tumour concentrations. Int J Radiat Oncol Biol Phys 1984;10:1759-1763.

172. Ryan HE, Lo J, Johnson RS. HIF-1alpha is required for solid tumour formation and embryonic vascularisation. EMBO J 1998;17:3005-3015.

173. Zhong H, De Marzo AM, Laughner E, Lim M, Hilton DA, Zagzag D, Buechler P, Isaacs WB, Semenza GL, Simons JW. Overexpression of hypoxia-inducible factor 1alpha is a positive factor in solid tumour growth. Cancer Res 1999;59:5830-5835.

174. Zelzer E, Levy Y, Kahana C, Shilo BZ, Rubinstein M, Cohen B. Insulin induces transcription of target genes through the hypoxia-inducible factor HIF-1alpha/ARNT. EMBO J 1998;17:5085-5094.

175. Zundel W, Schidler C, Haas-Kogan D, Koong A, Kaper F, Chen E, Gottschalk AR, Ryan HE, Johnson RS, Jefferson AB, Stokoe D, Giaccia AJ. Loss of PTEN facilitates HIF-1-mediated gene expression. Genes Dev 2000;14:391-396.

176. Jiang BH, Jiang G, Zheng JZ, Lu Z, Hunter T, Vogt PK. Phosphatidylinositol 3-kinase signalling controls levels of hypoxia-inducible factor 1. Cell Growth Differ 2001;12:363-369.

177. Tacchini L, Dansi P, Matteucci E, Disiderio MA. Hepatocyte growth factor signalling stimulates hypoxia inducible factor-1 (HIF-1) activity in HepG2 hepatoma cells. Carcinogenesis 2001;22:1363-1371.

178. Gorlach A, Diebold I, Schini-Kerth VB, Berchner-Pfannschmidt U, Roth U, Brandes RP, Kietzmann T, Brusse R. Thrombin activates the hypoxia-inducible factor-1 signalling pathway in vascular smooth muscle cells: Role of the p22(phox)-containing NADPH oxidase. Circ Res 2001;89:47-54.

179. Sandau KB, Faus HG, Brune B. Induction of hypoxia-inducible-factor 1 by nitric oxide is mediated via the PI 3K pathway. Biochem Biophys Res Commun 2000;278:263-267.

180. Schindl M, Schoppman SF, Samonigg H, Hausmaninger H, Kwasny W, Gnant M, Jakesz R, Kubista E, Birner P, Oberhuber G. Overxpression of hypoxia-inducible factor 1α is associated with an unfavourable prognosis in lymph node-positive breast cancer. 2002;8:1831-1837.

181. Birner P, Schindl M, Obermair A, Plank C, Breitenecker G, Oberhuber G. Overexpression of hypoxia-inducible factor 1 alpha is a marker for an unfavourable prognosis in early-stage invasive cervical cancer. Cancer Res 2000;60:4693-4696.

182. Mayer N, Wree A, Hockel M, Leo C, Pilch H, Vaupel P. Lack of correlation between Expression of HIF-1α expression and oxygen status in identical tissue areas of squamous cell carcinomas of the uterine cervix.

183. Haugland HK, Vukovic V, Pintilie M, Fyles AW, Milosevic M, Hill RP, Hedley DW. Expression of hypoxia-inducible factor-1α in cervical carcinomas: correlation with tumour oxygenation. Int J Radiat Oncol Biol Phys 2002;53:854-861.

184. Sivridis E, Giatromanolaki A, Gatter KC, Harris AL, Koukourakis MI. Association of hypoxia-inducible factors 1α and 2α with activated angiogenic pathways and prognosis in patients with endometria carcinoma. Cancer 2002;95:1055-1063.

185. Koukourakis MI, Corti L, Skarlatos J, Giatromanolaki A, Krammer B, Blandamura S, Piazza M, Verwanger T, Schnitzhofer G, Kostandelos J, Beroukas K. Hypoxia inducible factor (HIF-1a and HIF-2a) expression in early esophageal cancer and response to photodynamic therapy and radiotherhapy. Cancer Res 2001;61:1830-1832.

186. Takahashi R, Tanaka S, Hiyama T, Ito M, Kitadai Y, Sumii M, Haruma K, Chayama K. Hypoxia-inducible factor-1alpha expression and angiogenesis in gastrointestinal stromal tumour of the stomach. Oncol Rep 2003;10:797-802.

187. Koukourakis MI, Giatromanolaki A, Sivridis E, Simopoulos E, Turley H, Talks K, Gatter KC, Harris AL. Hypoxia-inducible factor (HIF1A and HIF2A), angiogenesis, and chemoradiotherapy outcome of squamous cell head-and-neck cancer. Int J Radiat Oncol Biol Phys 2002;53:1192-1202.

188. Giatromanolaki A, Koukourakis MI, Sivridis E, Turley H, Talks K, Pezzella F, Gatter KC, Harris AL. Relation of hypoxia inducible factor 1α and 2α in operable non-small cell lung cancer to angiogenic/molecular profile of tumours and survival. Br J Cancer 2001;85:881-890.

189. Hui EP, Chan AT, Pezzella F, Turley H, To KF, Poon TC, Zee B, Mo F, Teo PM, Huang DP, Gatter KC, Johnson PJ, Harris AL. Coexpression of hypoxia-inducible factors 1α and 2α, carbonic anhydrase IX, and vascular endothelial growth factor in nasopharyngeal carcinoma and relationship to survival. Clin Cancer Res 2002;8:2595-2604.

190. Birner P, Gatterbauer B, Oberhuber G, Schindl M, Rossler K, Prodinger A, Budka H, Hainfellner JA. Expression of hypoxia-inducible factor-1 alpha in oligodendriogliomas: its impact on prognosis and on neoangiogenesis. Cancer 2001;165-171.

191. Aebersold DM, Burri P, Beer KT, Laissue J, Djonov V, Greiner RH, Semenza GL. Expression of hypoxia-inducible factor-1α: a novel predictive and prognostic parameter in the radiotherapy of oropharyngeal cancer. Cancer Res 2001;61:2911-2916.

192. Birner P, Schindl M, Obermair A, Breitenecker G, Oberhuber G. Expression of hypoxia-inducible factor 1α in epithelial ovarian tumours: its impact on prognosis and on response to chemotherapy. Clin Cancer Res 2001;7:11661-1668.

193. Blancher C, Moore JW, Robertson N, Harris AL. Effects of ras and von hippel-lindau (VHL) gene mutations on hypoxia-inducible factor (HIF)-1α, HIF-2α, and vascular endothelial growth factor expression and their regulation by the phosphatidylinositol 3'-kinase/Akt signalling pathway. Cancer Res 2001;61:7349-7355.

194. Laughner E. HER2 (neu) signalling increases the rate of hypoxia-inducible factor 1alpha (HIF-1alpha) synthesis: novel mechanism for HIF-1-mediated vascular endothelial growth factor expression. Mol Cell Biol 2001;21:3995-4004.

195. Gingras AC, Raught B, Gygi SP, Niedzwiecka A, Miron M, Burley SK, Polakiewicz RD, Wyslouch-Cieszynska A, Aabersold R, Sonenberg N. Hierarchical phosphorylation of the translation inhibitor 4E-BP1. Genes Dev 2001;15(21):2852-64.

196. Alvarez-Tejado M, Alfranca A, Aragones J, Vara A, Landazuri MO, Del Peso L. Lack of evidence for the involvement of the phosphoinositide 3-kinase/Akt pathway in the activation of hypoxia-inducible factors by low oxygen tension. J Biol Chem 2002;277:13508-13517.

197. Arsham AM, Plas DR, Thompson CB, Simon MC. Phosphatidylinositol 3-Kinase/Akt signalling is neither required for hypoxic stabilisation of HIF-1α. Nor sufficient for HIF-1-dependent target gene transcription. J Biol Chem 2002;277:15162-15170.

198. Baek JH, Jang JE, Kang CM, Chung HY, Kim ND, Kim KW. Hypoxia-induced VEGF enhances tumour survivability via suppression of serum deprivation-induced apoptosis. Oncogene 2000;19:4621-4631.

199. Conrad PW, Rust RP, Han J, Millhorn DE, Beitner-Johnson D. Selective activation of p38alpha and p38gamma by hypoxia. J Biol Chem 1999;274:23570-23576.

200. Conrad PW, Freeman TL, Beitner-Johnson D, Millhorn DE. EPAS1 trans-activation during hypoxia requires p42/p44 MAPK. J Biol Chem 1999;274:33709-33713.

201. Wang GL. Jiang BH, Semenza GL. Effect of protein kinase and phosphatase inhibitors on expression of hypoxia-inducible factor 1. Biochem Biophys Res Commun 1995;216:669-675.

202. Minet E, Michel G, Mottet D, Raes M, Michiels C. Transduction pathways involved in hypoxia-inducible factor-1 phosphorylation and activation. Free Radical Biol Med 2001;31:847-855.

203. Hur E, Chang KY, Lee E, Lee SK, Park H. Mitogen-activated protein kinase kinase inhibitor PD98059 blocks the transactivation but not the stabilisation or DNA binding ability of hypoxia-inducible factor-1 α . Mol Pharmacol 2001;59:1216-1224.

204. Richard DE, Berra E, Pouyssegur J. p42/p44 mitogen-activated protein kinases phosphorylate hypoxia-inducible factor 1alpha (HIF-1α) and enhance the transcriptional activity of HIF-1. J Biol Chem 1999;274:32631-32637.

205. Minet E, Arnould T, Michels G, Ronald I, Mottet D, Raes M, Remacle J, Michiels C. ERK activation upon hypoxia: involvement in HIF-1 activation. FEBS Lett 2000;468;53-58.

206. Sutter CH, Laughner E, Semenza GL. Hypoxia-inducible factor 1alpha protein expression is controlled by oxygen-regulated ubiquitination that is disrupted by deletions and missense mutations. Proc Natl Acad Sci 2000;97:4748-4753.

207. Gherardi E. Hepatocyte growth factor--scatter factor: mitogen, motogen, and met. Cancer Cells 1991;3:227-232.

208. Ueoka Y, Kato K, Kuriaki Y, Horiuchi S, Terao Y, Nishida J, Ueno H, Wake N. Hepatocyte growth factor modulates mobility and invasiveness of ovarian carcinomas via Ras-mediated pathway. Br J Cancer 2000;82:891-899.

209. Grant DS, Kleinman HK, Goldberg ID, Bhargava MM, Nickoloff BJ< Kinsella JL, Polverini P, Rosen EM. Scatter factor induces blood vessel formation in vivo. Proc Natl Acad Sci USA 1993;90:1937-1941.

210. Tacchini L. Hepatocyte growth factor signalling stimulates hypoxia inducible factor-1 (HIF-1) activity in HepG2 hepatoma cells. Carcinogenesis 2001;22:1363-1371.

211. Sodhi A, Monanter S, Patel V, Zohar M, Bais C, Mesri EA, Gutkind JS. The Kaposi's sarcoma-associated herpes virus G protein-coupled receptor up-regulates vascular endothelial growth factor expression and secretion through mitogen-activated protein kinase and p38 pathways acting on hypoxia-inducible factor1aplpha. Cancer Res 2000;60:4873-4880.

212. Rak J, Mitsuhashi Y, Sheehan C, Tamir A, Viloria-Petit A, Filmus J, Mansour SJ, Ahn NG, Kerbel RS. Oncogenes and tumour angiogenesis: differential modes of vascular endothelial growth factor up-regulation in ras transformed epithelial cells and fibroblasts. Cancer Res 2000;60:490-498.

213. Peterson JK, Houghton PJ. Integrating pharmacology and in vivo cancer models in preclinical and clinical drug development. Eur J cancer 2004;40:837-844.

214. Parliament MB, Allalunis-Turner MJ, Franko AJ, Olive PL, Mandyam R, Santos C, Wolokoff B. Vascular endothelial growth factor expression is independent of hypoxia in human malignant glioma spheroids and tumours. Br. J. Cancer, 2000;82:635-641.

215. Durand RE, Raleigh JA. Identification of nomproliferating but viable hypoxic tumour cells in vivo. Cancer Res 1998;58:3547-3550.

216. Walton MI, Bleehen NM, Workman P. Effects of localised tumour hyperthermia on pimanidazole (Ro 03-8799) pharmacokinetics in mice. Br J Cancer 1989;59:667-673.

217. Olive PL, Chaplin DJ, Durand RE. Pharmacokinetics, binding and distribution of Hoechst 33342 in spheroids and murine tumours. Br J Cancer 1985;52:739-746

218. Semenza GL, Roth PH, Fang HM, Wang GL. Transcriptional regulation of genes encoding glycolytic enzymes by hypoxia-inducible factor 1. J Biol Chem 1994; 269:23757-23763.

219. Bennewith KL, Durand RE. Quantifying transient hypoxia in tumour xenografts by flow cytometry. Cancer Res 2004;64:6183-6189.

220. Yu AY, Frid MG, Shimoda LA, Wiener CM, Stenmark K, Semenza GL. Temporal, spatial, and oxygen-regulated expression of hypoxia-inducible factor-1 in the lung. Am J Physiol 1998;275:L818-L826.

221. Jewell UR, Kietikova I, Scheid A, Bauer C, Wegner RH, Gassmann M. Induction of HIF-1α in response to hypoxia is instantaneous. FASEB J 2001;15:1312-1314.

222. Vordermark D, Brown JM. Evaluation of hypoxia-inducible factor-1α (HIF-1α) as an intrinsic marker of tumour hypoxia in U87 MG human glioblastoma: in vitro and xenograft studies. Int J Radiat Oncol Biol Phys 2003;56:1184-1193.

223. Vordermark D, Katzer A, Baier K, Kraft P, Flentje M. Cell type-specific association of hypoxia-inducible factor-1α (HIF-1α) protein accumulation and radiobiologic tumour hypoxia. Int J Radiat Oncol Biol Phys 2004;58:1242-1250.

224. Stroka DM, Burkhard T, Desbaillets I, Wenger RH, Neil DA, Bauer C, Gassmann M, Candinas D. HIF-1 is expressed in normoxic tissue and displays an organ-specific regulation under systemic hypoxia. FASEB J 2001;15:2445-2453.

225. Vukovic V, Haugland HK, Nicklee T, Morrison AJ, Hedley DW. Hypoxia-inducible factor-1α is an intrinsic marker for hypoxia in cervical cancer xenografts. Cancer Res 2001;61:7394-7398.

226. Olive PL, Durand RE, Raleigh JA, Aquino-Parsons C. Comarison between the comet assay and pimonidazole binding for measuring tumour hypoxia. Br J Cancer 2000;83:1525-1531.

227. Raleigh JA, Chou SC, Arteel GE, Horsman MR. Comparisons among pimonidazole binding, oxygen electrode measruements, and radiation response in C3H mouse tumours. Radiat Res 1999;580-589.

228. Jiang B, Semenza GL, Bauer C, Marti HH. Hypoxia-inducible factor 1 levels vary exponentially over a physiologically relevant range of O_2 tension. Am Phys Soc 1996;271:C1172-1180.

229. Ling LL, Streffer C, Sutherland R Decreased hypoxic toxicity and binding of misonidazole by low glucose concentration. Int J Radiat Oncol Biol Phys 1986; 12: 1231-1234.

230. Durand RE, Raleigh JA. Identification of non-proliferation but viable hypoxic tumour cells in vivo. Cancer Res 1998;58:3547-3550.

231. Hori K, Zhang QH, Li HC, Saito S. Variation of growth rate of a rat tumour during a light-dark cycle" correlation with circadian fluctuations in tumour blood flow. B J Cancer 1995;71:1163-1168.

232. Hori K, Suzuki M, Tanda S, Saito S, Shinozaki M, Zhang QH. Circadian variation of tumor blood flow in rat subcutaneous tumours and its alteration by angiotensin II-induced hypertension. Cancer Res 1992;52:912-916.

233. Durand RE, Sham E. The lifetime of hypoxic human tumour cells. Int J Radiat Oncol Biol Phys 1998;42:711-715.

234. Janssen HLK, Haustermans KMG, Sprong D, Blommestijn G, Hofland I, Hoebers F, Blijweert E, Raleigh JA, Semenza GL, Varia MA, Balm AJ, Vand Velthuysen MF, Delaere P, Sciot R, Begg AC. HIF-1α, pimonidazole, and iododeoxyuridine to estimate hypoxia and perfusion in human head-and-neck tumours. Int J Radiat Oncol Biol Phys 2002;54:1537-1549.

235. Zagzag D, Zhong H, Scalzitti JM, Laughner E, Simons JW, Semenza GL. Expression of hypoxia-inducible factor 1 alpha in brain tumours: Association with angiogenesis, invasion and progression. Cancer 2000;88:2606-2618.

236. Haugland HK, Vukovic V, Pintilie M, Fyles AW, Milosevic M, Hill RP, Hedley DW. Expression of hypoxia-inducible factor-1α in cervical carcinomas: correlation with tumour oxygenation. Int J Radiat Oncol Biol Phys 2002;53:854-861.

237. Nordsmark M, Loncaster J, Aquino-Parsons , Chou SC, Ladekart M, Havsteen H, Lindegaard JC, Davidson SE, Varia M, West C, Hunter R, Overgaard J, Raleigh. Measurements of hypoxia using pimonidazole and polarographic oxygen-sensitive electrodes in human cervix carcinomas. Radiother Oncol 2003; 67: 35-44.